UCONN LIBRARY

University of Connecticut
OpenCommons@UConn

Doctoral Dissertations | University of Connecticut Graduate School

5-5-2015

Genetic Determinants of Skeletal Diseases: Role of microRNAs

Neha S. Dole
University of Connecticut - Storrs, ndole@uchc.edu

Follow this and additional works at: https://opencommons.uconn.edu/dissertations

Recommended Citation
Dole, Neha S., "Genetic Determinants of Skeletal Diseases: Role of microRNAs" (2015). *Doctoral Dissertations*. 763.
https://opencommons.uconn.edu/dissertations/763

Genetic Determinants of Skeletal Diseases: Role of microRNAs

Neha S. Dole, Ph.D.
University of Connecticut, 2015

Abstract

Genetic factors account for 60-80% of variability in bone mineral density, and thereby play an important role in predisposition to osteoporosis, a prevalent skeletal disease. Understanding the genetic determinants underlying bone mass may improve prognosis and provide novel targets for therapeutic intervention. Single nucleotide polymorphisms (SNPs) associated with bone mass have been recognized in protein coding and non-coding genes, including microRNAs (miRNAs, miRs). Given the role of miRNAs as key post-transcriptional regulators modulating skeletal phenotype, our goal was to investigate the function of specific miRNAs in osteoblasts and osteoclasts, and understand how SNPs can modify miRNA function.

A single nucleotide polymorphism in osteonectin 3' untranslated region regulates bone volume and is targeted by miR-433. The function of a bone mass associated SNP (rs1054204, cDNA base 1599) in the 3' untranslated region (UTR) of human osteonectin gene was examined by developing and analyzing novel 3'UTR knock-in mouse models. These studies demonstrated that rs1054204) alters osteonectin expression in bone and leads to variability in trabecular bone volume. The underlying mechanism for SNP modulation of osteonectin regulation may involve differential targeting by miR-433, which is a negative regulator of osteoblast differentiation. rs1054204 also modulated

skeletal response to bone anabolic intermittent PTH. This work validates the association of rs1054204 with bone mass, and assigns a physiological function to a common osteonectin allele, providing support for its role in the complex trait of skeletal phenotype.

Function of miR-365, -99b and -451 in osteoclasts. During RANKL induced osteoclastogenesis in vitro expression of miR-365 and -99b is induced, while miR-451 is downregulated. We demonstrated that miR-99b is a crucial positive regulator of osteoclast differentiation, whereas miR-365 negatively regulates osteoclast formation. Computational analyses predict mTOR, PI3 kinase/AKT, and calcium signaling pathways to be top targets of miR-99b and -365 in osteoclasts. Following computational predictions, we optimized a RISC immunoprecipitation protocol in osteoblastic and osteoclastic cells, to identify miRNA targets in an unbiased manner.

Together our studies expand the current understanding of miRNAs in regulating skeletal phenotype and contribute to the pool of SNP variants needed for individualized fracture risk assessment.

Genetic Determinants of Skeletal Diseases: Role of microRNAs

Neha S. Dole

B.S., Dr. D.Y. Patil Institute, 2008
M.S., Texas Tech University, 2010

A Dissertation

Submitted in Partial Fulfillment of the

Requirements for the Degree of

Doctor of Philosophy

at the

University of Connecticut

2015

Copyright by

Neha S. Dole

2015

APPROVAL PAGE

Doctor of Philosophy Dissertation

Genetic Determinants of Skeletal Diseases: Role of microRNAs

Presented by

Neha S. Dole B.S., M.S.

Major Advisor _____

Anne Delany

Associate Advisor _____

Archana Sanjay

Associate Advisor _____

Sun-Kyeong Lee

Associate Advisor _____

Carol Pilbeam

University of Connecticut
[2015]

ACKNOWLEDGEMENTS

I would like to express my special appreciation and thanks to my advisor Dr. Anne Delany. She has been a tremendous mentor to me, encouraging me to think critically, and push myself to be a better research scientist. Our discussions on research, career and personal life have been invaluable.

I would also like to thank my committee members, Dr. Sun-Kyeong Lee, Dr. Archana Sanjay and Dr. Carol Pilbeam for all your guidance and motivation throughout my research. I would also like to thank Catherine Kessler for her technical help for my research project. I would especially like to thank Tiziana Franceschetti and Spenser Smith for their friendship and support, which has made my Ph.D. a fun experience.

A special thanks to my family. Words cannot express how grateful I am to my mother, brother and father for all of their sacrifices, support and motivation. I would also like to thank to my beloved husband for his immense patience, support and encouragement throughout this experience.

TABLE OF CONTENTS

LIST OF TABLES

LIST OF FIGURES

CHAPTER 1

Introduction

Genetic determinants of skeletal diseases: role of microRNAs

The skeleton is a unique organ, due to its diversity in function. It provides mechanical support for muscular activities, physical protection to internal organs and serves as a mineral repository for systemic homeostasis. Osteoporosis is a skeletal disease characterized by low bone mass, deterioration of bone microarchitecture and decreased bone strength, causing bone fragility and increased risk of fracture. Fracture is one of the leading causes of morbidity and mortality in the elderly population. According to the National Osteoporosis Foundation (NOF), more than 9.9 million Americans over the age of 50 have osteoporosis and an additional 43.1 million have low bone density. Assuming the same frequency of prevalence, NOF estimates ~20% increase in the number of osteoporotic and osteopenic individuals by 2020 [1]. In order to create novel therapeutics for bone loss and to identify risk factors for increased fracture prevalence, it is important to understand the molecular mechanisms controlling the physiology of bone, as an organ.

Bone formation

Bone is a highly dynamic tissue; during embryonic development cells forming bone are derived from mesenchymal cells of the neural crest and lateral and paraxial mesoderm. The neural crest cells give rise to the axial skeleton, while the lateral and paraxial mesoderm form the appendicular skeleton [2]. Bone formation is initiated through condensation and subsequent

differentiation of mesenchymal cells into osteochondral progenitors, which give rise to bone and cartilage. Bone can be formed through two distinct processes, intramembranous and endochondral ossification. In intramembranous ossification, osteochondral progenitors can directly differentiate into osteoblasts, giving rise to the flat bones such as those in the craniofacial region. While in endochondral ossification, which occurs in long bones, the progenitors differentiate into chondrocytes that form a cartilagenous template, which is subsequently replaced by bone.

Bone remodeling

Following bone formation, bone modeling is necessary for growth of the skeleton, and determines the size, shape and density of bone. A second process, bone remodeling, is crucial for mineral homeostasis, renewal of bone and repair of microdamage that can occur in response to mechanical stress.

Bone remodeling, performed by teams of osteoblasts and osteoclasts, occurs in small packets known as basic multicellular units (BMUs), and the cycle consists of 4 distinct phases: activation, resorption, reversal and formation [3, 4]. Remodeling can be triggered either in response to microdamage or by hormones and local factors in response to fluctuations in calcium and phosphate homeostasis. Microdamage-induced bone remodeling is initiated by osteocytes (mineralized osteoblasts) in proximity to the microcrack locus. This frequently results in localized osteocyte apoptosis, activation of osteoblasts and recruitment of osteoclast precursors to the resorption site. Activated osteoblasts express key cytokines that promote osteoclast precursors to differentiate into mature bone resorbing osteoclasts. In addition, osteoblasts also

secrete matrix metalloproteinases (MMPs), including MMP-13 that degrades osteoid on the bone surface, thereby providing surface domains for osteoclast attachment (Figure 1.1).

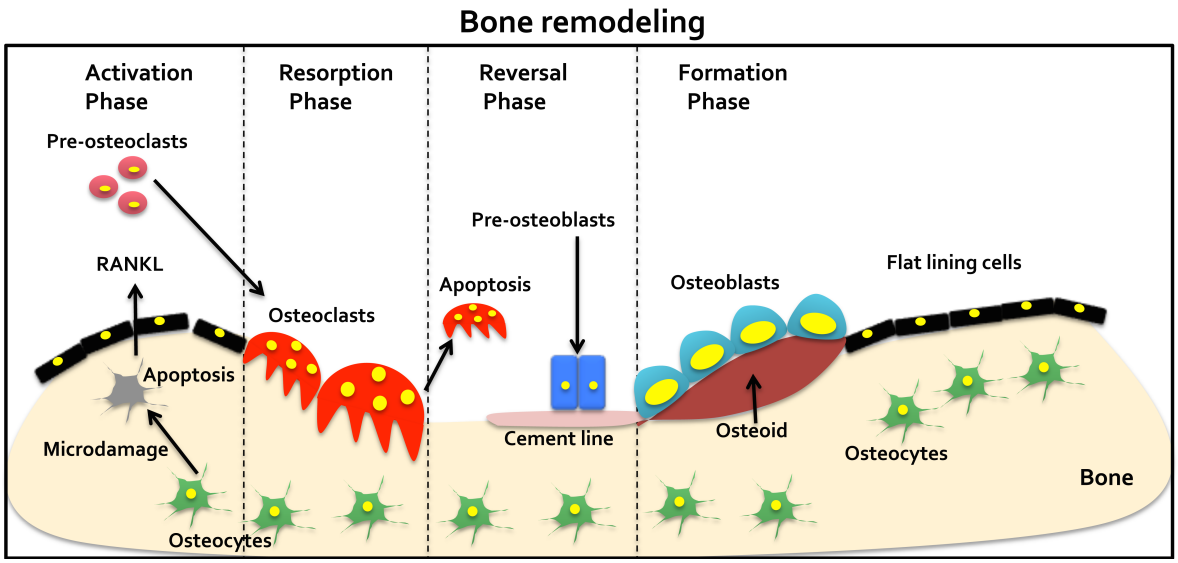

Figure 1.1 Schematics of bone remodeling. Remodeling starts with osteocyte apoptosis and RANKL mediated pre-osteoclast recruitment (Activation Phase), followed by osteoclastogenesis. Osteoclasts resorb bone (Resorption Phase) thus allowing the release of factors usually stored in the bone matrix, which recruit osteoblasts in the reabsorbed area (Reversal Phase). Once recruited, osteoblasts produce the new bone matrix, and promote its mineralization (Formation Phase).

During the bone resorption phase, osteoclasts attach to the bone surface through the sealing zone and enclose a resorption pit. Osteoclasts generate H^+ and HCO_3^- ions through carbonic anhydrase II enzyme activity; the H^+ ions are secreted into the resorption pit through the H^+ATPase proton pump. HCO_3^- ions are pumped out of the cell by Cl^-/HCO_3^- exchanger leading to an increase in intracellular Cl^-, which is secreted into the resorption pit by ClC-7

(chloride channel type 7). The acidified environment created in the resorption pit leads to the demineralization of bone matrix. Subsequently, proteolytic enzymes like Cathepsin K and matrix metalloproteinases (MMP-9) degrade the organic phase of bone matrix. Following the completion of resorption, osteoclasts undergo apoptosis, which marks the reversal phase. In this phase, the irregular cavities formed from resorption are corrected and a 'cement line' is formed, onto which osteoblasts can lay a uniform bone matrix. The exact details of this phase are not clear. However, it may involve additional degradation of collagen and deposition of some proteoglycans to form the cement line. It is also not clear whether macrophage or osteoblast lineage cells play a role in the reversal phase. During the final "formation" phase of the remodeling cycle, local osteoblast precursors are recruited to the resorbed site. Recruited precursors undergo osteogenic differentiation and active mature osteoblasts deposit newly synthesized osteoid at the resorbed site (Figure 1.1) [3, 4].

Osteoblasts

The bone forming osteoblasts are derived from multipotent mesenchymal stem cells with the potential to differentiate into alternate fates including the adipogenic, chondrogenic, myogenic and fibroblastic lineage. In response to appropriate stimuli, mesenchymal cells commit and differentiate into osteoprogenitors that give rise to matrix synthesizing mature osteoblasts, flat bone lining cells and matrix-embedded osteocytes. During osteogenic differentiation, spindle-shaped osteoprogenitors transform into pre-osteoblasts that proliferate and differentiate into osteoblasts. On the bone surface, osteoblasts appear as specialized cuboidal cells containing large golgi apparatus, extensive endoplasmic reticulum network, and a unique plasma membrane that enables them to synthesize and secrete a myriad of extracellular matrix proteins [5, 6].

Depending on the developmental stage, the extracellular matrix proteins synthesized by osteoblasts differ. For example, the pre-osteoblasts for the most part synthesize and secrete type I collagen and fibronectin, while the immature osteoblasts secrete alkaline phosphatase. The more mature osteoblasts secrete bone sailoprotein followed by osteocalcin, that associates with mineralized matrix [5]. Osteoblasts exert a tight regulation on osteoclastogenesis; they can promote osteoclast formation by expressing two crucial cytokines, macrophage colony-stimulating factor (M-CSF) and receptor activator of nuclear factor-κB ligand (RANKL) [7, 8]. The former is necessary for proliferation and survival of osteoclast precursors, while the latter is necessary for osteoclast formation. Osteoblasts can also inhibit osteoclast formation by synthesizing osteoprotegerin (OPG, TNFRSF11B), a soluble decoy receptor for RANKL. OPG inhibits osteoclastogenesis by blocking the RANKL-RANK interaction [8-10].

Osteoblast commitment and differentiation are intricately regulated by transcriptional and post-transcriptional mechanisms. The two major transcription factors critical for osteoblast commitment and differentiation are Runx2 and Osterix [11]. Runx2 belongs to the runt- domain gene family and is crucial for osteoblastic commitment of multipotent mesenchymal cells (MSCs) and bone development. While the globally Runx2 deficient mice have impaired endochondral and intramembranous bone development, deletion of Runx2 in committed osteoblast using 2.3kb-Col1a1-Cre leads to reduced postnatal bone growth [12-14]. Moreover, deletion of Runx2 activity in mature osteoblasts using osteocalcin-Cre results in an osteopenic phenotype with reduced osteoblastic activity [15, 16]. Osterix (Osx) belongs to the zinc finger DNA-binding protein family of transcription factors and is crucial for osteoblastic lineage commitment. Despite development of a cartilagenous skeleton, Osx-null mice lack bone and

suffer embryonic lethality [11]. Osx acts downstream of Runx2 during lineage commitment; deletion of Osx in committed osteoblasts (2.3kb-Col1a1-Cre) leads to osteopenia in growing mice [17, 18]. These transcription factors are often elicited through key signaling pathways for bone formation, including the BMP and Wnt pathways.

Bone morphogenetic proteins (BMP) are well known inducers of ectopic bone formation, and are crucial for osteoblast commitment and function. Deletion of BMP-2/4 in limb bud mesenchyme with Prx1-Cre leads to severe bone defects due to absence of osteoblast differentiation. Similarly, 2.3kb-Col1a1- Cre driven BMP4 deletion in early osteoblasts results in defective bone formation and growth. Moreover, overexpression of truncated dominant negative BMPR-IB (BMP receptor), driven by the 2.3kb-Col1a1 promoter, leads to dwarfism with lower bone volume and bone formation rate [19-23].

The importance of the canonical Wnt/β-catenin pathway is bone homeostasis was demonstrated through identification of rare human mutations in the Wnt co-receptor LRP5 (low density lipoprotein receptor related protein). LRP5 variants with a negative effect on Wnt signaling can cause osteoporosis pseudoglioma, and variants positively affecting Wnt signaling can cause Van Buchem disease and Sclerosteosis. Construction and analysis of LRP5-null mice confirmed the role of this locus in bone mass, and allowed study of the underlying mechanisms involved [24]. Moreover, Wnt/β-catenin signaling is essential for osteoblast lineage commitment, which was demonstrated by Prx1-Cre driven-β-catenin deletion mouse, which conditionally deleted β-catenin in limb mesenchyme. In these mice, the absence of β-catenin blocked osteoblastic differentiation, and osteochondral precursors differentiated into

chondrocytes instead [25, 26].

Osteoclasts

Multinucleated osteoclasts are hematopoietic lineage cells that originate from common myeloid progenitors (CMPs) near the bone surface. Co-culture of bone marrow or spleen cells with stromal cells led to the identification of M-CSF and RANKL as key cytokines for osteoclastogenesis [27, 28]. These cytokines are sufficient and essential for recruitment of osteoclast precursors, osteoclast commitment, survival, differentiation and function. Upon commitment of CMPs to the osteoclast lineage, the mononuclear precursors proliferate, migrate and fuse together to form multinucleated osteoclasts, that are subsequently activated to resorb bone [29].

Activated resorbing osteoclasts are structurally distinct and undergo cytoskeletal rearrangements during resorption, leading to their polarization and segregation of the plasma membrane into special domains. Polarized osteoclasts reorganize their nuclei, endoplasmic reticulum and golgi network towards the apical region of the cell, away from the resorption site. In contrast, the numerous mitochondria, lysosomes and vacuoles are reorganized towards the resorption site [29-31]. The plasma membrane in activated osteoclasts segregates into a basolateral membrane, sealing zone, and a ruffled border surface. The basolateral membrane faces the vascular marrow, while the sealing zone and the ruffled border face the bone surface. Osteoclasts attach to the bone matrix through the sealing zone and some studies implicate integrins like αvβ3 in mediating osteoclast attachment [32]. The sealing zone is enriched in podosomes, which are foot-like projections that form actin rings. Formation of actin rings is crucial for osteoclast attachment and resorption. The ruffled borders are finger-like membrane projections that extend into the resorption pit and facilitate resorption. Ruffled borders are

formed from the fusion of intracellular vesicles with plasma membrane, and are equipped with ion transporters. Extensive vesicular trafficking through the ruffled border creates an acidic environment in the resorption pit that leads to degradation of bone matrix [29, 32]. The ruffled border also releases lysosomal enzymes like Cathepsin K that degrades the collagenous bone matrix in resorption pit. The degraded bone matrix is taken up by osteoclasts through the ruffled borders and released into the vascular marrow through the secretory domain of the basolateral membrane (Figure 1.2) [29-31].

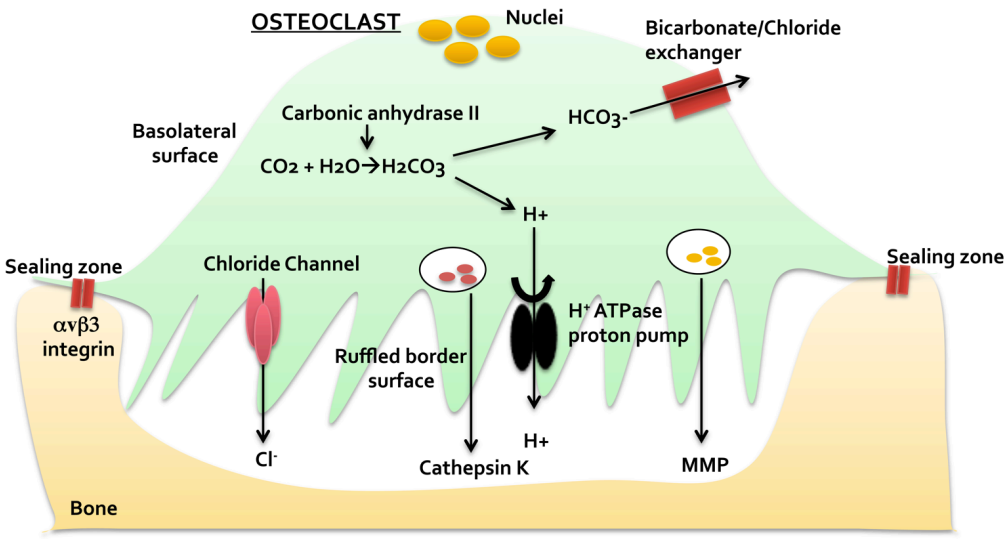

Figure 1.2 Mechanism of bone resorption by osteoclasts. Osteoclasts attach to the bone matrix at sealing zones via αvβ3 integrins. Resorption is initiated by Carbonic anhydrase II enzyme that generates H^+ and $HCO3^-$ ions; H+ is transported into the resorption pit by H+ATPase proton pump located in the ruffled border. $HCO3^-$ ions are exchanged for Cl^- by $Cl^-/HCO3^-$ exchanger at the non-resorptive surface. Chloride channels (ClC-7) located in the ruffled membrane pump the Cl− into the resorptive pit. Demineralized organic bone matrix is degraded by cathepsin K, an acid protease and MMP-9 (matrix metalloproteinase 9) secreted into the resorptive pit.

An early requirement for osteoclastic commitment of CMP is expression of transcription factors PU.1, MITF (microphtalmia transcription factor) and c-Fos, which induce expression of M-CSF receptor (M-CSFR) [28, 33-35]. M-CSFR belongs to receptor tyrosine kinase family and upon ligand binding activates several signaling cascades including ERK and PI3K/ Akt pathways for osteoclast precursor proliferation and survival [35]. M-CSF receptor binding also promotes expression of RANK (RANKL receptor) by osteoclast precursors; thereby priming them for RANKL induced osteoclastogenesis. Moreover, MCSF signaling also activates Rac, that mediates osteoclast migration and resorption [36]. RANKL-RANK binding leads to recruitment of adaptor proteins, TRAFs (tumor necrosis factor receptor associated factor), to activate several signaling cascades. The two most well recognized are TRAF -2 and -6; together they activate downstream signaling pathways of NF-κB, c-Jun N-terminal kinase (JNK), and NFATc1 [37-39]. NFATc1 is one of the master transcription factors, activated by multiple signaling cascades to induce osteoclastogenesis. Many studies have shown that NFATc1, in combination with PU.1, MITF and NF-**κ**B, induces expression of osteoclastic genes such as, Cathepsin K, Tartrate-resistant acid phosphatase (*Acp5, Trap*), and Calcitonin receptor [40-42].

MicroRNAs (miRNAs, miRs)

More recently, the importance of the key post-transcriptional regulators, microRNAs (miRNAs, miRs) in regulating bone cells has been appreciated. MicroRNAs are small, endogenous, single-stranded RNAs that regulate expression of protein encoding genes. miRNAs assembled in the RNA induced silencing complex (RISC) directly bind to the target mRNAs and mediate downregulation of their expression by mRNA degradation and/or translational suppression. For most part, miRNAs bind to the 3' untranslated region (UTR) of target mRNAs, however, miRNA binding sites can also be present in the coding region and 5' UTR [43, 44].

In osteoblasts, the importance of miRNAs was demonstrated by targeted deletion of the key miRNA processing enzyme, Dicer, in osteoblast precursors using ColIa1-Cre, and in mature osteoblasts using osteocalcin-Cre. Dicer deletion in osteoprogenitors prevents their differentiation and impairs bone formation, leading to embryonic lethality. While Dicer deletion in mature osteoblasts delayed their differentiation, and a high bone mass phenotype was ultimately observed [45]. This suggests a temporal activity of miRNAs in bone formation. Moreover, the importance of miRNA regulation in osteoclastogenesis was also demonstrated in vivo in the Ctsk-Cre Dicer-null mice. Abrogation of miRNA biogenesis in osteoclasts resulted in an osteopetrotic phenotype, with increased bone mass and decreased osteoclast number and resorption activity [46]. Given the overall importance of miRNAs in bone biology, there is a growing body of data describing the function of individual miRNAs in osteoblasts and osteoclasts [47, 48]. However, there is little known about how sequence variants might impact the activity of miRNAs in skeletal cells.

Sequence variations and gene regulation

Sequence variations such as insertions, deletions, copy number variants and single nucleotide polymorphisms (SNPs) are responsible for genomic diversity. Recent studies have identified approximately 38 million SNPs in the human genome, representing the majority of gene variants [49]. Although most numerous, individual SNPs are small changes. Depending on its location, a SNP may impact gene function or expression or it may be silent. For the most part, determining the functional consequence of SNPs or other gene variants has lagged behind the identification and cataloging of the sequence variants, themselves.

In the field of skeletal biology, bone mass phenotype is known to be a complex and highly heritable trait. Linkage studies, in conjunction with candidate gene studies, have identified some rare genetic variants with a high impact on bone phenotype, most notably variants of LRP5. More recently, GWAS (genome wide association study) has identified 62 genome-wide significant loci associated with bone mineral density (BMD) [50, 51]. Some of these loci contain candidate genes with known function in pathways important in bone physiology, such as canonical Wnt signaling, the RANK-RANKL-OPG system, and endochondral ossification. However, only chromosomal regions have been determined, and the genes or mechanisms underlying the linkage with BMD are not yet identified. For the most part, the SNPs identified are common variants, and likely have a small effect size. Presently, less than 6% of the variance in femoral neck BMD can be explained by the GWAS-identified loci. [52].

It may be relatively straightforward to determine whether SNPs in the protein-coding region of a gene, or within intronic areas that affect splicing, might cause changes in protein function or abundance, and thereby, phenotype. However, the functional impact of SNPs in untranslated regions (UTRs), promoter/enhancer regions or regulatory RNAs can be more difficult to evaluate. Since only 1-2% of genome comprises protein coding sequence, it is imperative to recognize and understand the potential function of SNPs in non-protein coding regions. With regard to regulatory region SNPs and bone mass, the alpha 1 type I collagen (Col1A1) gene was one of the first to be studied. In a cohort of post-menopausal women, BMD-associated SNPs in the promoter and intronic region of Col1A1 were reported. In vitro, these SNPs were associated with altered bone matrix mineralization and collagen gene expression by affecting binding of transcription factors, Nmp4/CIZ and Sp1, respectively [53-57].

At conserved sites within the human genome, the largest proportion of variants is within UTRs [49]. Remarkably, a study comparing GWAS-SNP sets found an enrichment of trait-associated variants in 3' UTRs, compared with 5' UTRs or coding sequences (CDS) [58]. The 3' UTR is recognized as a critical control region, with the potential to regulate mRNA stability, translation and localization. Moreover, many binding sites for microRNAs (miRNAs, miRs) are found in 3' UTRs.

SNPs and miRNAs

There are increasing reports of SNPs that can interfere with miRNA function. Such polymorphisms can occur in the miRNA target site of a mRNA (miR-TS-SNPs) or in the miRNA genes themselves (miR-SNPs) [59-61]. miR-TS-SNPs present at or near a miRNA binding site in a protein coding gene could modulate miRNA function by creating or eliminating a miRNA binding site in that target mRNA [62]. The functional impact of a miR-TS-SNP on phenotype largely depends on whether the corresponding miRNA is expressed in a particular tissue, as well as the expression of other possibly compensatory miRNAs. For example, miRs and their targets can be expressed in a tissue specific manner, and a miR-TS-SNP might only be of functional consequence if the targeting mRNA is expressed in the same tissue. These considerations could provide some basis for understanding tissue-restricted phenotype associated with some common SNPs. A recent study used an in silico approach to investigate potential mechanisms for the association of certain SNPs in disease pathogenesis. They identified potential pathways impacted by trait-associated 3' UTR SNPs, as well as whether SNPs could

affect splicing, polyadenylation site usage, secondary structure and miRNA binding [58]. This approach can be utilized to analyze the available GWAS data to interpret biological relevance of miR-SNPs in multifactorial diseases and outline novel pathways to explore experimentally [58].

In contrast to miR-TS-SNPs, SNPs in miRNA genes (miR-SNPs) are relatively rare. It is estimated that only ~10% of human miRNA genes contain SNPs; and SNPs in the region corresponding to the mature miRNA are the most rare (<~1%) [60, 63]. Since a single miRNA could target hundreds of genes and regulate multiple pathways, a polymorphism in a miRNA gene leading to functional impairment could impact all the regulatory pathways involving that miRNA. Thus, there appears to be considerable selective constraint on the transmittance of miR-SNPs.

In terms of trying to understand the function of mutations or polymorphisms in miRNA genes and targets, the cancer field has been in the forefront. Because of such work, some miR-TS-SNPs and miR-SNPs have become part of panels that can be used to help assess cancer risk, prognosis and/or response to therapies [64]. Similar work in the field of skeletal biology is in its infancy. However, some miRNAs and mRNA targets important in malignancy are also important in bone or cartilage. Therefore, studies performed in the context of cancer can also be relevant for understanding the function of miRNA gene and target polymorphisms in skeletal biology. Accumulating evidence suggests that SNPs in human miRNA genes (pri-, pre- or mature) can influence predisposition to skeletal disease, including osteoporosis. Although long non-coding RNAs (lncRNAs) are also frequently targeted by miRNAs, contain SNPs, and can impact skeletal physiology, there is relatively little known about the function of lncRNAs in the skeleton

[65-67]. Consequently, in reviewing the published data on sequence variants in miRNAs and miRNA targets, the following discussion will be restricted to protein coding genes and miRNAs that could have an impact on the skeleton. Moreover, many studies have associated miRNA SNP variants with a particular phenotype. However, few studies have identified a potential mechanism involved. Therefore, this review will also be restricted to work demonstrating molecular mechanisms.

miRNA biogenesis and function

Biogenesis of miRNAs is a complex, multistep process in which a long hairpin-containing transcript undergoes sequential maturation into a short single stranded miRNA. SNPs or mutations that alter the sequence of the pri-miRNA can have a dramatic effect on processing; therefore, before discussing SNPs in miRNA coding genes, it is important to first consider the steps in miRNA biogenesis (Figure 1.3).

MicroRNA biogenesis most frequently begins with RNA polymerase II mediated transcription of miRNA encoding genes into a long transcript termed primary miRNA (pri-miRNA). MicroRNA genes can reside in the intergenic regions of the genome, as well as within the intronic and exonic regions of protein-coding genes [68]. Generally miRNAs in the same cluster are co-transcribed, however additional post-transcriptional regulatory mechanisms exist and may contribute to alterations in the expression profile of miRNAs in a cluster. Transcription of intergenic miRNAs is regulated through dedicated promoters, while the intragenic miRNAs can share promoters with host genes. However, recent evidence suggests that several intron-

encoded miRNAs also possess independent promoters that are subject to classical regulation by transcription factor binding, DNA methylation and histone modifications [69].

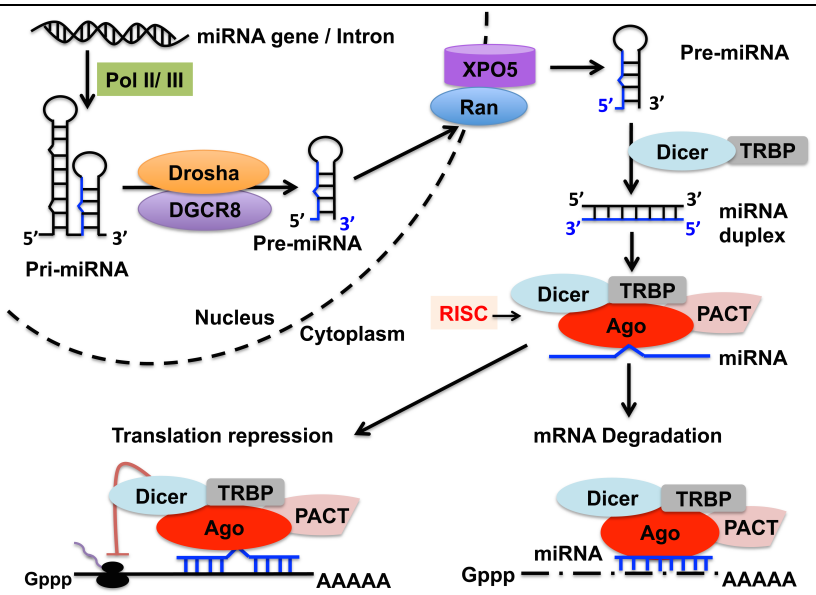

Figure 1.3 MicroRNA biogenesis pathway. Pri-miRNAs transcribed from miRNA genes by RNA polymerase (Pol) II are processed into pre-miRNAs by Drosha/DGCR8. Pre-miRNA is pumped into cytoplasm by XPO5 and further processed into a miRNA duplex by Dicer/TRBP complex. The leading strand of duplex that forms mature miRNA is indicated in blue. The mature miRNA strand assembles with Ago, incorporated in the RNA-induced silencing complex (RISC). Depending on the degree of complementarity of the seed sequence of miRNA and 3'UTR of the target mRNA, miRNA-RISC down regulates gene expression by either translational repression or mRNA degradation.

XPO5-Exportin 5; DGCR8-DiGeorge syndrome critical region gene 8; TRBP-TAR RNA binding protein; Ago- Argonaute; PACT, protein activator of PKR.

Like any other Pol II transcript, the structure of pri-miRNAs is comprised of a 5'-cap and 3'-poly-A tail, which flanks 2 or more hairpin structures; and each hairpin consists of an imperfect double stranded stem (~30 base pairs) and a short terminal loop. The pri-miRNA is further sliced into a shorter (~60-80 base) hairpin structure termed precursor miRNA (pre-miRNA) by a Microprocessor complex. This complex includes two major proteins: DGCR8 (DiGeorge critical region 8) and Drosha (RNase III enzyme family). The DGCR8 protein contains domains for binding Drosha and double stranded RNA, thereby recruiting the pri-miRNA to the Drosha RNase domain, which cleaves the pri-miRNA ~22 nucleotides upstream from the base of the terminal loop stem [70]. The precision in Drosha mediated cleavage is guided by unique motifs in the pri-miRNA (at the base and terminal loop of stem) and discrepancies in the motif signature or length can result in varied pre-miRNAs [71-73]. The Microprocessor complex also contains accessory proteins like DEAD-box helicases (p68 and p72) that function as post-transcriptional regulators of miRNA biogenesis. For example, R-SMAD interaction with the p68 helicase enhances pri-miR-21 processing by the Microprocessor complex [74]. Although majority of pri-miRNAs undergo canonical processing, some miRNAs bypass Drosha and are generated by alternative splicing of introns. (Figure 1.3) [75].

Following processing in the nucleus, pre-miRNAs are pumped to cytoplasm by exportin-5 (XPO5), which binds to the stem of the hairpin and exports the pre-miRNA in a Ran-GTP dependent manner [47, 76-78]. In the cytoplasm, pre-miRNAs are further processed into roughly symmetric miRNA duplexes by the Dicer complex. This complex consists of proteins TRBP (Tar RNA binding protein) and Dicer (RNase III enzyme family). The TRBP protein contains domains for binding Dicer and the pre-miRNA. The Dicer/TRBP complex binds to the 2

nucleotide long 3' overhang of the pre-miRNA and cleaves 22 nucleotides upstream from the base of the double stranded stem, resulting in formation of a miRNA duplex. Previously, the Dicer RNase III enzyme was implicated to function only as a slicer but recent structural studies indicate Dicer has an inherent capacity to selectively recognize and process diverse precursors. Subsequently, the miRNA duplex is loaded onto a particular Argonaute protein (Ago 1-4, typically Ago2) that, together with Dicer/TRBP, forms the RNA induced silencing complex (RISC).

A single stranded mature miRNA is assembled from the RISC-miRNA duplex through duplex unwinding and processing by Ago [69, 79-83]. In case of a perfect complementarity in the center of the miRNA duplex, the mature miRNAs are formed through direct slicing by Ago2. The passenger strand of the duplex often undergoes degradation; however in some cases both strands of duplex are loaded into the RISC [84, 85]. Selection of the guide strand from the miRNA duplex is governed by thermodynamics; the strand with the least stable 5' end bases in the duplex forms the mature miRNA that is loaded into RISC. Recent studies also suggest that Dicer/TRBP interaction also partly influences that strand selection [86]. Interestingly, not all pre-miRNAs undergo Dicer mediated processing. For example miR-451 is processed from Ago2 mediated slicing of the pre-miRNA stem [69].

The RISC-Ago-bound mature miRNA binds to a complementary region on target mRNAs, and the target binding is predominantly based on Watson-Crick base pairing. In particular, complementarity of bases in the 'seed' region, nucleotides 2-8 in the 5' end of the miRNA, has been considered crucial for miRNA action [78, 87]. Non-canonical interactions in

the seed region, consisting of G:U base pairing and bulges, were previously shown to compromise miRNA targeting [88]. However, it is now evident that these non-canonical interactions are indeed tolerated during miRNA-target binding [89]. Moreover, supplementary base pairing within nucleotides 12-17 in the 3'end of miRNA can enhance miRNA target recognition [90]. Interestingly, Ago2 has been reported to aid in miRNA binding site recognition, due to its own, independent binding preference to selected mRNA sequence motifs [91].

miRNAs negatively regulate the expression of target mRNAs by repressing translation and by decreasing mRNA stability [78, 92]. For the most part, the miRNA-RISC initially blocks translation by inhibiting the function of cap-binding initiation factor eIF4E, reducing elongation and enhancing translation termination, leading to formation of destabilized nascent peptides. Recent studies also indicate that miRNAs mediate translation repression of target genes by causing shortening of the poly-A tail. The destabilized transcripts with short poly-A tails are subsequently deadenylated, decapped and degraded [93]. MicroRNA mediated mRNA degradation is achieved by hydrolysis of phosphodiester backbone of target mRNA and altogether both mechanisms lead to repression in gene expression [94]. Current studies indicate that both translation repression and mRNA decay occur in conjunction during miRNA-mediated post-transcriptional regulation [93, 95]. These reports indicate that during the early phase of regulation, miRNAs repress translation, whereas mRNA decay might be the prominent mechanism of miRNA mediated post-transcriptional regulation later [95]. In addition, there is increasing evidence that selected miRNAs can be imported back into the nucleus, to alter the processing or function of other miRNAs [94, 96].

SNPs altering microRNA biogenesis and function

MicroRNAs regulate skeletal development and homeostasis by targeting multiple genes and pathways. Thus, SNPs that alter expression and/or function of a single miRNA could function as a dominant variant of skeletal phenotype. SNPs that compromise miRNA expression can occur in the miRNA gene promoter, termed miR-P-SNPs, or in miRNA genes (miR-SNPs). SNPs that compromise miRNA function can occur in the seed binding region of mature miRNA.

(I) miR-P-SNPs: SNPs in miRNA promoters

miRNA promoters are regulated by mechanisms similar to those regulating promoters of protein encoding genes. Following detection of transcriptional elements in pri and pre-miRNA genes, transcription factor binding sites (TFBS) near promoters of several miRNAs have been recognized [97, 98]. SNPs in these TFBS can modulate miRNA expression by, (1) altering the binding affinity of TFBS to transcription factors or (2) abolishing an existing TFBS or (3) creating a novel TFBS (Figure 1.4). With the discovery of many more SNPs in human miRNA genes, databases like miRGen 2.0 and dPORE-miRNA were developed to bioinformatically predict SNPs in miRNA promoters. Such studies estimated that ~20,000 SNPs prevail in human miRNA promoters [99, 100]. Despite these elaborate predictions, information on the impact of miR-P-SNPs on disease risk is limited. The mechanism by which miR-P-SNPs affect miRNA regulation is known for only a few miRNAs.

As an example, let us consider the impact of miR-P-SNP rs57095329 on miRNA regulation. This SNP is located within 1 kb of the miR-146a transcription start site and was first identified as strongly associated with risk of SLE (systemic lupus erythromatosis), a chronic autoimmune disorder [101]. This association was later validated in a meta-analysis of GWAS that included cohorts of European and Asian descent [102]. The studies in SLE linked the risk-associated minor allelic variant rs57095329-G (A>G, minor allele frequency (MAF) 0.14 in 1000 Genomes Project) with reduced miR-146a promoter activity, leading to low mature miRNA levels. Moreover, the risk allele was also shown to reduce binding affinity of Ets1 to the miR-146a promoter [101]. In bone, the Ets1 transcription factor, which enhances miR-146a promoter activity, is also known to interact with CbfA1/Runx2, which is the quintessential factor for osteogenesis [119].

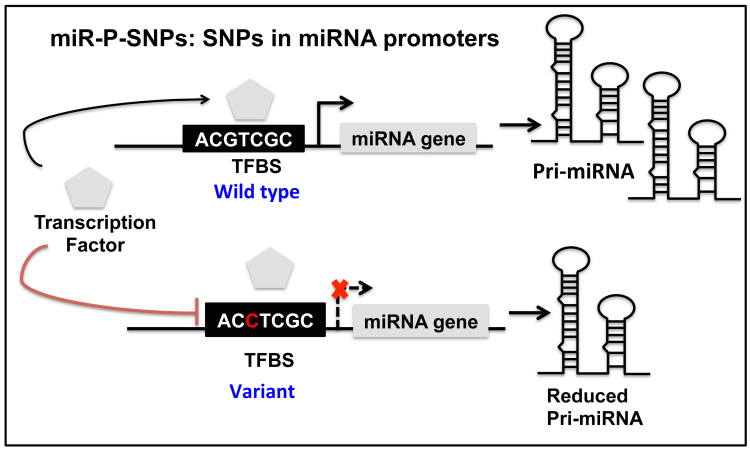

Figure 1.4 Schematics of miR-P-SNPs. SNPs in the regulatory transcription factor-binding site (TFBS) near the promoter of miRNA gene can alter miRNA expression.

Overall this study demonstrated that the miR-P-SNP modulated transcription factor binding to miR-146 promoter thereby altering its expression. Interestingly, apart from SLE, miR-

146a has been also implicated in rheumatoid arthritis (RA), an autoimmune disease affecting skeletal tissues [103-105]. In RA, where joint destruction occurs due to chronic inflammation, miR-146a has been shown to suppress osteoclastogenesis [104, 105]. However, an association between the SLE-linked miR-P- SNP, rs57095329, and RA has not yet been examined.

(II) miR-SNPs: miRNA gene SNPs

The multistep processing of long transcripts into short miRNAs relies heavily on the secondary structure of each transcript. Polymorphisms in miRNA genes that modulate RNA secondary structure can impair subsequent processing, and reduce mature miRNA levels (Figure 1.5).

Pri-miR-SNP:

Mechanistic studies examining the effect of a pri-miRNA SNP on processing have been described for miR-125a. SNP rs12975333 (G>T), located in the stem region of pri-mi125a, has been shown to modulate miRNA expression and activity. Specifically, the minor allele variant (T) was shown to decrease binding of pri-miR-125a to the DGCR8 component of the miRNA biogenesis machinery. This leads to defective pri- to pre-miR processing and low mature miR-125a levels. Moreover, in congruence with the decreased expression of mature miRNA, an increase in levels of miR-125a targets was also observed in rs12975333 (T) containing cells [59].

In addition to affecting processing, rs12975333 is retained by the mature-miRNA and was shown to impair miR-125a-mediated translational repression. Specifically, the T variant of rs12975333 impairs the seed-binding region of miR-125a, and reduces repression on the miR-

125a target gene, Lin-28 [59]. Lin-28 is a RNA binding protein that acts as a translational enhancer of IGF2 [106]. Remarkably, such SNPs that reside in the seed-binding region of mature miRNAs are quite rare, which might reflect their profound impact on cell physiology (Figure 1.5) [60, 61].

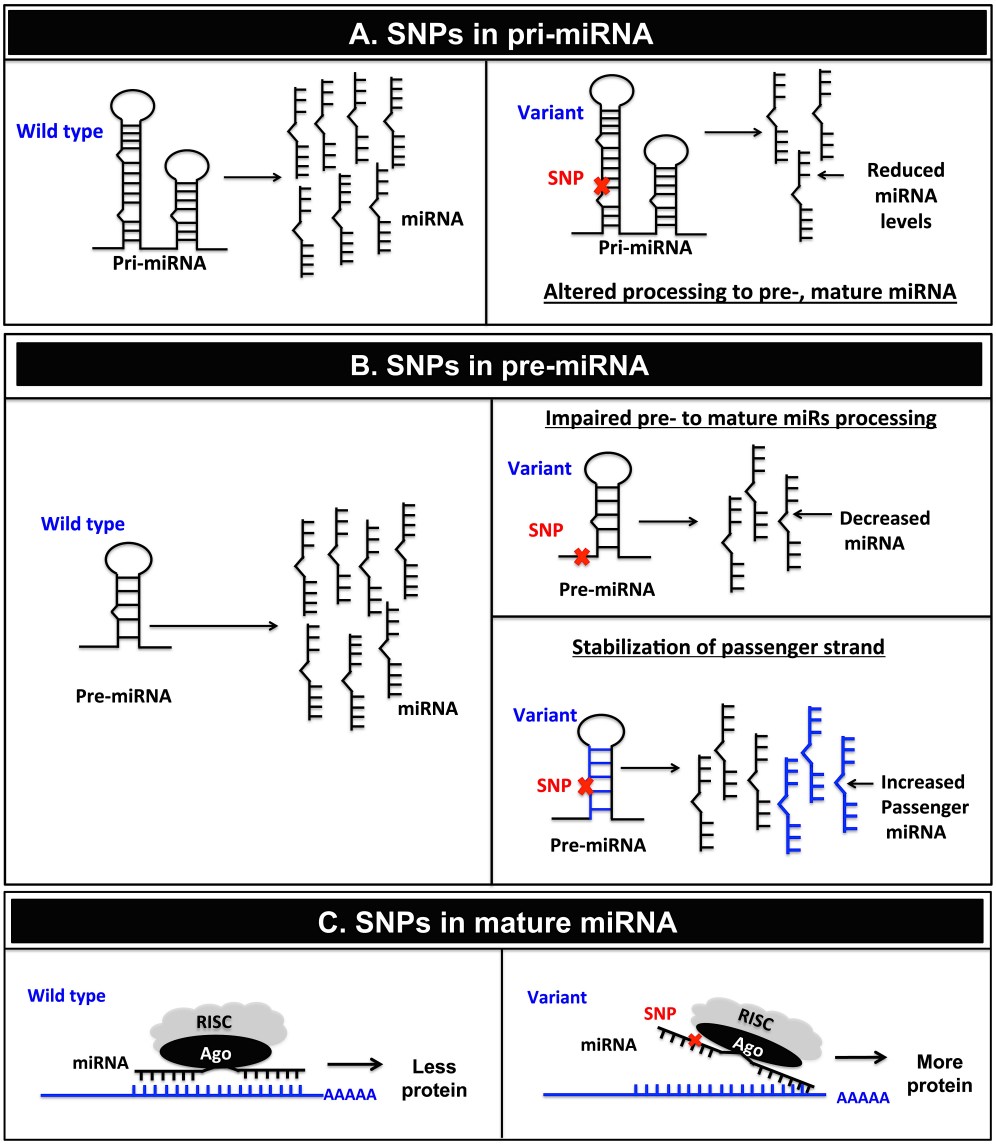

Figure 1.5. Schematics of miR-SNPs. SNPs in pri- and pre- and mature miRNAs are likely to affect miRNA processing and subsequent mature miRNA levels. SNPs in mature miRNA can alter their activity.

Pre-miR-SNP:

One example of a pre-miRNA SNP that can modulate mature miR expression and activity is illustrated by SNP rs2910164 in pre-miR-146a. SNP rs2910164 (G>C, MAF 0.458 in CSAgilent Project) was mapped to the passenger strand in the stem in pre-miR-146a, and was associated with the risk of various cancers, such as papillary thyroid carcinoma (PTC), prostate cancer, breast cancer, gastric cancer, ovarian cancer, esophageal squamous cell carcinoma, hepatocellular carcinoma [107-113]. The mechanism for SNP rs2910164-mediated alterations in mature miR-146a levels has been examined in studies of PTC and nasopharyngeal carcinoma (NPC), where GC heterozygosity was linked to high PTC risk, while C allele homozygosity has been associated with increased NPC risk [108, 114]. In both PTC and NPC, the risk associated allele C resulted in lower miR-146a levels, due to impaired Drosha-mediated processing of the pre-miRNA. Apart from impairing Drosha processing, this SNP has been suggested to stabilize the passenger strand leading to increased regulation of miR-146a target genes-TRAF6 and IRAK1 (Figure 1.5). In PTC patients, GC heterozygotes were shown to generate two passenger strands, -146a*G and -146a*C along with the leading strand [107]. It is possible that these alternate passenger strands could target different mRNAs. Although rs2910164 was previously linked to RA, a later meta-analysis disproved this association [115, 116].

Altogether, these seminal studies elegantly demonstrate the impact of miRNA- SNPs on miRNA processing and targeting.

(III) miR-TS-SNPs: SNPs in miRNA target sites

Polymorphisms in the miRNA target site (miR-TS-SNPs) can either abrogate an existing miRNA binding site or create a novel site in the 3' UTR of target genes. Compared with SNPs in miRNA genes, miR-TS-SNPs in 3' UTRs are more abundant [60, 61]. Again, studies in the field of cancer genetics have led the way, with regard to identifying the function of miR-TS-SNPs in several target genes with known functions in bone, such as BMPRI (bone morphogenetic protein receptor I).

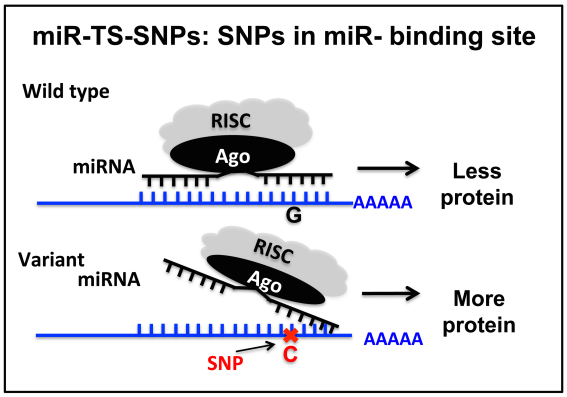

Figure 1.6. **Schematics of miR-TS-SNPs.** SNPs in miRNA target site (TS) can strengthen or reduce binding between the miRNA and its mRNA target. Moreover, such SNPs can create a novel site or destroy an existing target binding sites, ultimately modulating target gene expression.

Bone morphogenetic proteins (BMPs) are bone anabolic factors critical for development [117]. BMPs signal through their membrane bound receptors, BMPRI (IA and IB) and BMPRII, which form a homo- or heterotrimeric complex on ligand binding and activate a canonical Smad-mediated transcriptional program [118]. Both type I BMP receptors have distinct spatial and temporal expression patterns during embryogenesis [119-121]. In osteoblasts, BMPRI-B is crucial for commitment of mesenchymal precursors towards osteogenic lineage, while BMPRI-A appears to direct them towards adipocytic fate [21, 22]. Conditional deletion of BMPRI-B in

osteoblasts leads to decreased bone formation and growth [23]. Inhibition of BMP signaling can also lead to osteopetrosis due to impaired osteoclastogenesis and resorption, thereby indicating its importance in bone remodeling [20].

One case-control study linked SNP rs1434536 (C>T, MAF 0.404 in 1000 Genomes Project) in the BMPR-IB 3' UTR with increased risk of estrogen receptor-positive (ER+) breast cancer [122]. Previously, increased BMPR-IB mediated signaling in ER+ breast carcinoma was associated with high tumor grade, high tumor proliferation, cytogenetic instability and poor prognosis [123]. Interestingly, this SNP rs1434536 showed strong linkage with cancer associated SNPs from the CGEMS (Cancer Genetic Markers of Susceptibility) GWAS data set [122, 124]. Patients carrying the high risk rs1434536-T allele had increased BMPR-1B expression, and this allele demonstrated impaired binding of miR-125b binding to the BMPR-IB 3' UTR [122]. A second study demonstrated a similar mechanism for the rs1434536-T variant and higher prostate cancer risk [125]. Remarkably, the rs1434536-T allele was shown impart BMPR-IB mediated protection against endometriosis, due to diminished miR-125b directed repression [126]. SNP rs1434536-T is a common variant, and increased BMPRIB levels in individuals carrying this allele might contribute to higher bone mass.

SNPs in miRNAs important in the skeleton

miR-146a:

The human miR-146 family consists of 2 distinct isoforms, miR-146a and -146b, that have been mapped to human chromosomes 5q33.3 and 10q24, respectively [108]. miR-146a is expressed in articular cartilage and femur, as well as in non-skeletal tissues including prostate,

liver, breast, and hematopoietic cells [127-132]. An NF-κB binding motif near the transcription start site (TSS) of miR-146a has been recognized, and factors including TNFα, lipopolysaccharide or IL-1 β (interleukin-1β) have been shown to induce miR-146a expression [130, 133]. In turn, miR-146a limits the inflammatory response by targeting TRAF6 (TNF receptor associated factor 6) and IRAK1 (IL1 receptor associated kinase 1), which play a role in activating NF-κB signaling [130]. In osteoclasts, TRAF6 and IRAK1 mediate IL-1β induced activation of NF-κB signaling to promote osteoclast survival and activity [37, 134].

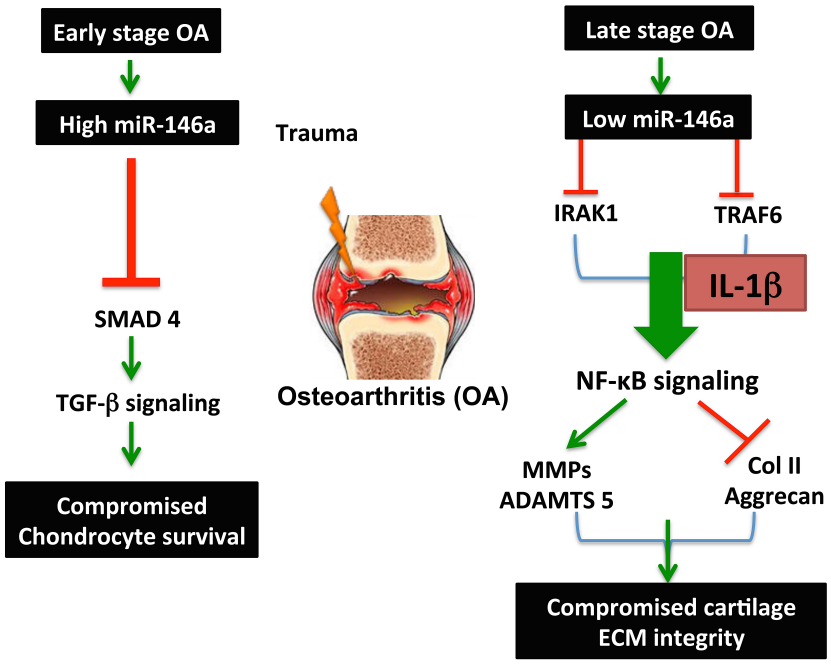

Figure 1.7 Potential model for miR-146a role in osteoarthritis. In early OA lesions, high levels of miR-146a are detected, which can suppress SMAD4/TGF-β signaling and enhance chondrocyte apoptosis. With progression of OA, miR-146a levels decline, which leads to loss of IL-1 β regulation. With increased IL-1 β/NF-κB signaling, expression of MMPs and ADAMTS5 is induced, while Col II and aggrecan expression is suppressed; together this exacerbates cartilage matrix degradation.

miR-146a has also been linked to the pathogenesis of osteoarthritis (OA) [133, 135, 136]. OA is characterized by the progressive degeneration of articular cartilage, primarily in response to mechanical injury. Studies have reported high levels of miR-146a in articular chondrocytes during the early stages of OA, whereas in the later stages, miR-146a levels decline [135-137]. miR-146a has been shown to target SMAD4, which might suppress TGF−β mediated chondrocyte survival [135, 136]. In the later stage of OA, when the synovium is inflamed, miR-146a is suggested to have a protective effect on articular cartilage by suppressing IL-1β signaling via TRAF6 and IRAK1 targeting. With decreased IL-1β signaling, expression of cartilage-degrading enzymes (MMP13 and ADAMTS5) is suppressed, while expression of cartilage matrix proteins such as aggrecan and type II collagen is highly induced [133].

miR-146a also plays a crucial role in regulating bone remodeling. It functions as a positive regulator in osteoblasts that drives commitment of mesenchymal stem cells to osteogenic rather than a chondrogenic fate. By targeting Smad 2/3, miR-146a regulates TGFβ signaling and indirectly downregulates expression of chondrocytic marker Sox9, and upregulates Runx2 [64]. In osteoclasts, miR-146a levels increase during differentiation, and miR-146a has been shown to inhibit both TNFα and RANKL induced osteoclast differentiation by mechanisms likely to include the targeting of TRAF6 and IRAK1, as well as other mRNAs [105, 138].

The miR-146a gene contains at least 2 functional SNPs. The SNP in the stem loop region of pre-miR-146a, rs2910164, discussed earlier, is a common variant that alters miRNA processing, whereas the miR-146a promoter SNP rs57095329 alters transcription factor binding. In addition, other SNPs in the promoter region of miR-146a have been recognized (rs17057381,

rs73318382, and rs6864584), although their function has not yet been ascertained. Given the role of miR-146a in regulating inflammation, autoimmunity, and skeletal homeostasis, it will be crucial to examine the functional impact of these other miR-146a SNPs, and determine whether they might be associated with skeletal diseases such as osteoarthritis and osteoporosis [115, 116].

miR-125:

The human miR-125 family comprises of three homologs: miR-125b1, -125b2 and -125a. Both miR-125b1 (on chromosome 11q23) and -125b2 (on chromosome 21q21) genes produce identical mature miR-125b. The miR-125a gene is located on chromosome 19q13.41, within a cluster also containing miR-99b and let-7e [59, 139].

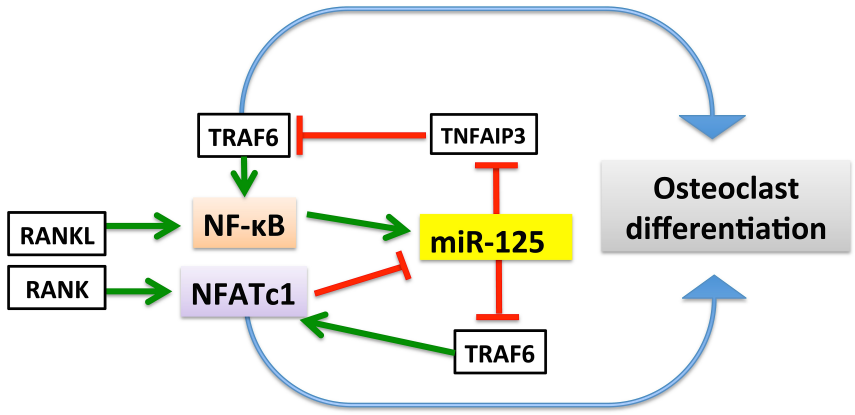

Figure 1.8 Potential model for miR-125a role in osteoclasts. miR-125a may fine tune osteoclast differentiation by regulating NF-κB and NFATc1 signaling. miR-125a has a feed forward regulatory mechanism with the NF-κB pathway, while it shares a feed back loop with NFATc1 signaling. miR-125a directly targets TRAF6 and TNFAIP3 genes crucial for both the signaling pathways.

In bone, miR-125a plays a crucial role in osteoclastogenesis. Upon RANKL stimulation, the p65 subunit of NF-κB has been shown to bind near the transcription start site of miR-125a

gene cluster, resulting in its upregulated expression [138, 140]. As discussed above, miR-125a negatively regulates NF-κB signaling by targeting the TRAF6 gene, thereby indicating a feedback mechanism [141]. Moreover, NFATc1, a transcription factor crucial for osteoclastogenesis, has been shown to repress miR-125a expression [141]. These data suggest that miR-125a levels are stringently regulated in osteoclasts, and may fine-tune differentiation. Impairment in miR-125a levels due to pri-miR-SNPs could modulate osteoclastogenesis and disrupt the balance in bone remodeling.

The other member of miR-125 family, miR-125b, has been shown to act as a negative regulator of osteoblastic differentiation by targeting the Cbf (core-binding factor) family members Cbf β and Runx2 [142]. miR-125b levels plummet in response to BMP 2/4 induced osteoblast differentiation [142, 143]. In congruence with its negative role, increased miR-125b levels were detected in serum and bone samples of osteoporotic patients [144]. miR-125b has been shown to confer protection against OA by directly targeting cartilage degrading enzyme aggrecanase-1 (ADAMTS-4). Reportedly, IL-1β suppresses miR-125b levels and upregulates aggrecanase-1 expression in OA chondrocytes [145].

Although 6 polymorphisms in pri-miR-125a (rs41275794, rs12975333, rs12976445, rs10404453, rs78758318, rs143525573) have been reported, only one of these (rs12975333) has been shown to be functional. In contrast, the miR-TS-SNP (rs1434536) in miR-125b binding site of BMPR-IB, discussed above, has been shown to have a dramatic effect on gene expression and disease progression [59, 146-149]. Given the function of the miR-125 family in both the

osteoblast and osteoclast lineage, it is of interest to determine whether these validated SNPs display any association with BMD.

miR-196a2:

The miR-196 family consists of 3 members, miR-196a1, -196a2, and -196b that are embedded in the highly conserved clusters of Hox (homeobox) genes. Located on chromosome 17, the miR-196a1 gene is lies within the Hoxb cluster, miR-196a2 lies on chromosome 12 within the Hoxc cluster, and miR-196b gene lies within the Hoxa cluster on chromosome 7. miR-196 isoforms show a high level of identity. Mature miR-196a isoforms are identical, while the mature miR-196b differs by a single base from the -196a isoforms. This sequence similarity suggests that they target same panel of mRNAs.

Hox genes regulate skeletal patterning and limb development by coordinating signaling pathways including, retinoic acid, BMP and TGF-β signaling [150, 151]. It is known that miR-196 family members play a crucial role in development of the axial skeleton, by regulating Hox genes (Hoxb8, Hoxc8, Hoxd8, Hoxa7), fine-tuning levels of HOX proteins in a temporal and spacial manner [152, 153]. miR-196a promotes commitment of mesenchymal stem cells (MSCs) towards the osteoblast lineage by targeting Hoxc8 [154, 155]. In osteoblasts, Hoxc8 acts as a negative regulator of differentiation and transcriptionally suppresses osteopontin (OPN). In turn, BMP signaling represses Hoxc8 activity through SMAD1 interaction with Hoxc8, and relieves repression on OPN transcription [156-158]. In addition to Hoxc8, miR-196a has also been shown to target Hoxb7 in MSCs. Over-expression of Hoxb7 has been shown to enhance the proliferative and osteogenic capacity of MSCs. In aging MSCs, an inverse correlation between

the levels of miR-196a and Hoxb7 were attributed to decreased osteogenic differentiation [155, 159].

Two miR-196a2 promoter region SNPs (rs35010275 and rs12304647) and one SNP in the pre-miRNA (rs11614913) have been studied in gastric cancer cohorts [160, 161]. Of these, miR-P-SNP rs35010275 (G>C; MAF 0.28 in 1000 Genomes Project), mapped within 1 kb of the miR-196a2 transcription start site, has been associated with gastric cancer risk in a Chinese population [160]. High levels of miR-196a detected in these patients were linked to the risk-associated allelic variant (G). Functional analyses indicated that rs35010275 modulated the interaction of nuclear proteins with DNA, leading to differences in miR-196a levels. Although the transcription factor complexes interacting with the SNP rs35010275 region were not identified, this study nicely demonstrates that the allele-specific differences in promoter region of a miRNA gene can alter promoter activity and modulate miRNA expression [160].

Another variant in the miR-196a2 precursor rs11614913 (C>T MAF 0.334 in 1000 Genomes Project) was associated with breast cancer risk [162]. Specifically, the T-allele was associated with decreased cancer risk and low miR-196a levels. Functional analysis revealed that the T variant leads to decreased mature miR-196a without affecting the pre-miR-196a2 levels, thereby indicating a miRNA processing defect [162]. Since Hox genes play a critical role in bone and cartilage, these common miR-196a variants may have an impact on skeletal phenotype.

miR-149:

The region encoding human miR-149 has been mapped to intron 1 of the glypican1 (GPC1) gene. This highly conserved miRNA is expressed independent of its host gene in a wide variety of non-skeletal tissues [163]. In the skeleton, expression of miR-149 has only been reported in chondrocytes, where it is upregulated in the presence of inflammatory cytokines IL-1β, IL-6 and TNFα. Furthermore, miR-149 has been shown to directly target these inflammatory cytokines in a feedback loop. In OA, dramatically decreased miR-149 expression has been suggested to exacerbate the inflammatory response [164, 165].

So far two SNPs have been mapped to pre-miR-149 at rs2292832 (C>T MAF 0.387 in 1000 Genomes Project), and rs71428439 (A>G MAF 0.144 in 1000 Genomes Project). Although the association of rs2292832 with cancer risk has been extensively studied, newer meta-analyses do not suggest an association between this SNP and cancer risk, and functional evidence for rs2292832 is lacking [166, 167].

In contrast, the mechanism for a SNP-mediated effect on gene regulation has been elegantly described for rs71428439 in the context of myocardial infarction (MI). Specifically, the risk associated variant rs71428439-G has been linked to decreased miR-149 expression. The SNP was predicted to alter the secondary structure of the pre-miR, yielding a less stable pre-miR-149-G. Functional analysis revealed that rs71428439-G modulates the pre- to mature miR processing, resulting in low levels of miR-149. In addition to defining mechanism, this study was unique in that it demonstrated the impact of rs71428439 on MI susceptibility in vivo. In a mouse model of MI, the infarct size and myocyte apoptosis was low in mice injected with precursor for

the miR-149- rs71428439-A variant, assigning a protective function against MI to rs71428439-A. This SNP is a common variant, and since miR-149 targets inflammatory cytokines, an association between this SNP and OA phenotype might be likely.

miR-27a:

The human miR-27 family comprises of two family members miR-27a and b. miR-27a is transcribed within a cluster on chromosome 19 that also contains miR-23a and miR-24-2, while miR-27b is transcribed in cluster on chromosome 9 with miR-23b, miR-3074 and miR-24-1. The mature miR-27a and b differ by only one nucleotide.

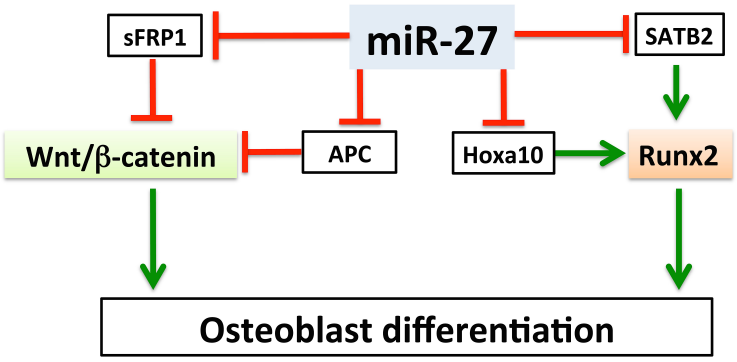

Figure 1.9 Potential model for miR-27a role in osteoblasts. miR-27 fine tunes osteoblast differentiation by positively regulating canonical Wnt signaling and negatively regulating Runx2 activation. miR-27a targets inhibitors of canonical Wnt pathway, APC and sFRP1, as well as promoters of Runx2 activity, SATB2 and Hoxa10.

In bone, miR-27 expression was reported to increase during osteoblastic differentiation in vitro. The miR-27 family promotes osteoblastogenesis by directly targeting and suppressing expression of inhibitors of Wnt/β-catenin signaling, sFRP1 (soluble frizzled related protein 1)

and APC (adenomatous polyposis coli) [126, 127]. Moreover, Runx2 binding sites were identified upstream of the transcription start site for the miR-27a cluster, where Runx2 negatively regulates its transcription. The miR-27a~miR-23a~miR-24-2 cluster was shown to target SATB2, which interacts with Runx2 to promote bone formation. Inhibition of the miR-27a~miR-23a~miR-24-2 cluster by Runx2 establishes a positive feedback loop [168]. In addition, miR-27a has been shown to target Hoxa10, which promotes osteoblast differentiation through Runx2-dependent and –independent mechanisms [169]. This provides another potential mechanism for the pro-osteoblastic effects of miR-27a repression.

So far two SNPs have been reported in pre-miR-27a at rs895819 (A>G MAF 0.364 in 1000 Genomes Project) and rs11671784 (G>A MAF 0.007 in 1000 Genomes Project). Notably, G variant of rs895819 has been associated with decreased risk of breast, renal and nasopharyngeal cancer [170]. The G variant was shown to aberrantly increase miR-27 expression in colorectal cancer, although the subsequent mechanism of SNP action was not validated [171]. Recent studies linking rs11671784 (G>A) to gastric cancer risk have elegantly demonstrated that the SNP impaired miRNA biogenesis. The risk associated allele rs11671784-G was shown to result in an aberrant processing of pre-miRNA leading to increase mature miR-27 levels. Subsequent increase in gastric tumorigencity associated with G variant was attributed to decreased expression of miR-27 target gene Hoxa10 [172].

miR-124:

Mature miR-124 arises from three different pri-miR structures encoded by independent genes. Genes encoding miR-124-1 and miR-124-2 have been mapped to chromosome 8, while

miR-124-3 gene is located on chromosome 20. Mature miR-124 is evolutionarily conserved and highly expressed by neurons in brain [173]. In the skeleton miR-124 is expressed by both osteoblasts and osteoclasts [174, 175]. In osteoblasts, miR-124 expression decreases during differentiation and it negatively regulates osteoblast formation by targeting Dlx2, Dlx3 and Dlx5 genes that are critical for osteogenic commitment [175]. Notably, miR-124 has also been shown to suppress expression of chondrocyte marker genes like Sox9 and Aggrecan [176]. In contrast, miR-124 has been shown to increase dramatically during commitment of human mesenchymal stem cells to adipocyte lineage [175]. Thus, miR-124 may promote adipogenic differentiation at the expense of commitment to the osteo-chondral lineage. Interestingly miR-124 also suppresses osteoclastogenesis by targeting NFATc1, key transcription factor in osteoclasts; it also reduces osteoclast precursor proliferation and motility by targeting integrin B1 (ITGB1), RhoA and Rac1 [174]. In a rat inflammatory arthritis model, miR-124 injection was shown to ameliorate progression of the arthritic lesion by decreasing osteoclast formation [177].

Polymorphism rs531564 (G>C MAF 0.130 in 1000 Genomes Project) was detected in pri-miR-124-1 in a case-control Alzheimer's disease (AD) study. Although the SNP was not linked to AD, the study showed that pri-miR-124-1 rs531564–G variant led to decreased mature miRNA levels, likely due to alteration of pri-miR secondary structure [178]. Since rs531564 is a common variant, and because miR-124 impacts both osteoblast and osteoclast differentiation and function, it will be of interest to determine whether this SNP might be associated with bone phenotype.

Implication of miRNA associated variants in skeletal diseases

The relationship of genetic variations or mutations affecting miRNAs on skeletal disease risk and pathogenesis has only begun to be explored. As of today, there are only a handful studies demonstrating the role of miR-SNPs and miR-TS-SNPs in skeletal diseases such as osteoporosis and chondrodysplasia.

Osteoporosis is characterized by low BMD and increased fragility, [52]. Predisposition to osteoporosis partly depends on BMD accrual, which is highly influenced by genetics [52, 179]. One recent study associated a miR-TS-SNP, rs6854081 T>G (MAF 0.0855 in 1000 Genomes Project) located in the 3' UTR of FGF-2 (fibroblast growth factor 2) with BMD in a cohort of middle-aged Caucasian women. Using the poly-miRTS database, SNP rs6854081was shown to potentially interfere with miR-146a and -146b binding to FGF-2 [180]. FGF-2 is a potent mitogenic growth factor that is widely expressed in limb bud mesenchyme, chondrocytes, osteoblasts, osteoclasts and adipocytes. In osteoblasts, FGF-2 positively regulates osteoblast differentiation partly via Wnt signaling, and its absence leads to decreased bone mass [181-183]. Moreover, sustained FGF-2 signaling can also inhibit bone formation by maintaining osteoblastic precursors in a proliferative state, thereby preventing their differentiation [181, 182, 184]. In osteoclasts, FGF-2 also promotes recruitment of osteoclast precursors and their differentiation [182, 183, 185].

The minor allele of rs6854081 (G) was associated with low BMD, and higher FGF-2 levels were observed in the low BMD patients compared high BMD subjects [180]. It was

speculated that rs6854081G might relieve translational suppression of FGF-2, leading to increased FGF2 levels and enhanced osteoclastogenesis. In this study, FGF2 was not experimentally validated as a target of miR-146a and b, and it is possible that other miRNAs could be involved. However, this study did report a FGF2 3' UTR SNP and provided an implication for the role of miR-TS-SNPs in mediating variations in BMD [180].

Interesting, another miR-TS-SNP rs1054204 C>G (MAF 0.387 in 1000 Genomes Project), identified in the 3' UTR of non-collagen extracellular matrix protein osteonectin (SPARC), was recently associated with idiopathic osteoporosis [186, 187]. Using a novel set of mouse knock-in models, the minor allelic variant rs1054204-G was shown to contribute decreased levels of osteonectin, decreased trabecular bone volume, and a reduced bone-anabolic response to intermittent PTH1-34 treatment [186, 187]. Moreover, in vitro studies demonstrated a cell-autonomous effect of the variant on osteoblastic differentiation and mineralized matrix production. In bone, osteonectin facilitates collagen fibril assembly and promotes osteoblast commitment, differentiation, and survival [188, 189]. Global deficiency of osteonectin leads to development of low turnover osteopenia, with decreased bone formation [190]. The minor allelic variant rs1054204-G was shown to enhance osteonectin post-transcriptional regulation by creating a novel miR-433 target site in its 3'UTR [187]. Overall, this study provided a physiological function to a common miR-TS-SNP [187]. Other studies demonstrated that miR-433 can inhibit osteoblast differentiation and target Runx2 [187, 191].

Another novel study associated a mutation in pre-miR-2861 with osteoporosis in one kindred. miR-2861 is transcribed in a cluster with miR-3960, and this locus is found at

chromosome 9q34.11. In bone, miR-2861 is expressed by bone marrow mesenchymal precursors and osteoblasts; osteoclasts do not express miR-2861. During osteoblastic differentiation, BMP2 was shown to upregulate the miR-3960/2861 cluster and miR-2861 positively regulates osteoblast differentiation [192]. In a mouse model, downregulation of miR-2861 expression by systemic administration of a specific miRNA inhibitor decreased bone mass and osteoblast activity [193]. Remarkably, miR-2861 was shown to target HDAC5. In bone, HDAC5 is known to deacetylate Runx2, promoting its ubiquitin-mediated degradation. Thus, miR-2861 mediated inhibition of HDAC5 increases Runx2 acetylation and induces BMP2 stimulated osteoblast differentiation and function [194]. Moreover, subsequent studies revealed a positive feedback loop between Runx2 and the miR-2861 cluster, induced with BMP2 mediated osteogenesis [192].

Functional analyses revealed that the mutation in the osteopenic kindred mapped to the leading strand in the stem of pre-miR-2861, which caused decreased mature miRNA levels due to reduced miRNA processing. High levels of the miR-2861 target gene HDAC5 were attributed to decreased Runx2 protein in the bones of these patients. Although expansion of the linkage study to include unrelated osteoporotic patients and healthy controls did not reveal the presence of pre-miR-2861 mutations in either groups, this study highlights a functional miR-SNP variant with a profound impact on bone mass [193].

Another mutation that affects miRNA-mediated regulation was recently identified in X-linked Chondrodysplasia. Chondrodysplasias are genetic disorders of bone and cartilage, and can be caused by defects in the differentiation and proliferation of chondrocytes or in the

extracellular matrix of the cartilage. Phenotypically, this disorder is associated with platyspondyly (flattening of vertebral bodies along the axial skeleton), rhizomelia (shortening of femur and/or humerus), specific brachydactyly, hydrocephaly, facial dysmorphism and microphtalmia. X-linked chondrodysplasias represent irregularities that are more prevalent and severe in males [195]. A linkage study using X-linked polymorphic microsatellite markers mapped the disease locus for X-linked chondrodysplasia to a pericentromeric region within Xp11.3–q13.1 (Lod score = 3.30). The HDAC 6 gene was hypothesized to be a candidate gene in this locus, and exon sequencing revealed a variant (c.*281A>T) in the HDAC6 3' UTR [196].

In osteoblasts, HDAC6 is known to promote Runx2 activity by deacetylating and decreasing transcription of the Runx2 repressor, $p21^{WAF1}$ in pre-osteoblasts [197]. In articular chondrocytes, primary cilia that respond to mechanical strain regulate hedgehog signaling and indirectly decrease transcription of cartilage degrading enzymes (ADAMTS5, MMPs). Recent findings suggest that aberrant activation of hedgehog signaling in osteoarthritis can be suppressed by HDAC6-mediated disassembly of the primary cilium [198]. The HDAC6 variant (c.*281A>T) was localized to a miR-433 seed binding region in the 3' UTR, and was shown to interfere with miR-433 targeting. It is likely that upregulated HDAC6 may indirectly inhibit hedgehog signaling and lead to phenotypic defects of chondrodysplasias. Altogether, this study had demonstrated that HDAC6 3' UTR variant suppressed miR-433 mediated post-transcriptional regulation, causing overexpression of HDAC6 that could contribute to X-linked chondrodysplasia [196].

Table 1.1 Genetic variants associated with miRNAs					
	miRNAs	**SNP #**	**Alleles**	**Description**	**Reference**
miR-P-SNPs	miR-146a	rs57095329	A>G	G-decreased miR levels; TFBS modification	[101]
	miR-196a-2	rs35010275	G>C	C- decreased miR levels; TFBS modification	[160]
miR-SNPs	***Pri-miR***				
	miR-125a	rs12975333	G>T	T-decreased miR levels; DGCR8 binding	[59]
	miR-124	rs 531564	G>C	G-decreased miR levels	[178]
	Pre-miR				
	miR-146a	rs2910164	G>C	G-increased miR levels; stable alternative passenger strands	[107, 108]
	miR-196a-2	rs11614913	C>T	T-reduced miR levels	[162]
	miR-149	rs71428439	A>G	G-reduced miR levels	[199]
	miR-27a	rs11671784	G>A	G-reduced miR levels	[172]
	miR-2861 *	mutation	C>G	G-reduced miR levels	[193]
	mature-miR				
	miR-125a	rs12975333	G>T	T- impairs miR binding to lin-28	[59], [147]
miR-TS-SNPs	BMPR-IB	rs1434536	C>T	T-loss of miR-125b binding site	[122]
	FGF-2	rs6854081	T>G	G-loss of miR-146a, -b binding site	[180]
	SPARC	rs1054204	C>G	G-creates miR-433 binding site	[187]
	HDAC6 *	mutation	A>T	T-loss of miR-433 binding site	[196]

Conclusions

A growing number of GWAS have associated genomic loci with BMD and fracture risk. Within these intervals, SNPs in protein coding regions as well as UTRs and miRNA genes should be considered for functional validation. To date, only a limited number of studies have identified SNPs or mutations in miRNA genes and target binding sites relevant to BMD. However, miR-associated SNPs (miR-P-SNPs, miR-SNPs and miR-TS-SNPs) validated in other disease models have potential to inform studies of SNPs and bone mass. In particular, data on functional miR-associated SNPs (collated from other diseases), along with miRNA-target co-expression information and quantitative trait locus (QTL) mapping could provide some direction for investigation of miR-SNPs with the potential for relevance in skeletal diseases. Moreover, newer sophisticated bioinformatic tools such as Patrocles and PolymiRTS can be used in conjunction with existing GWAS data to determine whether a polymorphism of interest might also be miR-TS-SNPs. Given the polygenic nature of skeletal diseases like osteoporosis, addition of such miRNA-associated SNPs to the pool of existing BMD-associated SNPs could enhance the prognostic potential, if functionally validated.

However, the majority of SNP variants are likely to have a small impact on BMD. In addition to genetics, factors including age, lifestyle, hormonal status and co-morbidities can greatly influence the risk for fracture. Assigning a function to miR-SNPs requires in vitro studies, whereas assigning a physiological function to such SNPs could require in vivo mouse models in which the influence of other, non-genetic factors impacting bone mass can be minimized. The increased usage of genome editing technology, such as the CrispR-Cas9 system,

for the generation of novel mouse models will likely be instrumental in driving this field forward. However, to advance clinical application, it will be crucial to analyze functional miR-associated SNPs in larger and ethnically diverse populations. Moreover, it will likely be necessary to examine a large number of SNPs to achieve a significant enrichment in fracture prediction, compared with the prediction tools currently used. Nonetheless, it is a goal worth pursuing, as the studies performed will provide key insights into the function of miRNAs in skeletal tissue.

We summarized the mechanisms for miR-associated SNP regulation of miRNA function, and provided evidence suggesting of potential impact that variants of several miRNAs might have in regulating skeletal phenotype (Table 1.1). Lastly, we summarized the current findings of known miR-associated SNPs or mutations in skeletal diseases. miRNA based therapeutics are in clinical trials for selected malignancies, and the development of novel miRNA-based therapeutics for bone repair and regeneration is underway. Information on miRNA function in bone and cartilage, as well as information on genetic variants affecting miRNA function could help the clinicians develop a better plan for individualized treatment as well as predict the impact of drug efficacy, adverse reactions or toxicity along with disease risk.

CHAPTER 2

Research Aims and Hypotheses

High throughput approaches such as gene expression microarray or RNA sequencing have provided a wealth of information on how miRNA expression profiles change during the course of bone cell differentiation. However, an understanding of miRNA function in the osteoblasts or osteoclasts differentiation program remains largely undefined. Moreover, although it is appreciated that single nucleotide polymorphisms (SNPs) can affect miRNA function, the impact of such variants on skeletal phenotype is unknown. The overall goal of our studies is to understand how specific miRNAs in regulate osteoblast and osteoclast differentiation and function. Specifically, 1) we demonstrate that SNP in the human osteonectin 3' UTR leads to differential miR-433 targeting and regulates bone volume, 2) we identify the function of miR-365 and miR-99b in osteoclastogenesis

Chapter 3: Specific Aim1

Previously, osteonectin 3' UTR haplotypes that differed only at SNP 1599 (rs1054204) were associated with bone mass in a cohort of patients with idiopathic osteoporosis [186]. We hypothesized that SNP 1599 in the osteonectin 3' UTR leads to differential miRNA targeting and regulates bone volume. To test this hypothesis, we proposed the following aims:

(I) To determine whether SNP 1599 modulates osteonectin expression.

3’ UTR reporter constructs representing 2 SNP 1599 haplotypes will be transfected in hFOB1.19 cells (human fetal osteoblasts cell line) and the effect of SNP 1599 on osteonectin 3’ UTR function will be examined using luciferase 3’ UTR reporter assays. The effect of SNP 1599 on osteonectin expression in bone will be examined in human osteonectin 3’ UTR knock-in mice, by qRT-PCR and Western blotting.

(II) To determine whether SNP 1599 affects miR-433 regulation of the osteonectin 3’ UTR.

Using a computational approach and luciferase 3’ UTR reporter constructs, we will examine if SNP 1599 leads to differential targeting of osteonectin by miR-433. We will also examine the regulation and function of miR-433 in osteoblast differentiation by qRT-PCR and loss function studies.

(III) To examine the impact of SNP 1599 on bone volume.

Using microCT and histomorphometry, the effect SNP 1599 on bone volume will be examined in femurs of osteonectin 3’ UTR knock-in mice. The effect of SNP 1599 on osteoblast differentiation and mineralization will be examined in bone marrow stromal cell cultures derived from osteonectin 3’ UTR knock-in mice. Furthermore, the effect of SNP 1599 on intermittent parathyroid hormone (PTH) induced bone anabolic changes were monitored by microCT and histomorphometry.

Chapter 4: Specific Aim 2

Previously, we performed a microarray study examining the miRNA expression profile during osteoclastogenesis in an enriched population of murine osteoclast precursors. This study

suggested that expression of miR-365-3p, and -99b was highly upregulated in differentiating osteoclasts, while miR-451 levels were downregulated [138]. We proposed the following aims to validate the expression of these miRNAs and examine their function in osteoclast formation.

(I) To determine function of miR-356-3p, miR-99b-5p and miR-451 in osteoclasts.

Using qRT-PCR, the expression pattern of miR-365-3p, miR-99b-5p and miR-451 will be validated during early, middle, and late stages of osteoclastogenesis in cultures of murine osteoclast progenitors enriched by depletion of $B220^+$ and $CD3^+$ lymphocytes. RANKL induced expression of these miRNAs will be determined in primary murine osteoclast progenitors and RAW264.7 cells (monocytic cell line). Function of these miRNAs in osteoclast differentiation will be examined by TRAP staining osteoclasts obtained from the differentiation of primary murine bone marrow monocyte cultures transfected with specific miRNA inhibitors or mimics.

(II) To identify miRNA targets in osteoclasts.

Using computational prediction tools, a panel of genes potentially targeted by miR-365-3p and miR-99b in osteoclasts will be assembled. In order to identify miRNA targets in an unbiased manner we will optimize a RISC-RNA co-immunoprecipitation protocol for osteoblastic and osteoclastic cells.

Together, these studies will expand our understanding of role of miRNAs in osteoblasts and osteoclasts, and provide a how comprehensive view on how modulation in miRNA regulation can impact bone phenotype.

CHAPTER 3

A single nucleotide polymorphism in osteonectin 3' untranslated region regulates bone volume and is targeted by miR-433

Neha S. Dole, M.S.[1], Kristina Kapinas, Ph.D. [1],Catherine B. Kessler, B.S.[1], Siu-Pok Yee, Ph.D.[2], Douglas J. Adams, Ph.D.[3], Renata C. Pereira, Ph.D.[4], and Anne M. Delany, Ph.D.[1]

[1]Center for Molecular Medicine, [2]Gene Targeting and Transgenic Facility, [3]Department of Orthopaedic Surgery, University of Connecticut Health Center, Farmington, CT, U.S.A.;

[4] Mattel Children's Hospital, University of California, Los Angeles, CA, U.S.A.

Abstract

Osteonectin/SPARC is one of the most abundant non-collagenous extracellular matrix proteins in bone, regulating collagen fiber assembly and promoting osteoblast differentiation. Osteonectin-null and –haploinsufficient mice have low turnover osteopenia, indicating that osteonectin contributes to normal bone formation. In male idiopathic osteoporosis patients, osteonectin 3' UTR single nucleotide polymorphism (SNP) haplotypes that differed only at SNP1599 (rs1054204) were previously associated with bone mass. Haplotype A (containing SNP1599G) was more frequent in severely affected patients, whereas haplotype B (containing SNP1599C) was more frequent in less affected patients and healthy controls. We hypothesized that SNP1599 contributes to variability in bone mass by modulating osteonectin levels. Osteonectin 3' UTR reporter constructs demonstrated that haplotype A has a repressive effect on

gene expression compared to B. We found that SNP1599G contributed to a miR-433 binding site and miR-433 inhibitor relieved repression of the haplotype A, but not B, 3' UTR reporter construct.

We tested our hypothesis in vivo, using a knock-in approach to replace the mouse osteonectin 3' UTR with human haplotype A or B 3' UTR. Compared to haplotype A mice, bone osteonectin levels were higher in haplotype B mice. B mice displayed higher bone formation rate and gained more trabecular bone with age. When parathyroid hormone was administered intermittently, haplotype B mice gained more cortical bone area than haplotype A mice. Cultured marrow stromal cells from B mice deposited more mineralized matrix and had higher osteocalcin mRNA compared with A mice, demonstrating a cell-autonomous effect on differentiation. Altogether, SNP1599 differentially regulates osteonectin expression and contributes to variability in bone mass, by a mechanism that may involve differential targeting by miR-433. This work validates the findings of the previous candidate gene study, and it assigns a physiological function to a common osteonectin allele, providing support for its role in the complex trait of skeletal phenotype.

Introduction

Osteoporosis is a prevalent disorder characterized by low bone mineral density (BMD), deterioration of bone microarchitecture and increased incidence of fracture [200]; and genetic factors account for 60-80% of total variability in BMD [179]. Understanding the genetic determinants underlying bone mass may improve prognosis and provide novel targets for therapeutic intervention. In this regard, genome wide association studies (GWAS) and candidate

gene studies have associated allelic variants of genes such as estrogen receptor (ER)-α, transforming growth factor (TGF)-β, osteoprotegerin, and type I collagen A1 with bone mass [201-205]. However, only a few studies have demonstrated a mechanism whereby a polymorphism could contribute to bone mass phenotype. Indeed, a previous GWAS study in premenopausal women linked variations in BMD to genomic regions including 5q33-35 [206]. Although candidate genes in the 5q33-35 interval were not identified, this region contains the gene for osteonectin/Sparc (secreted protein acidic and rich in cysteine), one of the most abundant non-collagenous extracellular matrix proteins in bone. In osteoblasts, osteonectin promotes commitment, differentiation, and survival. Osteonectin also suppresses adipogenic differentiation of mesenchymal precursor cells. In vivo, osteonectin-null and –haploinsufficient mice develop low turnover osteopenia, characterized by reduced osteoblast and osteoclast number and surface, and low bone formation rate [188, 189, 207, 208]. Moreover, osteonectin-null mice accumulate less bone in response to intermittent administration of parathyroid hormone (PTH), the best bone-anabolic treatment clinically available at this time [208].

Based on these findings, we had previously performed a candidate gene study, to determine whether 3 single nucleotide polymorphisms (SNPs) in the 3' untranslated region (UTR) of osteonectin (Figure 3.1A) were associated with bone mass in a cohort of men with low turnover idiopathic osteoporosis, a disorder primarily attributed to genetic determinants [186]. Briefly, this cohort consisted of middle-aged Caucasian men with a BMD T score of less than -2.0 at the lumbar spine, who lacked known secondary causes for osteoporosis. The control subjects were age and body mass index matched to the patients, and had BMD T scores of more than 1.0 at the lumbar spine. As a group, the idiopathic osteoporosis patients had mean serum

PTH and IGF1 levels in the low normal range. Their indices of bone formation were significantly reduced, although eroded surface was not different between patients and their matched controls [209, 210]. In the osteoporotic cohort, prevalence of fragility fracture was 23% [186].

In this cohort, one of the two most common osteonectin 3' UTR haplotypes that we identified, haplotype A, was found at a higher frequency in the most severely affected osteoporotic patients, whereas the second most common haplotype, B, was found at a higher frequency in the healthy controls. In addition, haplotype B was associated with higher BMD in the patient population [186]. Osteonectin 3' UTR haplotype A contained the SNPs at cDNA bases 1046C_1599G_1970T, whereas haplotype B consisted of SNPs 1046C_1599C_1970T (Figure 3.1A). Since these BMD associated haplotypes differed only at cDNA base 1599, we hypothesized that SNP 1599 C>G (rs1054204) may impact osteonectin expression, and affect bone mass. The 3' UTR represents a powerful regulatory region, with the potential to modulate mRNA stability, translation and localization [211]. Polymorphisms in the 3' UTR have the potential to alter the secondary structure of the mRNA, as well as its interaction with trans-acting factors, such as microRNAs (miRNAs, miRs). miRNAs are small, endogenous non-coding RNAs that, for the most part, decrease the stability and/or translation of protein-encoding mRNAs. Recent studies have associated mutations or SNPs in miRNA binding with skeletal disorders. For example, a SNP in the 3' UTR of Fgf2 (fibroblast growth factor 2) that abrogates miR-146a and -146b binding sites, was linked to low BMD in osteoporotic patients [180]. Another study attributed a mutation in the binding site for miR-433 in the 3' UTR of Hdac6 (histone deacetylase 6) to the pathogenesis of X-linked chondrodysplasia [196].

In this study we show that human osteonectin SNP1599 differentially regulates gene expression and contributes to a miR-433 binding site. Specifically, 1599G, found in haplotype A, has a repressive effect on gene expression and osteoblastic differentiation compared to 1599C, which is found in haplotype B. Moreover, using novel knock-in mouse models, we demonstrate that compared to mice carrying human osteonectin haplotype A 3' UTR (SNP 1599G), mice with the haplotype B 3' UTR knock-in (SNP 1599C) have higher levels of osteonectin in bone, higher bone formation rate, increased trabecular bone volume with age, and a greater increase in cortical bone volume in response to the bone-anabolic PTH treatment. These data substantiate the relationship between osteonectin 3' UTR SNP 1599 and skeletal phenotype, validate our initial observations in the cohort of idiopathic osteoporosis patients, and suggest that SNP 1599 affects bone mass by modulating osteonectin expression.

Materials and methods

Generation of osteonectin 3' UTR haplotype constructs.

1.1 kb variants of human osteonectin 3' UTR (cDNA bases 1018-2123) representing haplotypes A and B found in idiopathic osteoporosis patients were PCR amplified from genomic DNA using appropriate primer sets (Forward: 5'-ggactagtatccactccttccacagtaccgaa-3' and reverse: 5'-cccaagctttgaaggatttgtgaaactcttcac-3'). Amplified fragments were cloned downstream of the Luciferase gene in pMIR-REPORT vector (Life Technologies) using SpeI and HinDIII restriction enzymes (Invitrogen). Haplotype 3' UTR constructs were confirmed with sequencing.

Cell Culture.

Human fetal osteoblastic 1.19 cell line (hFOB1.19) was purchased from American Type Culture Collection (ATCC number CRL-11372). These cells are homozygous for human osteonectin 3' UTR haplotype C (rs1053411G/C_rs1054204C/C_rs1059279G/G) (our unpublished data). hFOB1.19 cells were grown at 33.5° C in complete medium of 1:1 Dulbecco's modified Eagle's medium (DMEM)/Ham's F-12 medium without phenol red (Invitrogen, Fredrick, MD), supplemented with 10% fetal bovine serum (FBS) (Atlas Biologicals, Fort Collins, CO), 0.3 mg/mL G418/ geneticin (Calbiochem, Gibbstown, NJ), and 1X Penicillin/Streptomycin (Pen/Strep) (Invitrogen). hFOB1.19 cells were differentiated into osteoblasts in vitro by culturing confluent cells at 39.5° C in complete medium supplemented with differentiation cocktail: 100 μg/μL ascorbic acid, 10^{-8} M menadione (vitamin K), 5 mM β-glycerolphosphate (β-GP), and 10^{-7} M 1-25$(OH)_2$-Vitamin D_3 (all from Sigma, St Louis, MO) [212, 213].

Transfection and luciferase activity.

hFOB1.19 cells were seeded in 24-well plates and grown to 80% confluency prior to transfection. Using Fugene6 (Roche, Indianapolis, IN), cells were co-transfected with luciferase-osteonectin 3' UTR constructs (50 ng) and a constitutively expressed β-galactosidase (β-gal) plasmid construct (100 ng), as a control for transfection efficiency (Promega). The ratio of Fugene6 to DNA was optimized to 3:1. 18 hours post-transfection, cells were serum-deprived for 24 hours and lysed using Reporter Lysis Buffer (Promega). Luciferase activity (Luciferase assay system, Promega) was determined and normalized to β-gal activity (Galacton chemiluminescent assay system; Tropix, Bedford, MA). At least 2 different DNA preparations for each construct

were tested. In addition, hFOB1.19 cells were co-transfected with luciferase-haplotype constructs (25ng), β-gal expression plasmid (100ng) and miRNA inhibitors (80nM, Ambion) using X-tremeGENE reagent (X-tremeGENE: nucleic acid ratio 5:1; Roche). A scrambled miRNA inhibitor that does not interact with any known mammalian miRNAs was used as a negative control (Ambion). 18 hours post-transfection cells were serum-starved for 24 hours, lysed, and analyzed as described above. Each experiment was done with 4-6 replicates and at least three independent experiments were performed. Representative experiments are shown.

Generation of osteonectin knock-in mice.

A knock-in strategy was used to replace the mouse osteonectin 3' UTR with human haplotype A or haplotype B 3' UTR. These mouse models were generated at the Gene Targeting and Transgenic Facility (GTTF) at UCHC. Briefly, human osteonectin 3' UTR sequence consisting of the 1 kb 3' UTR, the consensus poly A site, and a G-T rich region was cloned into a mini targeting vector containing a neomycin resistance cassette flanked by lox P sites and mouse homology arms. The mini targeting vector was prepared in pL253 and recombined into a BAC (bacterial artificial chromosome, Children's Hospital Oakland Research Institute; BACPAC Resources Center) [214]. The resultant targeting vector contained 8-10 kb long mouse homology arms that enabled targeted insertion of human 3' UTR into mouse osteonectin gene at exon 10, in 129 embryonic stem cells. Mice with osteonectin haplotype A ($ON^{+/A}$) or haplotype B ($ON^{+/B}$) 3' UTR were crossed with Hprt-Cre transgenic mice, to excise the floxed neomycin cassette. $ON^{+/A}$ and $ON^{+/B}$ mice were back crossed 7 times into C57BL/6J. $ON^{A/B}$ breeding pairs were maintained to generate $ON^{A/A}$ and $ON^{B/B}$ mice for analysis.

Quantitative RT-PCR analysis.

Femurs and tibiae of 6-8 week old $ON^{A/A}$ and $ON^{B/B}$ mice, devoid of marrow, were flash frozen in liquid nitrogen and homogenized. RNA was extracted using miRNeasy mini kit (Qiagen, Valencia, CA). RNA was also isolated from hFOB1.19 cells grown to confluence and differentiated for up to 6 days. All RNAs were subjected to RQ1 DNase I treatment to minimize genomic DNA contamination (Promega, Madison, WI). miR-433 levels were determined using the TaqMan MicroRNA assay (Life Technologies, Grand Island, NY). miRNA levels were normalized to RNU48 (small nuclear RNA) in hFOB cells and to sno202 RNA in mouse BMSCs or bone extracts (recommended endogenous control for mice and human tissue by TaqMan MicroRNA assay).

Table 3.1. Primer sequences used for qPCR analysis.

Gene (m- mouse, h-human)	**Sequence**
h OC (sense)	5'-ACACTCCTCGCCCTATTG-3'
h OC (antisense)	5'-GATGTGGTCAGCCAACTC-3'
h ALP (sense)	5'-AAGAAAGGGGACCCAAGAAA-3'
h ALP (antisense)	5'-GTACTCTCTGCCTGCCCAAG-3'
m OC (sense)	5'-TGGTGCACACCTAGCAGACAC-3'
m OC (antisense)	5'-CCGCGGGCTTGGCATCTGT-3'
m Ibsp (sense)	5′-CGCCACACTTTCCACACTCTC-3′
m Ibsp (antisense)	5′-CTTCCTCGTCGCTTTCCTTCAC-3′

Alkaline phosphatase (ALP), osteocalcin (OC) and bone-sailoprotein (ibsp) mRNA levels were determined using MMLV-Reserve Transcriptase (Invitrogen) and iQSYBR Green Supermix (BioRad) and normalized to 18sRNA. Sequences of primers used of amplification of these genes are mentioned in Table 3.1. Samples were run in a Biorad I-Cycler real time PCR machine under the following conditions: 95°C-3min; 95°C-20s, 55°C-20s, 72°C-20s for 40 cycles. qRT-PCR experiments were performed at least thrice, with N=3 for each experiment, and each sample was analyzed in duplicate. Absolute quantification method was used to quantify the RNA levels. Representative experiments are shown.

Western blot analysis.

Femurs and tibiae were dissected from 6-8 week old male mice. Bones, void of marrow, were snap-frozen in liquid nitrogen, weighed and ground into a powder. Powdered bone (10 mg) samples were resuspended in 0.5 M EDTA pH 7.5, 1x protease inhibitor cocktail buffer and extracted overnight at 4°C. Samples were centrifuged at 13,000 rpm for 30 minutes at 4°C and supernatant, containing solubilized protein, was obtained for Western blot. Protein concentrations were determined by the Bradford assay, and equal amounts were subjected to Western blot analysis using rabbit anti-bovine osteonectin primary antibody (BON-1; gift of L. Fisher, NIDCR, NIH) (1:4000), rabbit anti-β-actin primary antibody (Abcam, 1:1000), and goat anti-rabbit-horseradish peroxidase conjugated secondary antibody (1:20,000) [215]. Bands were visualized by chemiluminescence (Cell Signaling) and relative band densities were determined using Image J software. Bands for osteonectin and β-actin were observed at 37 and 42 kDa respectively. Expression of osteonectin was normalized to β-actin. Bones from 4 mice were used

for each experiment, and data was obtained from 3 independent experiments. Pooled data are shown.

Osteoblast differentiation, mineralization and proliferation analysis.

BMSCs were harvested from femurs and tibiae of 6-8 week old $ON^{A/A}$ and $ON^{B/B}$ male mice and cultured for 6 days in media containing α-MEM and 10% FBS. For osteoblast differentiation cultured cells were re-plated at 275,000 cells/well in a 6-well plate, grown to confluence and differentiated for 2weeks. Differentiation was accomplished in the presence of 5 mM β-GP and 50 μg/ml ascorbic acid; and media was changed every 3 days. Cells was harvested at 1 and 2 weeks of differentiation and processed for RNA. For assessing mineralization, cultured BMSCs were re-plated at 110,000 cells/well in a 12-well plate, grown to confluence and differentiated for 4 weeks. At confluence (week 0) and thereafter at all the differentiation time points (weeks 1, 2, 3, and 4), cells were fixed in 3.7% formaldehyde and then stained with either 1% Alizarin red S pH 6.45 (Sigma) or 0.05% Crystal violet stain (Fisher Scientific). Alizarin red stain was extracted using 10% acetic acid and 10% ammonium hydroxide, and absorbance was quantified at 405nm. Crystal violet stain was extracted using methanol and measured at 570 nm. For proliferation assay, cultured BMSCs were re-plated at 10,000 cells/well density in a 96-well plate in media containing DMEM and 10% FBS. Cell proliferation was assessed over a period of 4 days using MTS CellTiter 96® AQueous One Solution cell proliferation assay kit (Promega, Madison, USA), according to the manufacturer's instructions. The number of metabolically active live cells was quantified at 490nm. Representative experiments are shown.

In vitro PTH treatment.

The effect of PTH on miR-433 expression was examined in vitro. BMSCs harvested from 6-8 weeks old C57/BL6 mice were cultured for 6 days in media containing α-MEM and 10% FBS. Cells were re-plated at 275,000 cells/well in a 6-well plate and grown to confluence. Confluent cultures were treated with 10 ng/ml rhPTH (1-34) (Bachem Torrance, CA) or vehicle alone (0.1% BSA in α-MEM) for 24 hours. Cells were harvested at 3, 6, 12 and 24 hours of treatment and processed for RNA.

To study bone-anabolic response, 10-week old male mice were injected subcutaneously with 40 μg/kg/day rhPTH (1–34) (PTH) (Bachem, Torrance, CA) or vehicle alone (2% heat-inactivated mouse serum in acidified saline), 5 days per week for 4 weeks. Mice received intraperitoneal injections of calcien (10 mg/kg) 10 and 3 days prior to euthanasia. Femurs were dissected and fixed in 70% ethanol [208]. All procedures were approved by the Animal Care Committee of the University of Connecticut Health Center.

MicroCT.

Cortical and trabecular morphometry was measured in femora within the mid-diaphysis and distal metaphysis, respectively, using conebeam micro-focus X-ray computed tomography (μCT40, Scanco Medical AG, Bassersdorf, Switzerland). Serial tomographic volumes were acquired at 55 kV and 145 μA, collecting 1000 projections per rotation at 300 μsec integration time. Three-dimensional 16-bit grayscale images were reconstructed using standard convolution back-projection algorithms with Shepp and Logan filtering, and rendered within a 12.3 mm field of view at a discrete density of 578,704 voxels/mm^3 (isometric 12-μm voxels). Segmentation of

bone from marrow and soft tissue was performed in conjunction with a constrained Gaussian filter to reduce noise, applying hydroxyapatite-equivalent density thresholds of 740 mg/cm^3 and 500 mg/cm^3 for the cortical and trabecular compartments, respectively. Volumetric regions for trabecular analysis were selected within the endosteal borders to include the secondary spongiosa of femoral metaphyses located 960 μm (~6% of length) from the growth plate and extending 1 mm proximally. Trabecular morphometry was characterized by measuring the bone volume fraction (BV/TV), trabecular thickness (Tb.Th), trabecular number (Tb.N), and trabecular spacing (Tb.Sp). Cortical morphometry was quantified within a 600 μm mid-diaphyseal span (50 serial sections) extending distally from the diaphyseal mid-point between proximal and distal growth plates. Cross-sectional measurements included average total (Ta. Ar. Or sub-periosteal) area, marrow area (Ma.Ar.), cortical area (Ct. Ar.) [216, 217].

Histomorphometry.

Undecalcified femurs were embedded in methyl methacrylate. 5 μm thick longitudinal sections were cut on a microtome (Polycut S, Leika Heidelberg, Germany) and stained with toluidine blue (pH 6.4). Static parameters of bone structure, formation and resorption were measured at the distal metaphyses (magnification 400x), 195 μm from the growth plate, in a total of 20 fields using an OsteoMeasure morphometry system (Osteometrics, Atlanta, USA). Dynamic bone parameters were obtained from unstained 10 μm sections examined by fluorescent light microscopy (Nikon, Tokyo, Japan). The mineral apposition rate was expressed in micrometers per day, and bone formation rate was expressed per unit of bone surface. The terminology and units used are those recommended by the Histomorphometry Nomenclature

Committee of the American Society for Bone and Mineral Research [217]. 4-6 mice per group were analyzed.

Statistics.

All the quantitative data are expressed as a mean ± SEM. Statistical significance was determined by one-way ANOVA with Bonferroni post-hoc test or Student's t-test.

Results

SNP 1599 modulates osteonectin 3' UTR function and represses haplotype A 3' UTR.

To determine the role of SNP 1599 in regulating the osteonectin 3' UTR, we cloned the 1 kb osteonectin 3' UTR, representing human haplotype A or B, into a Luciferase reporter construct. In these reporter constructs, the cloned sequence functioned as 3' UTR for the Luciferase gene, the transcription of which was constitutively driven by a strong promoter. The constructs were transiently transfected into hFOB1.19 cells, a conditionally immortalized human osteoblastic cell line. We found that the haplotype A 3' UTR construct had lower luciferase activity compared to haplotype B, suggesting that haplotype A, which was found at a higher frequency in the most severely affected osteoporosis patients, had a more repressive effect on gene expression (Figure 3.1B). These data indicate that SNP 1599 contributed to differences in osteonectin 3' UTR function.

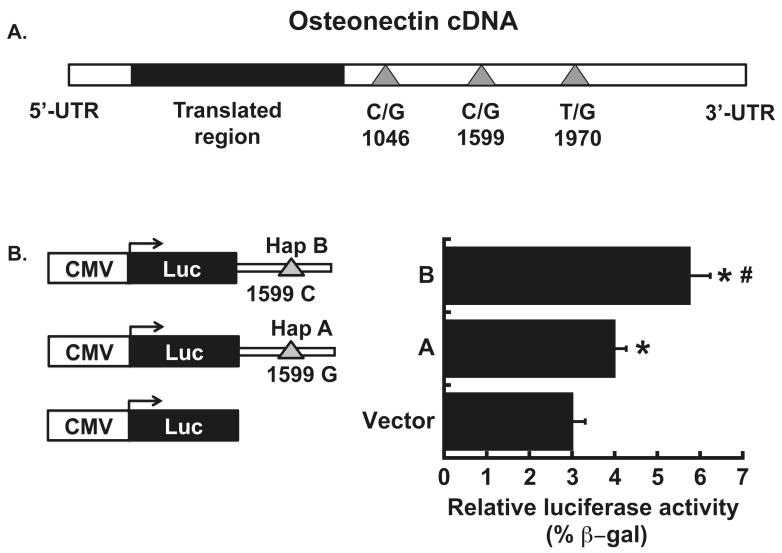

Figure 3.1. Osteonectin 3' UTR SNP 1599 regulates 3' UTR function (A) Schematic representation of the human osteonectin cDNA, and the characterized SNPs at bases 1046, 1599 and 1970 (grey triangles). (B) Human ON 3' UTR (cDNA bases 1018-2123) representing haplotypes A and B were cloned into pMIR-REPORT Luciferase vector. Luciferase activity was quantified in hFOB1.19 cells and normalized to β-galactosidase activity (*$p<0.05$ different from vector; # $p<0.05$ different from haplotype A, N=6).

SNP 1599 introduces a novel miR-433 binding site in haplotype A 3' UTR.

To determine whether miRNAs may mediate the differential regulation of osteonectin by SNP 1599G/C, we used RNAhybrid (http://bibiserv.techfak.uni-bielefeld.de/bibi/Tools.html) and miRbase v15.0 to assemble a panel of candidate miRNAs with the potential to interact with the region containing SNP 1599 [218]. The list of candidate miRNAs was further refined, based on whether or not SNP 1599 would facilitate or disrupt the interaction of the miRNA with the osteonectin 3' UTR. We observed the potential for differential interaction of miR-433-3p, miR-493-5p and miR-374a-3p in presence of 1599G (haplotype A), compared with 1599C (haplotype

B) (Table 3.2). Moreover, these miRNAs are expressed in hFOB1.19 cells. To test the hypothesis that the candidate miRNAs may differentially target haplotypes A and B in vitro, hFOB1.19 cells were transiently co-transfected with either haplotype A or B 3' UTR reporter constructs and inhibitor for miR-433-3p, miR-493-5p or miR-374a-3p. In the presence of miR-433 inhibitor, luciferase activity of the haplotype A construct was significantly increased compared to the non-targeting control, whereas activity of the haplotype B construct was not affected. In contrast, inhibitor for miR-374a-3p or miR-493-5p did not significantly increase luciferase expression from either haplotype A or B constructs (Figure 3.2A and Table 3.2).

Table 3.2. RNAhybrid analysis of putative miR-433, -493 and -374 binding sites in osteonectin 3' UTR. SNP 1599 G/C is indicated by underlined and larger font in the seed binding region of haplotype A or B 3' UTR.

miRNA	Haplotype A – SNP1599G	Haplotype B – SNP1599C
433	target 5′A GAAAGAUUCU G A 3′ ACUGA GGGGCU U**G**UUAUGA UGGCU CCUCGG GUAGUACU miRNA 3′UC A 5′	target 5′A GAAAGAUUCU GU**C** A 3′ ACUGA GGGGCU UUAUGA UGGCU CCUCGG AGUACU miRNA 3′UC GU A 5′
493-5p	target 5′ A AUU GGG U A 3′ GAAAG CU GCUGU**G** UAUGA CUUUC GA UGGUAC AUGUU miRNA 3′ UUA G 5′	target 5′ C AAAG C GG U 3′ UGAGAG AUU UG GC ACUUUC UGG AC UG miRNA 3′ UU GGA U A UU 5′
374a-3p	target 5′ C G C A 3′ U GGG UGU**G**UUAUGA A UCC ACAUAAUAUU miRNA 3′ GUGAAU G A 5′	target 5′ C G C **C** A 3′ U GGG UGU UUAUGA A UCC ACA AAUAUU miRNA 3′ GUGAAU G A U 5′

miR-433 targeting of haplotype A 3' UTR was also evaluated in hFOB1.19 cells using miR-433 mimic and a scramble mimic control. In the presence of miR-433 mimic, haplotype A 3' UTR luciferase activity was inhibited compared to the control, whereas haplotype B 3' UTR activity was not significantly affected (Figure 3.2B). These results suggest that SNP 1599 introduces a novel miR-433 binding site in haplotype A 3' UTR, which may contribute to differential regulation of osteonectin. However, our data do not preclude the possibility that other

miRNAs or trans-acting factors could also demonstrate differential regulation of the haplotype A and B 3' UTRs.

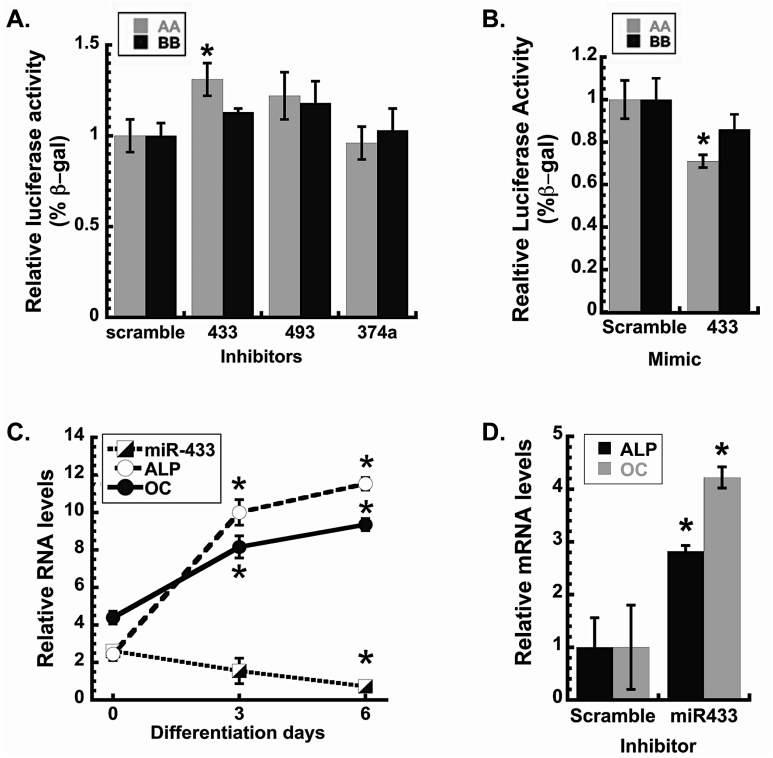

Figure 3.2. miR-433 represses haplotype A 3' UTR, and miR-433 decreases during osteoblastic differentiation, and inhibits differentiation . (A) Luciferase activity of haplotype A and B-3'UTR pMIR-report constructs in hFOB1.19 cells co-transfected with specific miRNA inhibitors or scramble control. Inhibitors for miR-433, -493 and -374a (A) and miR-433 mimic or scramble control mimic (B) were tested; luciferase activity was normalized to β-galactosidase activity (* $p<0.05$ different from scramble control, N=6). (C) miR-433, alkaline phosphatase (ALP) and osteocalcin (OC) RNA in hFOB 1.19 cells at confluence (0), and during osteoblastic differentiation. miR-433 normalized to RNU48; ALP and OC mRNA normalized to 18s RNA (*$p<0.05$ different from confluence, N=3). (D) ALP and OC RNA in hFOB1.19 cells transfected with miR-433 or scramble inhibitor and cultured in osteoblast differentiation medium for 3 days (*$p<0.05$ different from scramble inhibitor, N=3).

miR-433 expression decreases during osteoblastic differentiation.

Since miR-433 could differentially regulate the human osteonectin 3' UTR, we determined whether the expression of this miRNA was altered during osteoblastic differentiation, using hFOB1.19 cells as a model [212, 213]. Osteoblastic differentiation was induced using a vitamin D-containing cocktail, and after 3 or 6 days, mRNAs for the early osteoblastic marker alkaline phosphatase (ALP), and the mature osteoblast marker, osteocalcin (OC), were dramatically increased. In contrast, expression of miR-433 decreased during differentiation, such that miR-433 levels were lowest when osteoblastic differentiation markers were highest (Figure 3.2C). A similar phenomenon was reported by others when miR-433 levels were evaluated in a BMP2-treated murine pre-osteoblast cell line [191]. To determine the role of miR-433 in human osteoblastic differentiation, hFOB1.19 cells were transfected with either a miR-433 inhibitor or a scramble control inhibitor and subjected to osteoblastic differentiation for 3 days. Here, miR-433 inhibitor increased mRNA for the osteoblast markers ALP and OC, compared to the scramble control, confirming that miR-433 is a negative regulator of osteoblast maturation in vitro (Figure 3.2D).

SNP 1599 affects osteonectin expression in vivo.

Many mature miRNAs display sequence conservation across species, and the sequence of mature miR-433 is identical between mouse and human (miRBase). Whereas selected regions of the mouse and human osteonectin 3' UTR are highly conserved, such as the miR-29 binding sites in the proximal portion of the UTR [219], mouse and human osteonectin are not well conserved in the region containing human SNP1599 (UCSD Genome Browser). Therefore, to examine the

impact of SNP 1599 on osteonectin expression in bone in vivo, we used a knock-in strategy to replace the mouse osteonectin 3' UTR with the 1 kb human osteonectin 3' UTR, representing either haplotype A ($ON^{A/A}$) or haplotype B ($ON^{B/B}$) (Figure 3.3A). In relation to other mouse strains, C57Bl/6 mice have a low bone mass phenotype [220, 221].

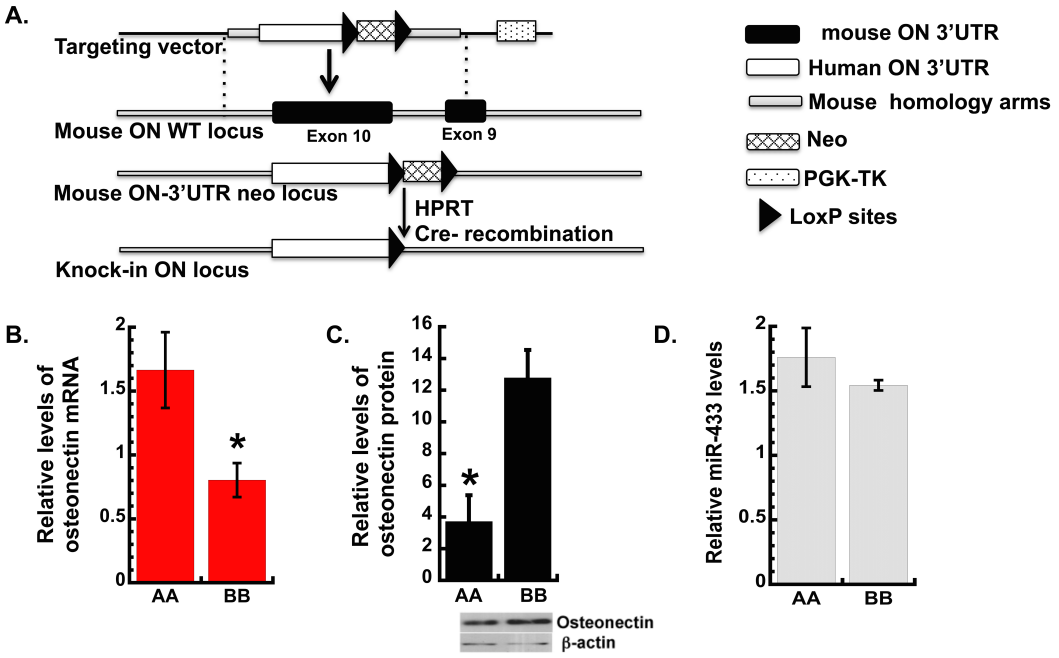

Figure 3.3: Osteonectin protein levels are higher in bone of haplotype B knock-in mice. (A) Schematics shows the strategy for generating haplotype A and B knock-in mice, mouse genome region from exon 10 and a part of intron 9 was replaced with a human osteonectin 3' UTR. (B) Osteonectin mRNA and (D) miR-433 levels was quantified by qRT-PCR using RNA isolated from the femurs of 6-8 week old $ON^{A/A}$ and $ON^{B/B}$ mice. Osteonectin mRNA levels were normalized to 18s RNA, miR-433 levels were normalized to sno202 RNA; (N=4 mice/ haplotype, * $p<0.05$ different from haplotype A). (C) Western blotting for osteonectin and β-actin in lysates from long bones of $ON^{A/A}$ and $ON^{B/B}$ mice (*$p<0.05$ different from haplotype B, N=3 mice/group).

We chose to examine the function of the human osteonectin 3' UTR haplotypes in the C57Bl/6 genetic background because our candidate gene study revealed an association between

osteonectin haplotype and bone mass only in the idiopathic osteoporosis patient group. We reasoned that the effect of the osteonectin 3' UTR haplotype might be most apparent in a low bone mass background, where other gene variants may not be sufficient to rescue a low bone mass phenotype. Moreover, we chose to limit our present analysis to males, to further mimic our previous study in male idiopathic osteoporosis patients.

Osteonectin transcript and protein levels in femur of homozygous haplotype A and B ($ON^{A/A}$ and $ON^{B/B}$) male mice were examined. Western blot analysis of protein extracts demonstrated 2-3 fold lower osteonectin levels in $ON^{A/A}$ femur in comparison to $ON^{B/B}$, indicating that SNP 1599 contributed to differential osteonectin accumulation in bone in vivo (Figure 3.3C). At the same time, qRT-PCR revealed a ~2 fold increase in osteonectin mRNA in femur of $ON^{A/A}$ mice compared with $ON^{B/B}$ (Figure 3.3B), while miR-433 levels were similar (Figure 3.3D). This apparent discrepancy may be related to the fact that the protein data represent the accumulation of osteonectin in bone tissue, whereas the RNA data represent a window of gene expression at 6-8 weeks of age. SNP 1599 affects changes in bone mass with age.

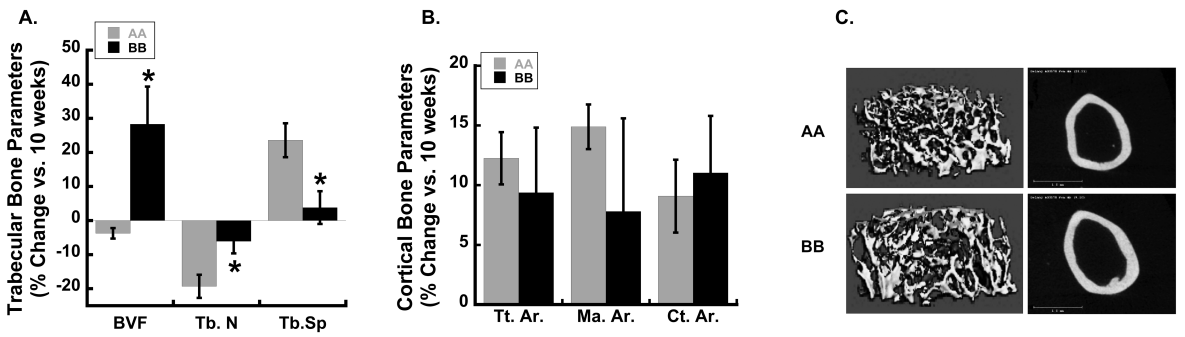

Figure 3.4. Gain in trabecular bone is higher in haplotype B knock-in mice. μCT analysis of changes in femoral bone from 10 to 20 weeks of age in $ON^{A/A}$ and $ON^{B/B}$ mice. (A) Changes in trabecular and (B) cortical bone compartments are shown. Trabecular bone volume (BVF), trabecular bone number (Tb.N) trabecular bone spacing (Tb.Sp.). Total (periosteal) area (Tt.Ar), marrow area (Ma.Ar), cortical area (Ct.Ar). *$p<0.05$ different from haplotype A, N=4-9 mice/group. (C) Representative μCT images from femora of 20 week old mice.

Using μCT, we analyzed the skeletal phenotype of male $ON^{A/A}$ and $ON^{B/B}$ mice at 10 and 20 weeks of age. The femurs of 10-week old mice $ON^{A/A}$ and $ON^{B/B}$ displayed similar trabecular and cortical bone parameters (Table 3.3). At 20 weeks of age, trabecular bone volume and trabecular thickness were significantly higher in $ON^{B/B}$ mice compared with $ON^{A/A}$ (Table 3.3). When the percentage change in trabecular bone parameters between 10 and 20 weeks was examined, the differences between the two genotypes became more apparent (Figure 3.4A and C). For example, between 10 and 20 weeks of age, $ON^{B/B}$ mice realized a 20-25% gain in trabecular bone volume fraction (BVF), while $ON^{A/A}$ mice did not. Trabecular number (Tb.N) decreased with age in both the genotypes, and the decrease was significantly less in $ON^{B/B}$ mice. Trabecular spacing (Tb.Sp.) increased between 10 and 20 weeks of age in $ON^{A/A}$ mice, but not in

$ON^{B/B}$ animals (Figure 3.4A and C).

In contrast, cortical bone area (Ct.Ar.) increased from 10 to 20 weeks of age in both genotypes, to a similar extent (Figure 3.4B and C). This was not unexpected, as the osteonectin-null and haploinsufficient mice display primarily defects in trabecular bone volume [208]. Overall, these data suggest that human osteonectin 3' UTR haplotypes A and B differentially affect the trabecular bone compartment, and that $ON^{B/B}$ gained more trabecular bone with age than $ON^{A/A}$ mice.

Table 3.3. µCT analysis of trabecular and cortical bone parameters in femur of 10-week and 20-week old male $ON^{A/A}$ and $ON^{B/B}$ mice. Trabecular bone volume fraction (BVF), trabecular bone number (Tb.N) trabecular bone spacing (Tb.Sp.) and trabecular thickness (Tb.Th.). Total (periosteal) area (Tt.Ar.), marrow area (Ma.Ar.), cortical area (Ct.Ar.); (10 weeks; N = 4-5 mice per group, 20 weeks; N = 8-9 mice per group) *p<0.05 different from haplotype A.

Trabecular	**AA**		**BB**	
	10 weeks	**20 weeks**	**10 weeks**	**20 weeks**
BVF (%)	12.60±0.01	12.20±0.00	11.70±0.02	14.80±0.01*
Tb.Th.(µm)	45.48±3.72	46.97±1.23	53.06±2.76	55.24±1.89*
Tb.N.(/mm)	5.20±0.33	4.20±0.18	4.47±0.30	4.23±0.14
Tb.Sp.(µm)	192.25±11.97	237.56±9.59	225.06±17.56	232.34±9.46
Cortical	**AA**		**BB**	
	10 weeks	**20 weeks**	**10 weeks**	**20 weeks**
Tt.Ar.(mm^2)	1.96±0.10	2.24±0.04	1.89±0.03	2.062±0.11
Ma.Ar.(mm^2)	1.08±0.04	1.24±0.02	1.00±0.03	1.08±0.08
Ct.Ar.(mm^2)	0.88±0.06	0.96±0.03	0.88±0.02	0.98±0.04

SNP 1599 modifies the bone anabolic effect of intermittent PTH.

Since intermittent administration of PTH is the best bone anabolic therapy currently available, we studied the response of $ON^{A/A}$ and $ON^{B/B}$ mice to this treatment. 10-week old male mice were injected daily with 40 µg/kg PTH (1-34) or vehicle, 5 days per week, for 4 weeks. µCT analysis showed that after 4 weeks of treatment, PTH significantly increased cortical bone area in both $ON^{A/A}$ and $ON^{B/B}$ mice, however the gain in cortical bone in $ON^{B/B}$ mice was nearly twice than that observed in $ON^{A/A}$ mice (Figure 3.5B and C, Table 3.4).

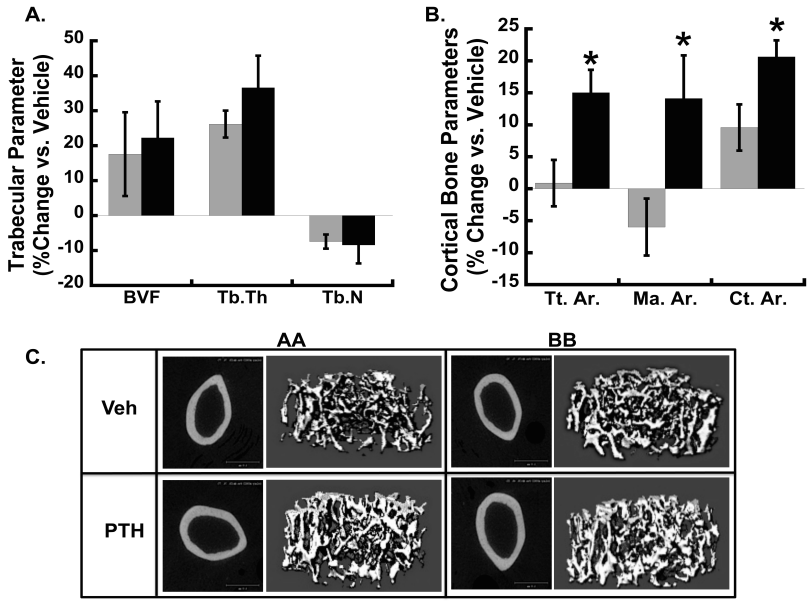

Figure 3.5: PTH induced gain of cortical bone area is greater in haplotype B knock-in mice. µCT analysis of femoral trabecular bone from 14-week old $ON^{A/A}$ and $ON^{B/B}$ mice that had been injected for 4 weeks with 40 µg/kg/day PTH or vehicle. (A) Percent change in trabecular bone parameters vs. vehicle in femur. (B) Percent change in cortical bone parameters vs. vehicle in femur. Trabecular bone volume (BVF), trabecular thickness (Tb.Th), trabecular bone number (Tb.N) Total (periosteal) area (Tt.Ar), marrow area (Ma.Ar), cortical area (Ct.Ar). (C) µCT images of femoral bones of vehicle and PTH treated $ON^{A/A}$ and $ON^{B/B}$ mice.

The PTH mediated increase in the total cross-sectional area (Tt.Ar.) was greater in $ON^{B/B}$ mice compared with $ON^{A/A}$ mice, providing a mechanism for increased cortical bone area. PTH mediated changes in marrow area (Ma.Ar.) did not reach significance (p=0.07) in either genotype (Figure 3.5B and C and Table 3.4). These data indicate that the bone anabolic effect of intermittent PTH was greater in $ON^{B/B}$ mice compared to $ON^{A/A}$. We also assessed changes in the trabecular bone at the femoral metaphysis of PTH or vehicle injected mice using microCT. Although the PTH-mediated increase in trabecular bone volume was not statistically significant, PTH did increase trabecular thickness and number to a similar extent in mice of both genotypes (Figure 3.5A, Table 3.4).

Table 3.4. μCT analyses of trabecular and cortical bone parameters in femur of vehicle and PTH injected $ON^{A/A}$ and $ON^{B/B}$ mice. 14-week old haplotype A and B knock-in mice that had been injected for 4 weeks with 40 μg/kg/day PTH or vehicle. Trabecular bone volume fraction (BVF), trabecular bone number (Tb.N) trabecular bone spacing (Tb.Sp.) and trabecular number (Tb.N.). Total (periosteal) area (Tt.Ar.), marrow area (Ma.Ar.), cortical area (Ct. Ar.). (N=4-6 mice per group) # $p<0.05$ different from corresponding vehicle injected mice of the same genotype. Data is represented as mean ± SEM.

Trabecular	**AA**		**BB**	
	Vehicle	**PTH**	**Vehicle**	**PTH**
BVF (%)	12.00±0.01	14.00±0.01	12.00±0.01	16.00±0.01
Tb.Th.(μm)	47.03±1.16	59.54±1.94#	46.40±2.54	61.65±3.81#
Tb.N.(/mm)	4.43±0.04	4.10±0.16 #	4.72±0.16	4.25±0.21
Cortical	**AA**		**BB**	
	Vehicle	**PTH**	**Vehicle**	**PTH**
Tt.Ar. (mm^2)	2.15±0.07	2.17±0.08	2.00±0.05	2.36±0.06 #
Ma.Ar. (mm^2)	1.22±0.06	1.15±0.05	1.10±0.03	1.21±0.07
Ct.Ar. (mm^2)	0.93±0.02	1.02±0.02 #	0.90±0.02	1.09±0.02 #

Histomorphometry was used to evaluate bone remodeling parameters and bone formation rate in femoral trabecular region of vehicle and PTH injected $ON^{A/A}$ and $ON^{B/B}$ mice [217]. Interestingly, osteoblast number was lower in vehicle treated $ON^{B/B}$ mice compared to $ON^{A/A}$, whereas bone formation rate (BFR) was higher in the vehicle treated $ON^{B/B}$ mice (Figure 3.6; Table 3.5). These data suggest greater bone forming activity, per cell, in $ON^{B/B}$ mice. With PTH treatment, osteoblast number and bone formation rate in both $ON^{A/A}$ and $ON^{B/B}$ mice were significantly increased, such that they were equivalent. Differences in osteoclast number and eroded surface were not seen between $ON^{A/A}$ and $ON^{B/B}$ mice, in the presence or absence of PTH treatment (Table 3.5).

Altogether, these data indicate that $ON^{A/A}$ mice have decreased bone formation compared with $ON^{B/B}$ mice, providing an explanation for the failure of $ON^{A/A}$ mice to increase trabecular bone volume from 10 to 20 weeks of age (Figure 3.4, Figure 3.6; Table 3.5).

To determine whether PTH might have a direct effect on miR-433 expression, wild type mouse BMSCs were cultured to confluence, serum-deprived, and treated with PTH or vehicle for 3, 6, 12 or 24 hours of treatment (Figure 3.7D). However, PTH treatment did not regulate miR-433 levels at any time point tested, suggesting that the actions of PTH on bone in vivo may not be related to direct effects on miR-433.

Table 3.5 Histomorphometric analysis of femoral trabecular bone of vehicle and PTH injected $ON^{A/A}$ and $ON^{B/B}$ mice. 14-week old haplotype A and B knock-in mice that had been injected for 4 weeks with 40 μg/kg/day PTH or vehicle (N = 4-6 mice per group) # $p<0.05$ different from the corresponding vehicle injected mice of the same genotype. * $p<0.05$ different from haplotype A mice in the same treatment group. Data is represented as mean + SEM.

Histomorphometry	**AA**		**BB**	
Formation	**Vehicle**	**PTH**	**Vehicle**	**PTH**
Osteoblast number (N.Ob/B.Pm, /mm^2)	1.64±0.26	6.28±1.16#	0.91±0.23*	6.39±1.52#
Mineralizing surface (MS/BS, %)	4.77±0.55	10.58±1.63#	7.34±0.90*	8.86±1.16
Bone formation rate ($\mu m^3/\mu m^2$/ day)	93.29±1.17	317.27±35.02#	168.36±21.90*	196.81±21.34
	AA		**BB**	
Resorption	**Vehicle**	**PTH**	**Vehicle**	**PTH**
Osteoclast number (N.Oc/B.Pm; /mm^2)	0.91±0.22	0.81±0.25	0.72±0.07	0.80±0.21
Osteoclast surface (Oc.S/BS, %)	2.54±0.64	2.27±0.66	1.97±0.21	2.26±0.10
Eroded surface (ES/BS, %)	5.67±1.14	5.63±1.05	4.76±0.53	5.29±0.38

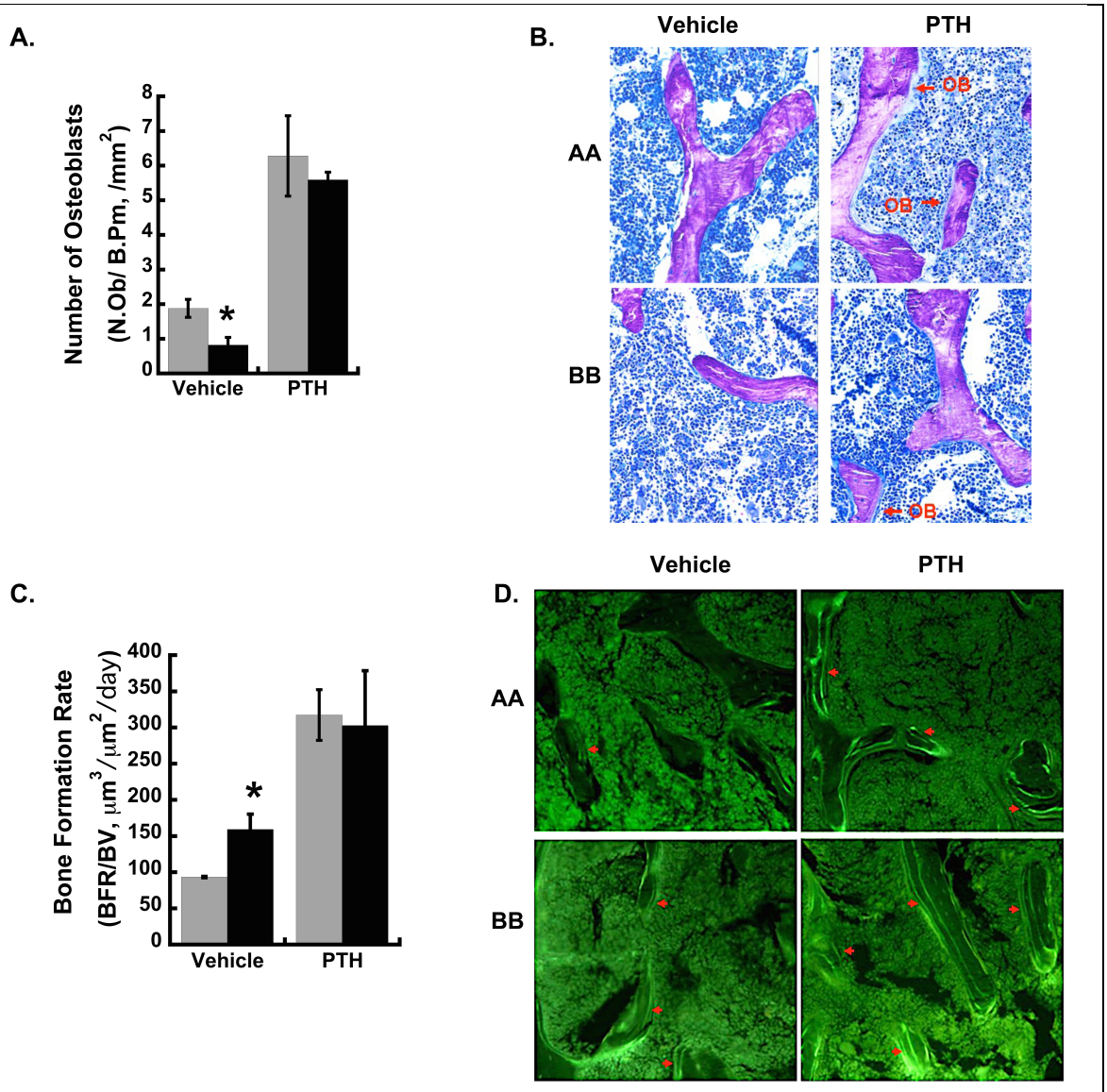

Figure 3.6: Bone formation rate is greater in haplotype B knock-in mice. Histomorphometric analysis of femoral trabecular bone from 14-week old $ON^{A/A}$ and $ON^{B/B}$ mice that had been injected for 4 weeks with 40 μg/kg/day PTH or vehicle. (A) Osteoblast number and (C) bone formation rate in femoral trabecular bones of vehicle and PTH treated $ON^{A/A}$ and $ON^{B/B}$ mice (*$p<0.05$ different from $ON^{A/A}$ mice, N=4-6/group). Red arrows indicate (B) toluidine blue stained osteoblasts and (D) calcien double labels.

Cell autonomous effect of SNP 1599 on osteoblastic differentiation and mineralized matrix deposition.

To determine whether the effect of SNP 1599 on bone formation was cell autonomous, we monitored osteoblastic differentiation markers in BMSCs from $ON^{A/A}$ and $ON^{B/B}$ mice cultured for up to 2 weeks. After 1 week of culture in osteoblast differentiation medium, $ON^{B/B}$ cells displayed significantly more osteocalcin and bone sialoprotein mRNA compared to $ON^{A/A}$ cultures (Figure 3.7E and F). After 2 weeks of culture, bone sialoprotein mRNA levels were no longer significantly different between genotypes, whereas osteocalcin mRNA remained elevated in $ON^{B/B}$ cultures. We also assessed mineralized matrix deposition in BMSCs undergoing osteoblastic differentiation in vitro. Mineralized matrix deposition was quantified using alizarin red staining, whereas differences in cell density were monitored by crystal violet staining. The stains were then solubilized and quantified; and alizarin red staining was normalized to crystal violet (Figure 3.7 A and B). Although both cultures were plated at the same density, crystal violet staining was greater in $ON^{A/A}$ compared to $ON^{B/B}$ cultures (Figure 3.7 B). Crystal violet staining peaked at week 2 in $ON^{A/A}$ cultures, and at week 3 in $ON^{B/B}$ cultures. However, despite the lower cell number, $ON^{B/B}$ cultures showed a greater alizarin red staining at weeks 3 and 4 of differentiation. After normalizing alizarin red staining by crystal violet, the difference in mineralized matrix deposition between $ON^{A/A}$ and $ON^{B/B}$ cultures became more apparent. This suggests that $ON^{B/B}$ osteoblasts deposited significantly more mineralized matrix per cell compared to $ON^{A/A}$ cultures, and support the in vivo observations (Figure 3.7A and B).

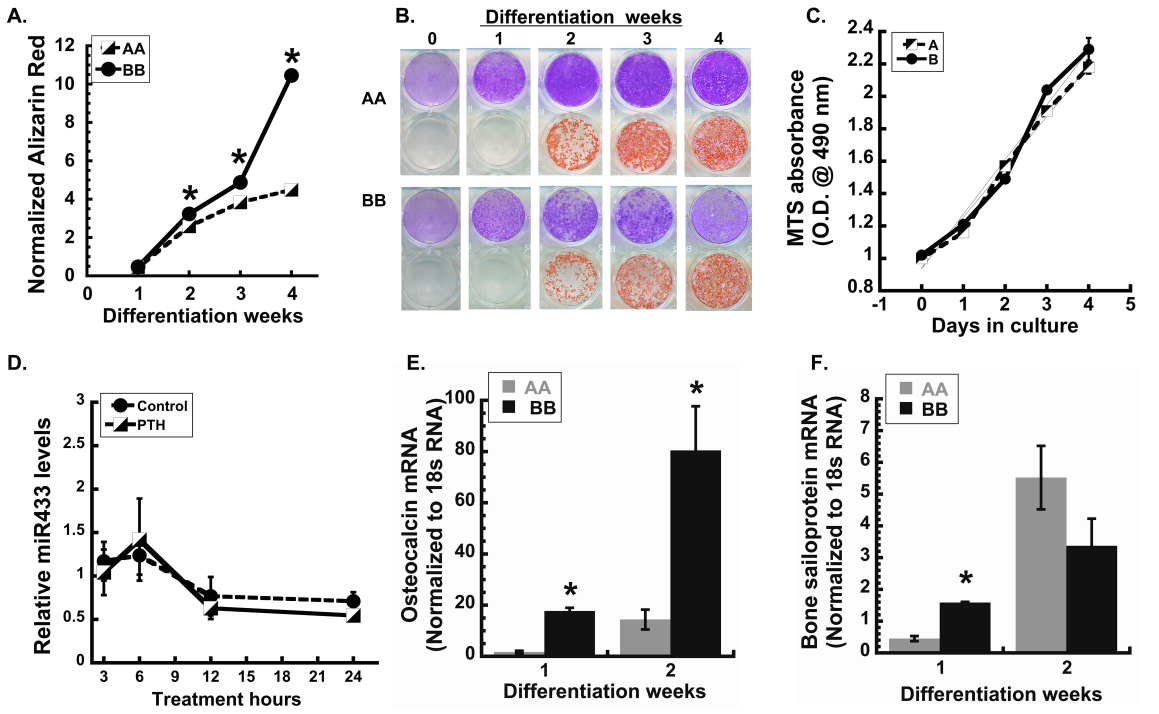

Figure 3.7. Osteoblast mineralization and differentiation capacity is higher in haplotype B mice. (A, B) Quantified alizarin red stain normalized to crystal violet in differentiated BMSCs from $ON^{A/A}$ and $ON^{B/B}$ mice indicate increased osteoblast mineralization/per cell equivalent in $ON^{B/B}$. (C) Growth of $ON^{A/A}$ and $ON^{B/B}$ BMSCs over 4 days of culture was assessed by MTS assay read at 490nm, (N = 6/ time point/assay/group). (D) Confluent BMSC cultures of C57/BL6 mice were treated with 10ng/ml PTH for 24 hours, miR-433 levels were quantified and normalized to sno202 RNA by qRT-PCR (N=3-4, data points are represented as mean ± SEM). (E) Osteocalcin and (F) Bone sailoprotein RNA in BMSCs from $ON^{A/A}$ and $ON^{B/B}$ mice undergoing osteoblastic differentiation for 2 weeks (*$p<0.05$ different from haplotype A, N=3). (*$p<0.05$ different from haplotype A, N = 4).

To determine whether there were inherent differences in the growth rate of $ON^{A/A}$ and $ON^{B/B}$ BMSCs, MTS assay was used to monitor the growth of sub-confluent cultures. We found

that the growth rate for $ON^{A/A}$ and $ON^{B/B}$ stromal cells did not differ (Figure 3.7C). Similarly, previous in vitro studies showed that osteonectin-null osteoblasts displayed decreased osteoblast maturation and mineralized matrix deposition, but no defects in cell growth [189]. The present in vitro studies support the concept that, in BMSCs, osteonectin levels do not impact cell growth, but have effects on osteoblastic differentiation.

Discussion

Skeletal phenotype is a complex genomic trait, and only a minute fraction of the genetic variants contributing to this phenotype have been identified. Further, the in vivo function of most osteoporosis associated polymorphisms identified through GWAS and candidate gene studies is not known [200]. In this study, we developed a novel knock-in mouse model to determine the in vivo impact of a human regulatory region polymorphism on skeletal phenotype. This model demonstrated that a SNP in the osteonectin 3' UTR can regulate osteonectin levels and bone volume, essentially validating the association between osteonectin 3' UTR SNP haplotypes and bone mass first identified in a cohort of Caucasian men with idiopathic osteoporosis [186]. Moreover, we identified a potential molecular mechanism by which this SNP regulates osteonectin expression, through differential targeting of a miRNA (Figure 3.8).

Bone matrix is enriched in osteonectin. This integrin-binding matricellular protein is important for regulating collagen matrix assembly and organization [222-224]. In fact, many connective tissue pathologies detected in osteonectin-null mice have been attributed to defective extracellular matrix composition [223-225]. In vitro and in vivo studies demonstrate that

collagen fibril organization is impaired in bone matrices of osteonectin-null mice, likely contributing to decreased bone mineralization [223]. In vitro, osteonectin promotes osteoblast survival, differentiation and matrix mineralization [189]. It is possible that extracellular matrix organization differs between $ON^{A/A}$ and $ON^{B/B}$ mice, which may contribute to differences in osteoblastic differentiation and mineralization; studies to address these questions are ongoing. Although we did not analyze osteonectin mRNA or protein levels in $ON^{A/A}$ and $ON^{B/B}$ mice after PTH administration, studies by Turner et al. (2007) showed that intermittent PTH administration increased osteonectin mRNA in bone of rats subjected to hind limb unloading [226].

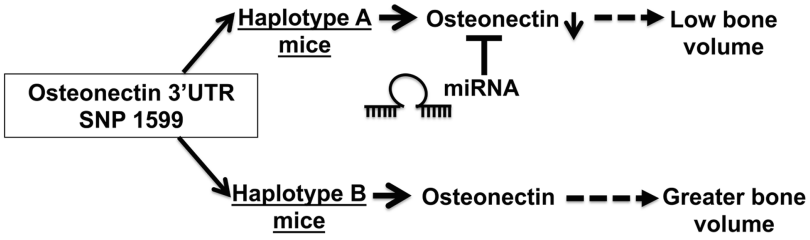

Figure 3.8. Working model for osteonectin 3' UTR SNP mediated effect on bone. In haplotype A knock-in mice, osteonectin levels in bone are lower compared to haplotype B knock-in mice. The osteonectin 3' UTR haplotype A is targeted by miRNA (miR-433), which may contribute to lower osteonectin and lower bone volume.

Previously, we reported that although osteonectin-null and haploinsufficient mice gain bone in response to intermittent PTH therapy, their bone-anabolic response was less than that seen in wild type mice. For the most part, the response of these mice to PTH could be related to osteonectin gene dosage [208]. Although the dose of PTH used in our previous study was higher than the one used in this report (80 vs. 40 μg/kg/day), our results suggest that higher levels of osteonectin in bone are associated with greater PTH-mediated bone gain, particularly with regard

to the cortical compartment (Figure 3.5B). It is possible that the higher levels of osteonectin in $ON^{B/B}$ mice could facilitate the anabolic response of bone to intermittent PTH treatment.

The expression of osteonectin is tightly regulated through mechanisms that alter transcription, mRNA stability, and translation [219, 227-232]. In osteoblasts, the osteonectin transcript is quite stable, with a half-life of >24 hours under conditions of transcription arrest [232]. Therefore, regulation of translation would likely provide the most rapid means of decreasing osteonectin synthesis. Recently, 2 evolutionarily conserved binding sites for the miR-29 family of miRNAs were found in the proximal region of the osteonectin 3' UTR [219]. Induction of miR-29 expression by canonical Wnt signaling provided potent repression of osteonectin protein synthesis, within one hour of treatment [219]. This example illustrates the efficiency by which miRNAs could regulate osteonectin levels.

In this study, we identified miR-433 as a miRNA that could play a role in regulating osteonectin expression. The mature miR-433 sequence is identical between mice and humans, and the organization of the miR-433 genomic locus conserved. Previously, miR-433 was shown to decrease during BMP2- induced osteoblastic differentiation of C3H10T1/2 cells, and to target the Runx2 3' UTR [191]. Our study confirms that miR-433 expression decreases during osteoblastic differentiation in human cells, and that miR-433 has an inhibitory effect on differentiation (Figure 3.2). We also demonstrated that SNP 1599 modulates the ability of miR-433 to regulate the human osteonectin 3' UTR (Figure 3.2). Although the effect of the miR-433 inhibitor on the haplotype A construct was modest, it is consistent with effects reported in other studies, and may reflect the relatively low level of miR-433 expression in the human osteoblast

cell line [212]. Moreover, osteonectin is expressed in multiple tissues, many of which likely have a complement of miRNAs that are distinct from that found in the bone cells. Other miRNAs might bind to the osteonectin 3' UTR, and differential binding of these miRNAs to the region containing SNP 1599 must be strongly considered.

Table 3.6. Osteonectin SNP 1599 (rs1054204) allele and genotype frequencies (from dbSNP summary for ss68954048).

Population ID	Ethnicity	Allele Frequency	Genotype Frequency
HapMap-CEU	European	C=0.533 G=0.467	C/G=0.433 C/C=0.317 G/G=0.250
HapMap-JPT	Asian	C=0.522 G=0.478	C/G=0.511 C/C=0.267 G/G=0.222
HapMap-YRI	Sub Saharan African	C=0.742 G=0.258	C/G=0.567 C/C=0.350 G/G=0.083

Others have examined the potential association of osteonectin SNPs with disease phenotype in systemic sclerosis, hepatocellular carcinoma, glaucoma, and keratoconus [233-237]. Although some studies have associated particular osteonectin 3' UTR SNPs and disease, these reports have not involved SNP 1599, nor have they described potential mechanisms. Osteonectin SNP 1599G is a common variant (Table 3.6) [238]. In a sample population of North Americans that are of African descent, frequency of the SNP1599G allele, present in haplotype A, is less than that for populations of European or Chinese descent (dbSNP summary for ss68954048). Studies have shown that, as a group, African Americans have higher bone mineral density compared to Caucasians [239, 240]. Although several candidate genes have been associated with BMD within these groups, it is not clear whether decreased frequency of SNP

1599G could play a part in this effect [241].

In the literature, there has been argument about whether the majority of phenotypic variance is driven by rare variants with large effects or by common variants with small effects [242]. Most likely, rare and common variants work together, in conjunction with gene-environment interactions, to specify phenotype. The present study was performed in an inbred mouse strain, and the animals were housed in well-controlled environmental conditions. These experimental parameters allowed us to decrease the impact of genetic variance and gene-environment interactions on trabecular and cortical bone phenotype. This permitted us to assign a physiological function to a common osteonectin allele, providing support for its contribution to the complex trait of skeletal phenotype.

Presently, estimation of a patient's risk of fracture is performed using models based on clinical, demographic and anthropomorphic information, such as BMD, previous fracture, a parent with hip fracture, smoking, glucocorticoid and alcohol use. Although valuable, the prognostic performance of these models could be improved especially in case of idiopathic osteoporosis. Including genetic profiling data for an individual could help improve accuracy of risk assessment and better inform treatment decisions [243]. Osteonectin SNP 1599 could be of importance to consider in investigations of idiopathic osteoporosis. However, the impact of a single variant on fracture risk is small, and identification of many more gene variants with an impact on the skeleton is necessary before real gains in fracture prediction can be realized [243, 244]. Data such as those reported here will contribute to the pool of SNP variants needed for individualized risk assessment and fracture prevention.

CHAPTER 4

Function of miR-365, -99b and -451 in osteoclasts

Portions of this chapter have been published in:

Pathway analysis of microRNA expression profile during murine osteoclastogenesis

Tiziana Franceschetti, M.S.*[1], Neha S. Dole, M.S.*[1], Catherine B. Kessler, B.S.[1], Sun-Kyeong Lee, Ph.D.[2], and Anne M. Delany, Ph.D.[1]

* These authors contributed equally to the work.

Abstract

Osteoclast formation and function are tightly regulated by transcriptional, post-transcriptional and post-translational mechanisms. This stringent control is critical to prevent excessive or insufficient bone resorption and to maintain normal bone homeostasis. microRNAs (miRNAs) are key post-transcriptional regulators that repress expression of target mRNAs controlling osteoclast proliferation, differentiation, and apoptosis. With the goal of designing novel therapeutics for bone loss, it is critical to define the function of individual miRNAs in the osteoclast lineage.

Our previous miRNA expression profiling studies suggest that miRNAs-99b, -365 and -451 are dramatically regulated during the RANKL-driven osteoclastic differentiation of an enriched population of murine bone marrow osteoclast precursors. Here, we validated these miRNA expression data and demonstrate that miR-99b is crucial for osteoclast differentiation. In contrast, miR-365 appears to be a negative regulator of osteoclast formation, but a positive

regulator of overall osteoclast size. Computational analyses predicted mTOR, PI3 kinase/AKT, and Calcium signaling pathways to be top targets of miR-99b and -365 in osteoclasts. To identify miRNA targets in an unbiased manner, miRNAs and their targets are frequently co-immunoprecipitated with the RISC complex. We also optimized a RISC immunoprecipitation protocol for osteoblastic and osteoclastic cells. Overall, our study is unique in that we identified function of 2 miRNAs that are induced during osteoclastogenesis, and we report an optimized strategy for RISC-RNA immunoprecipitation in bone cells.

Introduction

Bone mass is a well-known determinant of bone strength, and reflects the net outcome of bone formation and resorption. Maintenance of healthy bone mass requires tight regulation on the number and activity of bone forming osteoblasts and bone resorbing osteoclasts. Imbalance in bone remodeling, with accelerated bone resorption, can result in bone loss, as that observed in post-menopausal osteoporosis patients. Novel therapeutic interventions to reduce such osteoclast-mediated bone loss require understanding of the molecular mechanisms regulating osteoclast formation and activity.

Osteoclastogenesis is an intricate process that involves the differentiation of common myeloid progenitors to monocyte precursors, commitment of these precursors to the osteoclast lineage, followed by the migration and fusion of osteoclast precursors into multinucleated polykaryons [9]. The two major cytokines essential and sufficient to induce osteoclastogenesis are macrophage-colony stimulating factor (M-CSF, CSF1) and receptor activator of nuclear

factor kappa-B ligand [7]. The is former required for proliferation and survival of osteoclast precursors, while the later is needed to drive osteoclastogenesis [41].

Osteoclast differentiation is regulated by transcriptional and post-transcriptional mechanisms. Transcription factors essential for osteoclastogenesis, including PU.1, MITF (microphtalmia associated transcription factor), and c-Fos are activated upon differentiation of the mutlipotent common myeloid progenitors, to mediate commitment of monocytic precursors to osteoclast lineage. PU.1 drives differentiation of monocytic precursors towards the osteoclast and macrophage lineage [245-247]. This was essentially demonstrated by the lack of osteoclasts and macrophages in PU.1$^{-/-}$ mice, although these mice contained functional monocytes. In conjunction with MITF, PU.1 drives expression of osteoclast genes such as RANK, Cathepsin K (Ctsk), tartrate resistant acid phosphatase 5 (TRAP/Acp5), osteoclast-associated receptor (Oscar), osteopetrosis-associated transmembrane protein 1(Ostm1) and Chloride channel 7 (Clcn7) [34, 40, 42, 248, 249].

In addition to promoting their osteoclastic commitment, c-Fos prevents commitment of monocytic precursors to the dendritic lineage [33]. Although c-Fos$^{-/-}$ mice contain macrophages, they lack osteoclasts, indicating that c-Fos functions downstream of PU.1 in the transcription program of osteoclast commitment. c-Fos is also necessary for upregulation of RANK expression in pre-osteoclasts upon M-CSF signaling [250-252]. Following osteoclast commitment, RANKL signaling induces NFATc1 (nuclear factor of activated T-cells) expression. NFATc1 functions as a master transcriptional regulator, driving osteoclastic differentiation of mononuclear osteoclast precursors into polykaryonic mature osteoclasts that

resorb bone [253]. RANKL activates NFATc1 through two pathways: calcium-calmodulin signaling and by activating NF-κB, which directly binds to NFATc1 promoter [35, 252, 254]. Interestingly, NFATc1 complexes with other transcription factors including PU.1, MITF, NF-κB and c-Fos, to induce expression of osteoclast genes such as Ctsk, Oscar, TRAP and Calcitonin receptor [40-42].

In addition to regulation at the level of transcription, post-transcriptional mechanisms also play fundamental role in osteoclastogenesis, and miRNAs are critical post-transcriptional regulators of gene expression. The importance of miRNAs in osteoclast biology was initially demonstrated by 2 studies that deleted a key miRNA-processing enzyme, Dicer, in cells of the osteoclast lineage. Dicer deletion mediated by a CD11b-Cre transgene abrogated miRNA biogenesis in the monocytic cells that give rise to osteoclasts. CD11b-Dicer$^{-/-}$ mice developed osteopetrosis, due to decreased osteoclastogenesis and bone resorption [255]. Moreover, Cathepsin K-Dicer$^{-/-}$ mice also developed mild osteopetrosis, due to impaired miRNA biogenesis in mature osteoclasts [46]. Subsequently, the function of only a few miRNAs in osteoclasts has been revealed. For example, overexpression of miR-155 was shown to block osteoclastogenesis, and downregulate MITF expression. Being highly expressed in macrophages, the negative role of miR-155 in osteoclasts suggests that it promotes commitment of monocytic precursors to the macrophage lineage, at the expense of osteoclastogenesis [256-258]. In contrast, the PU.1 transcription factor was shown to induce expression of miR-223 during osteoclastogenesis, and inhibition of miR-223 decreases osteoclast formation. The positive role of miR-233 in osteoclasts was illustrated by its targeting of the NFIA (nuclear factor I-A) gene, a transcription factor that suppresses MCSF mediated signaling in osteoclasts [255, 259, 260].

Although the overall importance of miRNAs in the osteoclast lineage is recognized, there is little information about the function of specific miRNAs in osteoclasts [104, 174, 255, 258, 259, 261, 262]. In human genome, although there are a limited number of miRNAs, their effect is substantial, as a single miRNA may regulate hundreds of genes. Indeed, > 30% of protein coding genes are estimated to be targeted by miRNAs [87]. This makes it difficult to predict the effects a single miRNA might have on cell phenotype. For designing miRNA-based therapeutics for pathologies caused by excessive or insufficient osteoclast activity, a thorough understanding of the function of specific miRNAs and their panel of target genes will be necessary.

Recently, a microarray study in RAW264.7 cells (murine monocyte cell line) documented a panel of miRNAs that were up or down regulated during osteoclastic differentiation [263]. Information on miRNAs expressed during differentiation of primary bone marrow cells into osteoclasts was, however, still lacking. Moreover, osteoclast formation, which begins with mononuclear cells and ends with polykaryons, is quite a dramatic cellular metamorphosis and it is likely that the miRNA expression profile may differ at every stage of osteoclastogenesis. Thus, it is crucial to examine miRNAs expressed at different stages of osteoclast formation and not just at the endpoints of the process.

Therefore, we profiled miRNAs expressed during the early, middle and late stages of osteoclastogenesis in an enriched osteoclast progenitor population from murine bone marrow. The resulting data set was unique in that it was derived from a primary cell population with decreased heterogeneity, and it revealed miRNAs expressed during different stages of osteoclastogenesis, providing a better insight on the role of miRNAs in this process.

Cluster analysis of these data revealed panels of miRNAs expressed during early, middle and late stages of osteoclastogenesis. Of note, miR-365-3p and miR-99 family members (consisting of miR-99a, -99b and -100) were strongly up regulated during osteoclastogenesis. [263]. Presently, there is not much was known about these miRNAs. The goal of our study was to investigate the function of these miRNAs in osteoclast differentiation, and to identify some potential target genes in osteoclasts.

We validated that expression of miR-365-3p, -99b-5p and -451 during osteoclastogenesis in a population of primary murine bone marrow cells enriched for osteoclast progenitors, as well as in RAW264.7 cells. Through gain and loss of function studies, we determined their role in osteoclast differentiation. Our computational predictions of miR-365-3p and -99b-5p targets and their pathway analysis suggest potential molecular mechanisms involved. Lastly, in an effort to design an unbiased approach to identify miRNA target genes, we optimized an Ago-RNA-immunoprecipitation protocol for osteoblastic and osteoclastic cells. In summary, our approach provides an outline of fundamental methodology that can be utilized for studying miRNA function in osteoclasts.

Materials and Methods

Ethics statement.

All animal protocols were approved by the Institutional Animal Care and Use Committee at the University of Connecticut Health Center (protocol 100435-0315).

Cell culture.

Primary osteoclast precursor cultures were established using bone marrow from 6-8 week old C57BL/6 male mice, which had been enriched for osteoclast precursors by depletion of B220/CD45R-positive and CD3-positive cells (B and T lymphocytes, respectively). Briefly, bone marrow was isolated from femurs, tibias, and humeri, and depleted of erythrocytes by treatment with ammonium-chloride-potassium (ACK) buffer (Gibco Life Technologies, Grand Island, NY) [264]. Cells were incubated with Phycoerythrin (PE)-conjugated primary antibodies for CD45R and CD3 (eBioscience, San Diego, CA), and with magnetically labeled anti-PE microbeads (MiltenyiBiotec, Auburn, CA). Magnetic-Activated Cell Sorting (MACS®) Column Technology (MiltenyiBiotec, Auburn, CA) was used to capture CD45R and CD3 positive cells in the column, and the flow-through contained a population of cells enriched for monocytic and non-lymphoid lineage cells.

Cells were cultured in α-MEM (Gibco Life Technologies, Grand Island, NY) supplemented with 10% FBS (Fetal Bovine Serum, Atlas Biologicals, Fort Collins, CO) and 30 ng/ml murine recombinant Macrophage Colony-Stimulating Factor (M-CSF) (eBioscience, San Diego, CA). Bone marrow-derived osteoclast precursor cells were cultured in the presence of 30 ng/ml M-CSF and 30 ng/ml murine recombinant RANKL (eBioscience) for up to 5 days.

RNA-immunoprecipitation studies were performed in the human fetal osteoblastic hFOB1.19 cell line (CRL-11372) and the mouse monocytic RAW264.7 cell line (TIB-71TM), purchased from American Type Culture Collection. hFOB1.19 cells were grown at 33.5°C in DMEM/ F12 media (Gibco Life technologies, Grand Island, NY) supplemented with 10% FBS

(Lonza, BioWhittaker ™) and 1% penicillin/ streptomycin. RAW264.7 cells were cultured in DMEM (Gibco Life technologies, Grand Island, NY) supplemented with 10% FBS (Atlas Biologicals, Fort Collins, CO) and 1% penicillin/streptomycin. For osteoclastic differentiation, RAW264.7 cells were cultured in 30 ng/ml RANKL.

In Vitro Osteoclast Formation Assay

Cells were fixed with 2.5% glutaraldehyde in PBS, and TRAP activity was detected according to the manufacturer's instructions using the Acid Phosphatase Leukocyte (TRAP) kit (Sigma-Aldrich). Osteoclast cultures were imaged using light microscopy and TRAP positive cells with more than 3 nuclei were counted as osteoclasts. CellSens Dimension software (Olympus) was used to measure osteoclast area. N=6. Data shown are representative of 2 independent experiments.

Quantitative Real time PCR

miRNA expression levels were analyzed using the TaqMan MicroRNA Assay (Life Technologies, Grand Island, NY). According to the manufacturer's instructions, 22.5 ng of RNA were reverse transcribed with specific primers to generate cDNA. The expression of miR-365-3p, miR-99b-5p, and miR-451 was detected by qPCR in a MiQ qPCR cycler (Bio-Rad). miRNA levels were normalized to U6 small nuclear RNA (RNUB6) levels, using the absolute quantification method. Data are presented as mean ± SEM. Data were analyzed by one-way ANOVA with Bonferroni post-hoc test, as appropriate (KaleidaGraph, Synergy Software, Reading, PA).

Inhibitor or mimic transfection and osteoclastogenesis

Bone stromal cells (BMSCs) isolated from long bones of 6–8-week-old C57BL/6 mice were cultured overnight to reduce the amount of stromal cells. Enrichment in monocyte precursor population was achieved by subjecting the non-adherent cells to density gradient centrifugation with Ficoll (GE Healthcare, Piscataway, NJ). Bone marrow-derived monocytes (BMMs) were plated at 30,000 cells/well in 96-well plates and cultured in α-MEM supplemented with 10% FBS (Atlas) in the presence of 10 ng/ml M-CSF for two days. Subsequently, cells were transfected with anti-miRNA inhibitors or miRNA mimics (Dharmacon) or non-targeting controls at 50 nM concentration using HiPerFect transfection reagent (Qiagen, Valencia, CA). 6 hours post-transfection, osteoclast differentiation was induced with M-CSF (30 ng/ml) and RANKL treatment (30 ng/ml), and osteoclast formation was evaluated by TRAP staining.

RNA Immunoprecipitation (RNA-IP)

We performed RNA-IP in hFOB1.19 and RAW264.7 cell lines, to optimize the technique for osteoblast and osteoclast lineage cells. To determine if the technique can be efficient to immunoprecipitate RISC-associated RNAs, we chose to examine levels of miR-29 family members (a and c), as they are expressed in both lineages. Cells were grown to confluence, harvested by scraping in ice cold PBS (5ml/ plate), and washed in PBS (5ml/ plate, 2 washes). For hFOBs 15-20 x 10^6 cells (corresponding to 5-7 10 cm plates, ~3x10^6 cells/ plate), and for RAW264.7 2 x 10^6 cells (corresponding to 1 10 cm plate, ~10x10^6 cells / plate) were used for preparing cell lysates. Cells were incubated in polysome lysis buffer (275 ul for hFOB1.19 or 600 ul for RAW264.7 cells) [PLB composition- 100 mM KCl, 5 mM $MgCl_2$, 10 mM HEPES, pH7.0, 0.5% NP-40, 1 mM DTT, 400 uM Vanadyl ribonucleoside complexes

(VRC), protease inhibitor cocktail (1x- Halt^{TM}, Thermo Scientific)] for 10 minutes on ice, and homogenized (5 passes through a 21G gauge needle with a 1 ml syringe). Protein G Dynabeads (Invitrogen) were rinsed and blocked with 1 mg/ml BSA and 0.5 mg/ml yeast tRNA (50 ul of beads with 450 ul of blocking solution) for 30 minutes. Following the initial blocking step, beads were incubated with 5 ug of monoclonal anti-AGO (2A8) or IgG antibody (Millipore) in PBS for 2 hours (200 ul). Beads were then washed in lysis buffer (25 mM Tris-HCl at pH 8.0, 150 mM NaCl, 2 mM $MgCl_2$, 0.5% NP-40 and 5 mM DTT). Cell lysate was clarified by centrifugation at 13,000 rpm for 30 minutes (4 ºC), added to anti-Ago or IgG labeled beads, and incubated from 4 hours at 4 ºC. We found that overnight incubation of cell lysates with the antibody leads to protein degradation. After co-IP, stringency was achieved by sequential washes: beads were washed twice in lysis buffer containing 900 mM NaCl, 1% NP-40 and twice again in lysis buffer with 0.05% NP-40. Subsequently, beads were resuspended in buffer (40 mM Tris-HCl at pH 8.0, 10 mM $MgSO_4$, 1 mM $CaCl_2$, 200 U/ml RNasin) and aliquots were used for RNA and protein analysis. RNA was harvested using Qiazol and analyzed by qRT-PCR. Aliquots of lysate were mixed with an equal volume of 2X Lamelli sample buffer (62.5 mM Tris-HCl pH 6.8, 25% glycerol, 2% SDS, 0.01% bromophenol blue) and subjected to Western blot analysis [265, 266]. We were able to isolate ~250 ng of RNA from the immunoprecipitated complexes in hFOB 1.19 cells (15 x 10^6 cells) and ~850 ng of RNA from RAW264.7 cells (1.7 x 10^6 cells).

Western blot analysis

Equal volume of lysates in 2X Lamelli sample buffer prepared from hFOB1.19 cells (15 x10^6 cells) were analyzed by Western blot. AGO immunoprecipitation was confirmed by immunoblotting for Anti-pan Ago, clone 2A8 primary antibody (Millipore 1:1000) and goat anti-

mouse IgG- horseradish peroxidase conjugated secondary antibody (1:10,000). Bands were visualized by chemiluminescence (Cell Signaling) and relative band densities were determined using Image J software. The band for AGO protein was detected at ~95 kDa. The antibody has been reported to cross react with radixin, as shown by the band at ~70 kDa.

Results

Differential miRNA expression during in vitro osteoclastogenesis.

Although mouse bone marrow is a widely used source of primary osteoclast progenitors for in vitro analyses, it represents a highly heterogeneous population, containing monocytes, megakaryocyte precursors, macrophages, neutrophils, and higher percentages of lymphocytes. Flow cytometric analysis suggests that, after erythrocyte depletion, 25-30% of total bone marrow is $B220^{+}$ and 5-7% is $CD3^{+}$ (unpublished data, personal communication from Dr. SK Lee). Prior studies indicate that the $B220^{-}/CD3^{-}/CD11b^{-/lo}$ population in the bone marrow constitutes the fraction of osteoclast precursors that have the highest potency for osteoclast formation [267, 268]. We sought to decrease the heterogeneity in primary osteoclast precursor population before initiating osteoclastogenesis, by depleting the lymphocytic cells. Therefore, mouse bone marrow cells were subjected to MACS sorting using CD45R and CD3 antibodies. We cultured mouse bone marrow-derived osteoclast precursors in the presence of M-CSF and RANKL for up to 5 days. At days 1, 3, and 5 of culture, total RNA was harvested. Osteoclast differentiation was examined by TRAP staining, and we reported elsewhere a progressive increase in the expression of the osteoclast markers TRAP and Cathepsin K during this time [262].

Profiling expression of miRNAs during osteoclastogenesis.

Our miRNA microarray analysis showed that miR-99b levels increased by ~4.5 fold and miR-365 levels increased by ~ 11 fold from day 1 to day 5 of osteoclastogenesis. In contrast, miR-451 levels dropped ~30 fold by day 3 and were almost undetectable by day 5 of osteoclast differentiation [138]. Expression and function of these selected miRNAs had not been previously reported in the osteoclast lineage. We verified the results of our microarray using quantitative RT-PCR (qRT-PCR) and confirmed changes in the levels of miRNAs during differentiation. We observed that both miR-365-3p and miR-99b-5p expression progressively increased with osteoclast formation (Figures 4.1 A). Both miR-365-3p and miR-99b are well expressed and showed ~12 fold robust upregulation after 5 days of osteoclastogenesis.

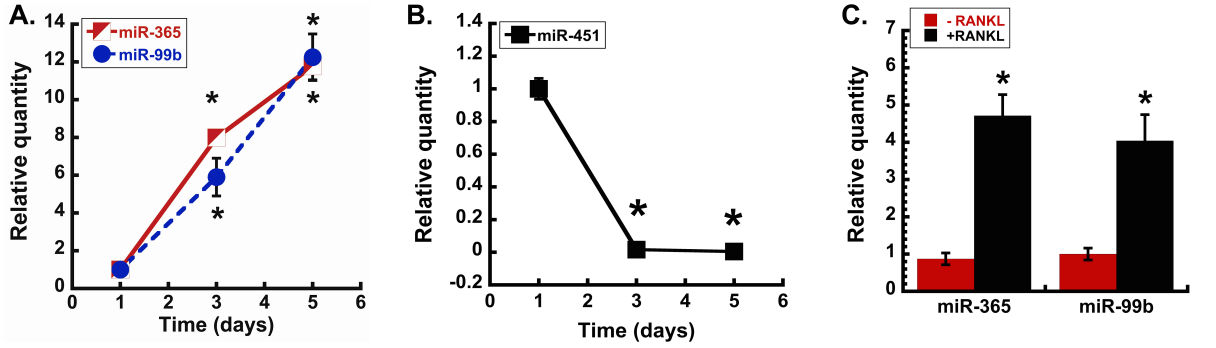

Figure 4.1. Expression profile of miR-99b-5p, miR-365-3p and miR-451 during osteoclastogenesis. Murine bone marrow cells depleted of the $CD45R^+$ and $CD3^+$ population were differentiated with 30 ng/ml M-CSF and RANKL for up to 5 days. Expression of miR-99b-5p, miR-365-3p (A) and miR-451 (B) was quantified and normalized to U6 RNA, n=4, *p<0.01 different from day 1. (C) Expression of miR-365-3p and miR-99b-5p in cells cultured for 3 days in 30 ng/ml M-SCF, and either in presence or absence of RANKL (30 ng/ml), miRNA levels were and normalized to U6 RNA, n=4, *p<0.01 different from M-CSF group.

In contrast, miR-451 expression dramatically decreased from day 1 to day 3, and was nearly undetectable day 5 of osteoclast differentiation (Figure 4.1 B). Differences in the fold changes detected by microarray and the qRT-PCR are attributed to sensitivity of the assays. qRT-PCR assay provides a wider dynamic range for miRNA detection compared to the microarray platform.

We then compared miRNA expression in cultures differentiated with and without RANKL for 3 days. qRT-PCR showed that at day 3, both miR-365 and miR-99b levels were ~4 fold higher in RANKL treated cultures compared to those grown in its absence. (Figure 4.1 C). miR-451 expression was not detected in the day 3 cultures treated with or without RANKL, thereby suggesting that the decrease in miR-451 levels during osteoclastogenesis was independent of RANKL (data not shown). It is likely that the high levels of miR-451 detected at day 1 in primary cultures is due to the heterogeneous mix of cells in our culture.

We further examined expression of the selected miRNAs during differentiation of RAW264.7 cells (murine monocytic cell line). RAW264.7 cells were cultured in the presence of RANKL for up to 4 days, to induce osteoclastogenesis. Total RNA was harvested at days 0, 1, 2, 3, and 4 of RANKL treatment. Expression of miR-451 was not detectable in RAW264.7 cells (data not shown). Although we detected miR-99b expression in RAW264.7 cells, there was no change in its levels during osteoclastic differentiation (Figure 4.2 A). miR-365 levels progressively increased, such that they were ~ 2.5 fold higher after 4 days of osteoclastogenesis in the RAW264.7 cells (Figure 4.2 B).

Likewise, another group performing miRNA microarray analysis in RAW264.7 cells treated with TNFα and RANKL showed an increase in miR-365 after 82 hours of treatment, whereas changes in miR-99b levels were not documented in that study [263].

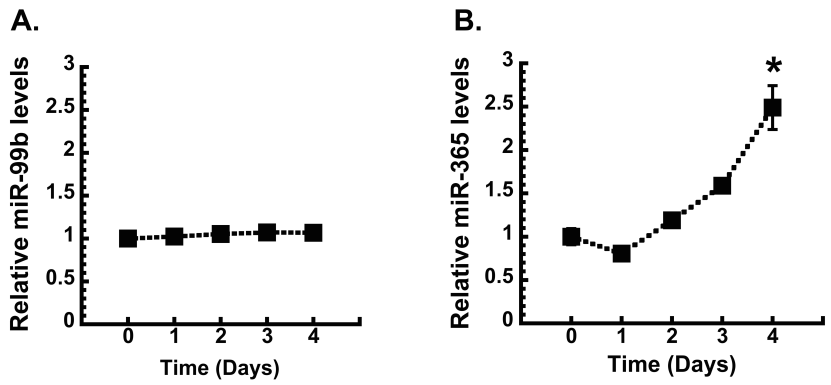

Figure 4.2. Expression of miRNAs in RAW264.7 cells stimulated with RANKL. RAW264. 7 cells were differentiated for up to 4 days into osteoclast with 30 ng/ml RANKL. Expression of miR-99b-5p (A) and miR-365-3p (B) was quantified and normalized to U6 RNA by qRT-PCR, n=4, *p<0.01 different from day 0.

Examining the role of candidate miRNAs in osteoclastogenesis

To determine whether the strongly up-regulated miRNAs had a positive role in osteoclastogenesis, bone marrow-derived monocytes (BMMs) were transiently transfected with inhibitors for miR-99b-5p or miR-365-3p. Osteoclast number and size were determined after 3 days of culture in the presence of RANKL. Inhibition of miR-99b activity resulted in a 50% decrease in osteoclast number compared to the control inhibitor, and the osteoclast size was also significantly reduced (Figure 4.3 A, B and C). This decline in osteoclast number and size indicates that miR-99b is crucial for osteoclast formation.

In contrast to miR-99b, inhibition of miR-365 increased osteoclast number, while decreasing osteoclast size. These data suggest that miR-365 may fine tune osteoclastogenesis, regulating osteoclast size and number in an opposing manner. In other cell types, miR-365 has been shown to target Cyclin D1 and CDC25A, as well as pro-apoptotic BAX [269, 270]. Thus, inhibition of miR-365 activity could lead to increased cell number, a potential explanation for the increased osteoclast number observed in our studies (Figure 4.3 A, and C). The increased levels of miR-365 during osteoclast differentiation could slow proliferation and increase survival.

Since miR-451 levels were dramatically decreased during osteoclast differentiation, to test its function, BMMs were transfected with a miR-451 mimic prior to RANKL-mediated differentiation. However, osteoclast number and size were not affected by the miR-451 mimic, suggesting that this miRNA may not have a significant role in osteoclastogenesis in vitro, although these data do not preclude potential actions in vivo (Figure 3.2 D and E). Several reports have revealed that miR-451 expression is required for erythroid differentiation and homeostasis [271, 272]. It is possible that the high levels of miR-451 observed in cultured osteoclast progenitors could reflect the presence of erythroid precursors.

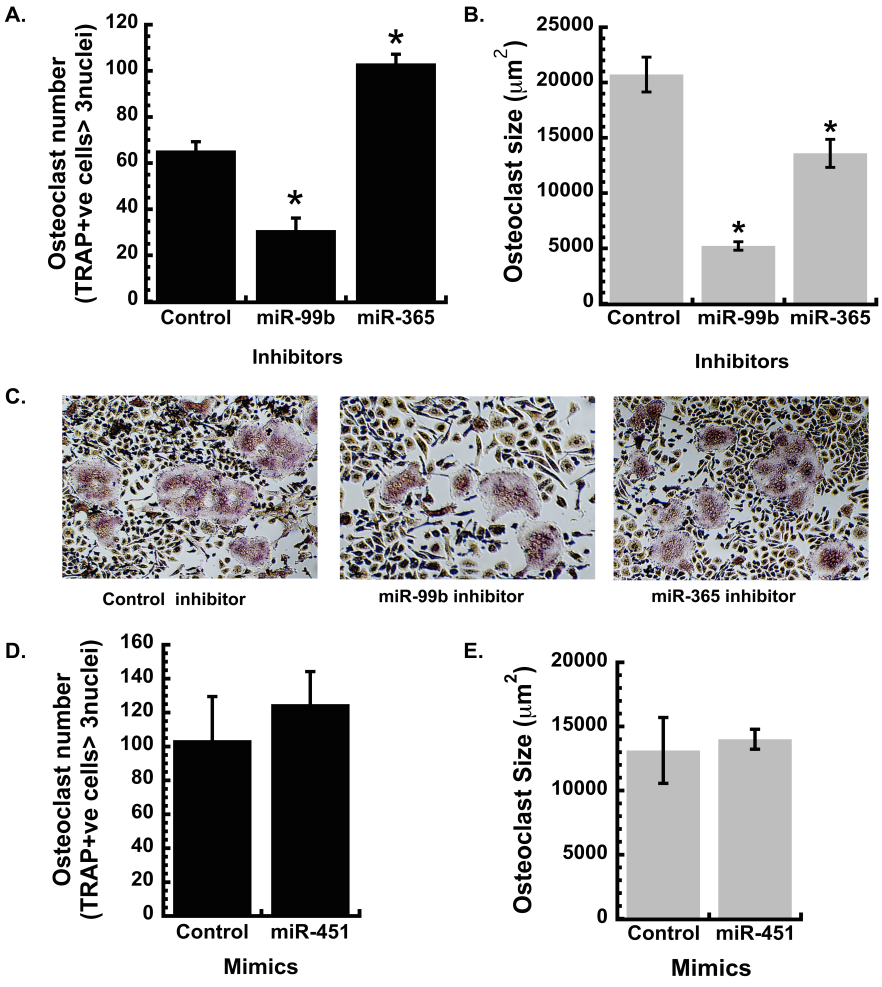

Figure 4.3. Function of miR-99b, -365 and -451 in osteoclasts. Primary BMMs were transfected with 50 nM miRNA inhibitors (A and B) or miRNA mimic (D and E) or the appropriate non-targeting control. Cells were differentiated into osteoclasts with treatment of M-CSF and RANKL (30 ng/ml each) for 3 days. Osteoclast formation was evaluated by TRAP staining. Osteoclast number and size, *$p<0.05$ different from control inhibitor (n=6). (C) Representative images of miR-99b, -365 and control inhibitor transfected osteoclasts (4x magnification).

Analysis of pathways targeted by miRNAs during osteoclastogenesis

Since a single miRNA can potentially target hundreds of genes, deciphering the role of miRNAs by identifying target genes can become cumbersome. However, miRNAs frequently target mRNAs important in a common signaling pathway. Therefore, some strategies for trying to refine lists of potential miRNA targets include pathway analysis. We used this bioinformatics approach in an attempt to understand to potential pathways and target genes regulated by our selected panel of miRNAs. MicroRNA target recognition, for most part, is thought to be nucleated by complementarity between the miRNA seed region and the mRNA target, and this forms the basis for many miRNA computational prediction algorithms designed. In addition to seed binding, secondary structure and complementarity in non-seed regions, as well as evolutionary conservation can also be taken into consideration for target prediction. The 3' UTR tends to be enriched for miRNA binding sites. Thus, many earlier computational strategies limited analysis to the 3' UTR of genes. More recently developed algorithms scan for miRNA-seed sequences in the 5' UTR and coding sequence (CDS), in addition to the 3' UTR.

We performed miRNA binding site prediction for miR-99b and miR-365 using three different computational prediction algorithms: DIANA-microT-CDS (v5.0) (http://www.microrna.gr/microT-CDS), miRanda (http://www.microrna.org/microrna/home.do) and TargetScan (http://www.targetscan.org/mmu_61/), in an attempt to achieve higher accuracy in target gene prediction [273-275]. We did not analyze potential targets for miR-451, since it does not appear to have an impact on osteoclastogenesis in vitro. Our analysis revealed 72 genes predicted as miR-99b targets by all three algorithms, while 1324 genes were predicted as miR-365 targets (Figure 4.4 A and 4.4 B). Using DIANA-miRPath (v2.0 software) we performed a

KEGG (Kyoto Encyclopedia of Genes and Genomes) pathway analysis that enabled us to predict global pathways that may be potentially regulated by a specified set of miRNAs. This algorithm retrieves potential miRNA targets genes from TargetScan, Pictar and DIANA-microT-CDS programs and fits them into all available KEGG pathways. The efficiency of miRNA-mRNA seed interaction and the number of predicted target genes are combined to calculate a P-value, to suggest potential pathways that might be regulated by the miRNA.

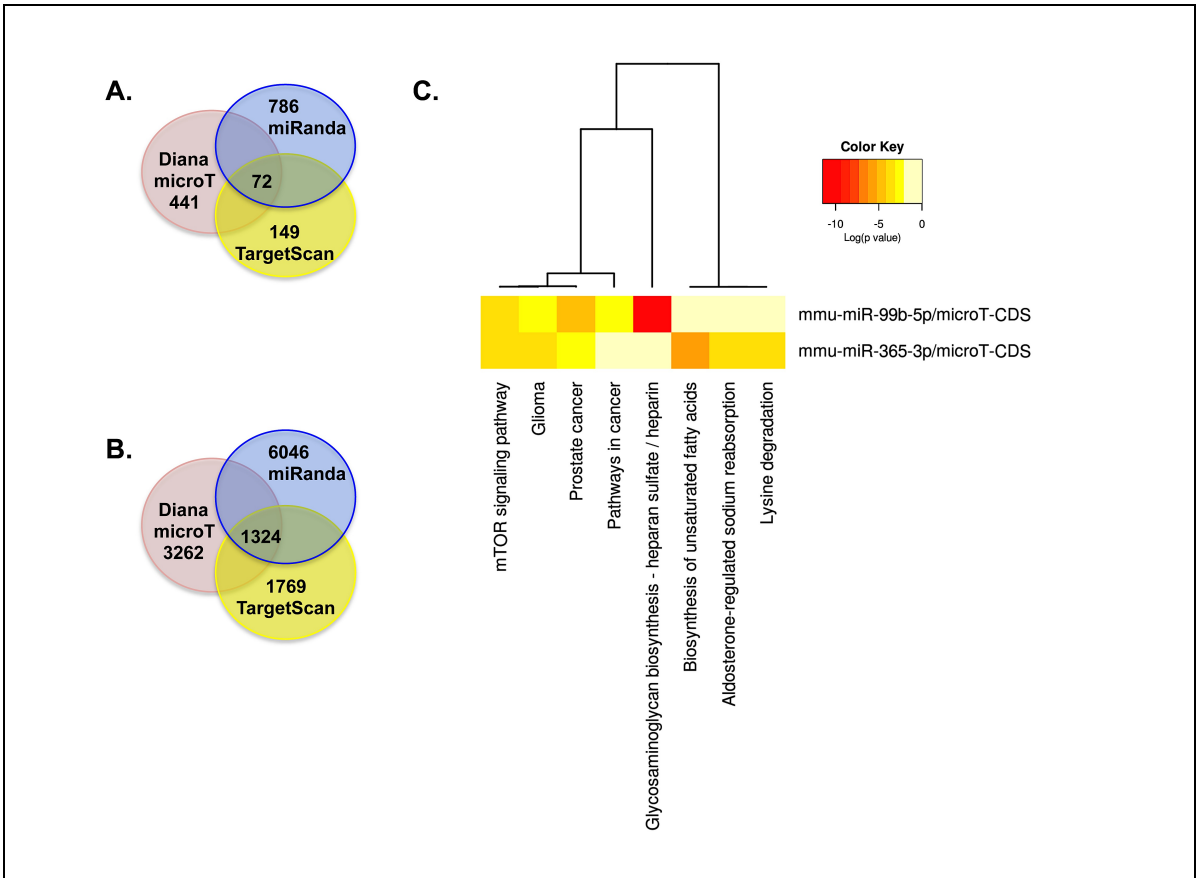

Figure 4.4. Pathway prediction analysis for miR-99b and miR-365. Computational prediction databases, DIANA-microT-CDS, TargetScan and miRanda together predicted (A) 72 common genes as miR-99b targets and (B) 1324 common genes as miR-365 targets. (C) Heat map of predicted pathways targeted by these miRNAs. Red color indicates lower p values.

Combined DIANA-miRPath analysis predicted heparin sulfate/heparin, prostate cancer, and mTOR signaling pathways are most likely to be targeted by miR-99b, whereas mTOR, gliomas and biosynthesis of unsaturated fatty acids are the top predicted pathways most likely to be targeted by miR-365 (Figure 4.4 C). Because the mTor pathway was predicted to be enriched for both miR-99b and miR-365 targets, this pathway was examined further (Figure 4.5). Predicted miR-99b targets in the mTOR pathway were mTor and the fg1r (insulin growth factor 1 receptor) (Table 4.1). Predicted miR-365 target genes regulating signaling in the mTOR pathway were Rheb (Ras homolog enriched in brain), p110 α subunit of PI3K (phosphotidylinositol-3 kinase catalytic subunit), and Ifg1 (insulin growth factor) (Table 4.2). The importance of mTOR signaling in osteoclastogenesis has been previously demonstrated. In osteoclasts, M-CSF signaling is crucial for osteoclast survival; this effect is mediated through mTOR. mTOR downregulates expression of Bim, a pro apoptotic gene and promotes osteoclast survival [276-278]. Moreover, recent studies demonstrated that inhibition of mTOR led to reduction in osteoclast formation and resorption [279-281].

miR-99b has been shown to directly target and downregulate mTOR and Akt1, thereby affecting mTOR/Akt/PI3K signaling pathway critical to mediate most cellular responses including proliferation, migration and survival [276-278]. miR-99b has been identified as a tumor suppressor in several cancer studies due to its role in regulating cell proliferation and migration. That the miRPath software detected miRNA-target interactions have already been validated reflects the promise of this approach.

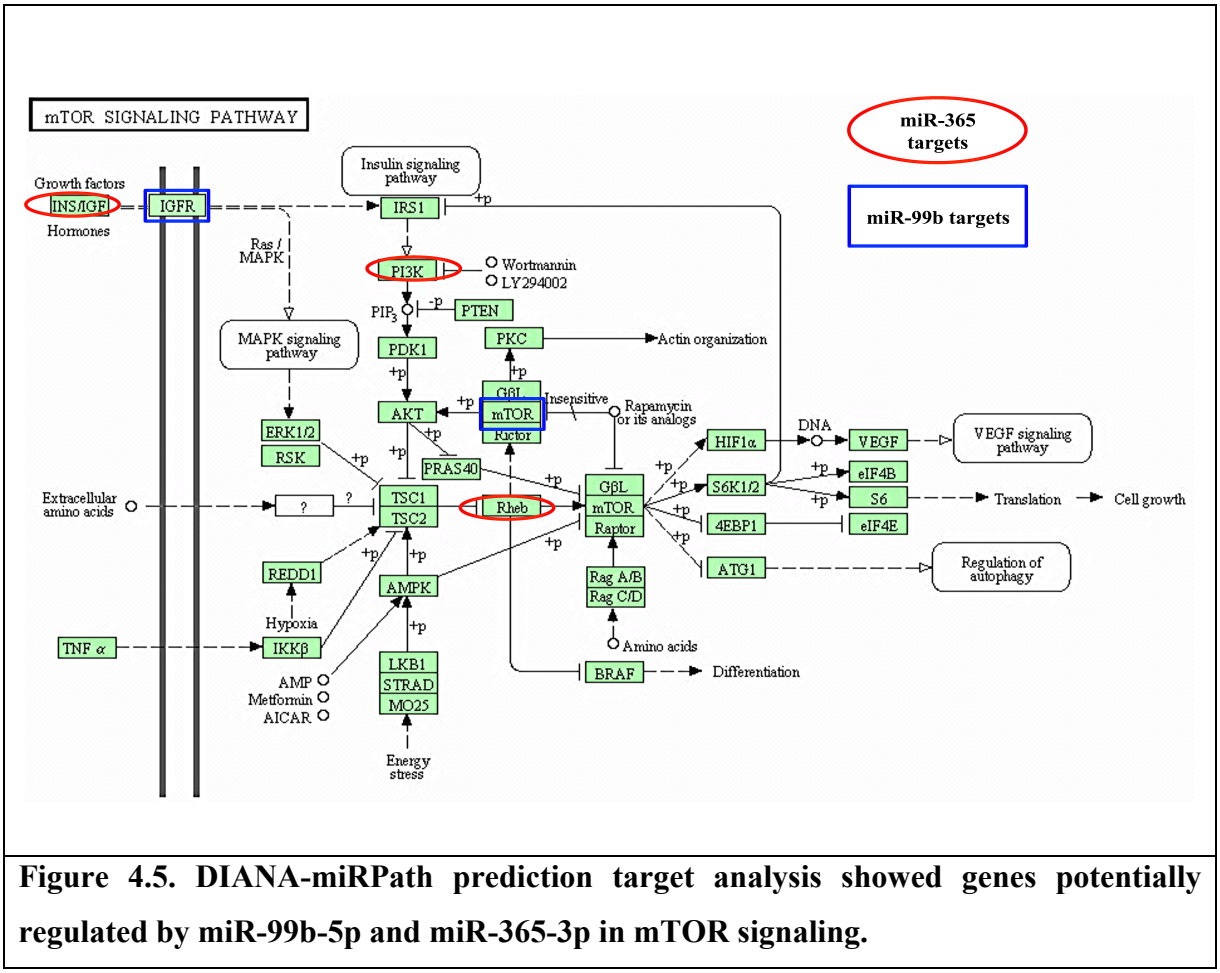

Figure 4.5. DIANA-miRPath prediction target analysis showed genes potentially regulated by miR-99b-5p and miR-365-3p in mTOR signaling.

Type I IGF receptor (IGF1R), predicated to be a miR-99b target, (Table 4.1) was recently validated as a miR-99b target [140]. In bone, IGF1 receptors are expressed by osteoblasts, osteocytes and osteoclasts. A positive role of IGF1/IGF1R signaling in promoting osteoblast commitment, differentiation and function has been previously demonstrated. Moreover, global deficiency of IGF1 decreases osteoclastogenesis by impairing the interaction of osteoclast precursors with osteoblasts [282, 283]. However, to definitely deduce the function of IGF1 signaling in osteoclasts, generating an osteoclast specific IGF1R deletion using CD11b or Cathepsin K-Cre mouse model would be necessary.

Table 4.1 Predicted binding sites for miR-99b-5p in the 3' UTR of target genes using miRanda computation database

miR-99b-5p target genes	mirSVR Score
3' gcGUUCCAGCCA--AGAUGCCCAc 5' mmu-miR-99b :||| | || :||||||| 5690:5' ucUAAGUCCAGUAGAUUACGGGUa 3' Igf1r	-0.0700
3' gcguuccagccaagAUGCCCAc 5' mmu-miR-99b ||||||| 275:5' ggguaacugagaaaUACGGGUu 3' Mtor	-1.2245

Rheb (Ras homolog enriched in brain) was predicted to be a miR-365 target. It belongs to the Ras superfamily of GTPases, and activates mTOR to regulate energy metabolism in cells. Nutrient deprivation decreases mTOR activity, to reduce energy-associated activities like cell growth, and prolonged nutrient deficiency comprises cell survival [284]. Rheb has been shown to be able to rescue mTOR function in nutrient starved conditions, thereby indicating its importance in promoting cell survival and growth [285]. Global deficiency of Rheb leads to embryonic lethality with abrogation of multiple organ development [286]; in bone however, the function of Rheb has not been examined.

PI3K is a major signaling pathway activated by M-CSF and RANKL during osteoclastogenesis and it promotes osteoclast differentiation, motility and bone resorption [287, 288]. PI3K are classified as type IA and IB, and there are three catalytic subunits for class IA PI3K, including p110–α (encoded by Pik3ca), p110-β (encoded by Pik3cb), and p110-δ (encoded by Pik3cd). Catalytic subunits bind to one of the regulatory subunits, such as p85–α and its splicing variants p55–α and p50–α (encoded by Pik3r1). miR-365 is predicted to target

p110 α catalytic subunit. In osteoclasts, p110–α has been recognized as the more dominant PI3K subunit and in vitro inhibition of p110- α isoform-mediated signaling of PI3K directly inhibits osteoclastogenesis and bone resorption in vitro [289]. Global deficiency of p110-α leads to embryonic lethality, and although the impairment in bone resorption due to deficiency of p85–α regulatory subunit specifically in osteoclasts (Ctsk-Cre) has been demonstrated, the function of p110- α has not been validated in vivo [288, 290]. Using these computational tools, both genes and pathways targeted by miR-99b and miR-365 in osteoclasts can be predicted, to provide a rationale for the selection of potential targets and pathways to be validated experimentally.

Table 4.2 Potential binding site for miR-365-3p in the 3'UTR of target genes using miRanda computation database

miR-365-3p target genes	mirSVR Score
3' uauuccuaaaaauccCCGUAAu 5' mmu-miR-365 |||||| 1156:5' aacuuauuuaaacuuGGCAUUu 3' Pi3kca	-0.0618
3' uauUCCUAAAAAUCCCCGUAAu 5' mmu-miR-365 | || ||||| |||||| 248:5' accAAGAAUUUUAUCGGCAUUa 3' Rheb	-0.6501
3' uauuccuaaaaaUCCCCGUAAu 5' mmu-miR-365 | ||||||| 144:5' aacauuacaaagAUGGGCAUUu 3' Igf1	-0.8632

RNA immunoprecipitation

Although the bioinformatic tools can provide a vast pool of potential target genes for a specific miRNA, these target predictions are based on a certain set of assumptions, and there is still much we do not know about miRNA-target interactions. With the goal of providing an experimental, unbiased, high throughput approach for detecting miRNA target genes, RNA-immunoprecipitation techniques have been developed. These techniques exploit the RISC-miRNA-mRNA interaction, and RNA sequencing or microarray analysis. Together with bioinformatic analysis, this approach can provide enrichment in miRNA target genes and insight into the regulatory pathways that might be impacted by a test miRNA [291-293].

The technique is frequently performed by over expressing the test miRNA in cells, followed by pulldown of RISC proteins, which leads to the capture of test miRNA-enriched target genes. RISC proteins are frequently immunoprecipitated using an antibody against the essential RISC component, AGO. As an alternative, cells can also be transfected with a construct expressing a tagged RISC protein (i.e. c-myc-tag, 6x-histidine-tag, biotin-tag), allowing RISC immunoprecipitation using antibody against the tag [294].

mRNAs bound to immunoprecipitated RISC are then analyzed by a high throughput approach such as microarray, in a process termed RIP-ChIP (ribonucleoprotein immunoprecipitation followed by microarray chip analysis) or sequencing termed RIP-Seq (ribonucleoprotein immunoprecipitation followed by high-throughput sequencing). Comparison of RISC-bound mRNA targets in cells overexpressing a miRNA versus a control miRNA provides the panel of mRNAs that may be potentially enriched in the miRNA targets. Based on the previously established approaches for RISC pull down, we sought to optimize an AGO pull

down technique as a first step for identification of miRNA targets in osteoblast and osteoclast lineage cells. Since different AGO (1-4) proteins vary in their preference for binding miRNAs and have different efficacies [85, 295], we chose to use 2A8 anti-AGO antibody for RISC immunoprecipitation [296]. This antibody recognizes all four AGO proteins from mouse and human, making it applicable for miRNA pull down in RAW264.7 cells (derived from a mouse source) and hFOB 1.19 cells (derived from a human source). Initial immunoprecipitation of RISC was performed in hFOB1.19 cells using 2A8 antibody, and as a negative control, a non-immune IgG was used. Protein samples were prepared from total cell lysate (input), lysate that was bound to anti-AGO or IgG, and the unbound material from immunoprecipitation. Immunoblotting indicated presence of AGO (band corresponding to ~95kDa) in total cell lysate and the lysate fraction bound to anti-AGO. With 2A8-immunoprecipitation, ~7 fold more AGO protein was captured compared to the total cell lysate. A band at ~70 kDa, corresponding to the actin binding protein Radixin was also detected due to its cross reaction with 2A8 antibody (Figure 4.6 A). Radixin has no known role in miRNA regulation [296] and was also detected in the total cell lysate, and the unbound fractions. Interestingly, radixin was detected in the IgG bound lysates, but not Ago-bound.

To examine miRNA coimmunoprecipitation with AGO, we performed qRT-PCR using RNA obtained from AGO- and IgG- pull down. In hFOB1.19 cells, qRT-PCR demonstrated that more than ~900 fold enrichment in miR-29a was achieved through AGO-IP compared to IgG negative control (Figure 4.6 B). We performed the same procedure in RAW264.7 cells subsequently and showed ~ 300 fold enrichment in miR-29c using qRT-PCR (Figure 4.6 C). In conclusion, we confirmed the consistent efficiency of our AGO immunoprecipitation and this

optimized protocol will provide a firm foundation toward future studies aimed at identifying miRNA targets in osteoblasts and osteoclasts, in a non-biased manner.

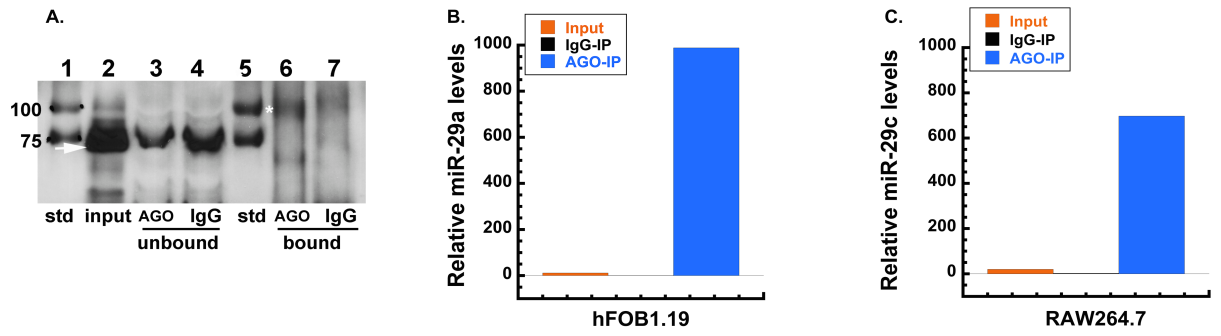

Figure 4.6. Argonaute coimmunoprecipitates are enriched for miRNAs. Lysates from hFOB1.19 cells were immunoprecipitated with anti-AGO or IgG (negative control) antibody. Immunoblotting for AGO in hFOB1.19 cells, samples include input: total lysate, Ago-, IgG-unbound and bound proteins (A). AGO1-4 band (~70-95kDa) (asterisk); radixin cross-reactive band (~70kDa) (arrow). RNA samples obtained from hFOB1.19, input: total lysate RNA, IgG- and AGO- bound RNA and AGO- bound RNA. Transcript levels of miR-29a were quantified and normalized to RNU48 endogenous control (B). RNA samples obtained from RAW264.7 cells, input: total lysate RNA, IgG- and AGO- bound RNA and AGO- bound RNA. Transcript levels of miR-29c were quantified and normalized to U6 endogenous control (C).

Discussion

To summarize our findings, we showed that, in a population of primary murine bone marrow cells enriched for osteoclast progenitors, RANKL mediated osteoclastogenesis increased miR-99b and -365 levels, while miR-451 levels were down regulated. We demonstrated that in the down regulation of miR-99b impaired osteoclast differentiation, leading to reduced osteoclast

number and size. Our computational pathway predictions suggest that the positive role of miR-99b might involve fine-tuning of NF-κB signaling. In contrast, miR-365 was shown to negatively regulate osteoclastogenesis. Computational predictions suggest that both miR-99b and miR-365 may target genes important for mTOR signaling, which is crucial for osteoclast formation and apoptosis. With the goal of designing an unbiased approach to identify miRNA target genes, we optimized an AGO immunoprecipitation technique, to pull down miR-RISC-mRNA complexes for analysis in osteoblasts and osteoclasts.

miR-99b is transcribed in an evolutionary conserved cluster on mouse chromosome 17, which includes let-7e and miR-125a. All of which were significantly upregulated during osteoclastogenesis, as reported by our microarray data and by others [138, 140]. miR-99b belongs to miR-99 family that includes miR-99a and -100. Both miR-99a and -99b have a similar seed sequence, except for a single nucleotide difference, suggesting that they likely target the same genes. Interestingly, in our microarray, expression of miR-99a and miR-100 were also up regulated during osteoclastogenesis.

A recent study confirmed our findings about the positive role of miR-99b in human osteoclasts, and identified a NF-κB binding site near the transcription start site (TSS) of the miR-99b~let-7e~miR-125a cluster [140]. Chromatin immunoprecipitation demonstrated increased binding of p65 NF-κB to this region during osteoclast differentiation, providing a mechanism for the upregulation of miR-99b during osteoclastogenesis. Remarkably, their study also showed significant upregulation of miR-99b cluster in immature osteoclasts compared to macrophages

and dendritic cells, thereby indicating that this cluster might act as a regulatory switch for osteoclast commitment [140].

miRNA-99b is also upregulated in dendritic cells and monocytes during inflammation [299]. Furthermore, miR-99b was shown to directly target Tnfα, Tnfrsf4 (Tumor Necrosis Factor Receptor Superfamily, Member 4), and TRAF2 (TNF receptor-associated factor 2), in other cell types. This implies regulation of the TNFα (tumor necrosis factor α) signaling pathway, which promotes osteoclastogenesis [297, 299].

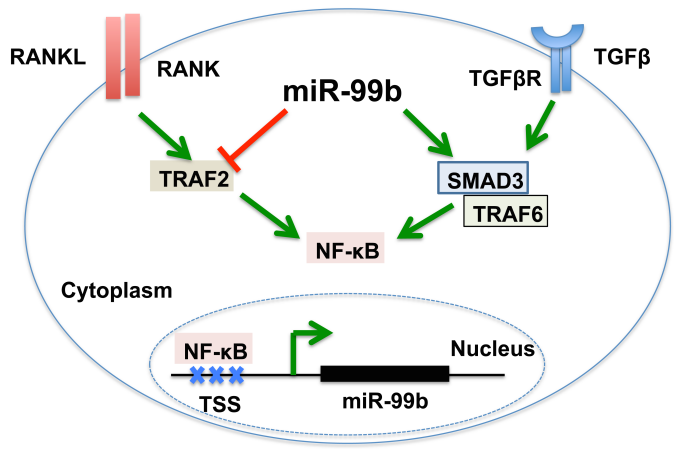

Figure 4.7. Potential working model for miR-99b role in osteoclastogenesis. miR-99b in osteoclasts may be potentially involved in fine-tuning of NF- κB signaling to promote osteoclast formation. miR-99b may potentially inhibit NF-κB expression by targeting TRAF2 gene [297]. While miR-99b induced SMAD3 phosphorylation leads to NF-κB activation through SMAD3/TRAF6 interaction [298]. NF-κB promotes miR-99b expression in osteoclasts [140].

During osteoclastic differentiation, membrane bound RANK mediates its signal transduction through TRAFs, to activate a series of downstream cascades including NF-κB, PI3K/Akt, p38/JNK and calcium/calmodulin pathways [37-39]. Together, these pathways

regulate cell proliferation, migration, differentiation and survival. miR-99b has been also shown to promote SMAD3 phosphorylation in cells of mouse mammary gland [298]. Interestingly, SMAD3 promotes osteoclast formation, and interacts with TRAF6-TAB1-TAK1 molecular complex [300]. In osteoclasts, upon RANKL stimulation, TRAF6 is recruited to form a complex with TAK1 (TGF-beta activated kinase 1, MAPKKK family member) and activate PI3K, MAPKs and NF-κB pathways [301]. This indicates that the upregulation in miR-99b during osteoclastogenesis may play a role in fine-tuning NF- κB signaling [28, 250]. Since inhibition of miR-99b decreased osteoclast differentiation, it is likely that the appropriate balance between these signaling pathways is important for the differentiation process.

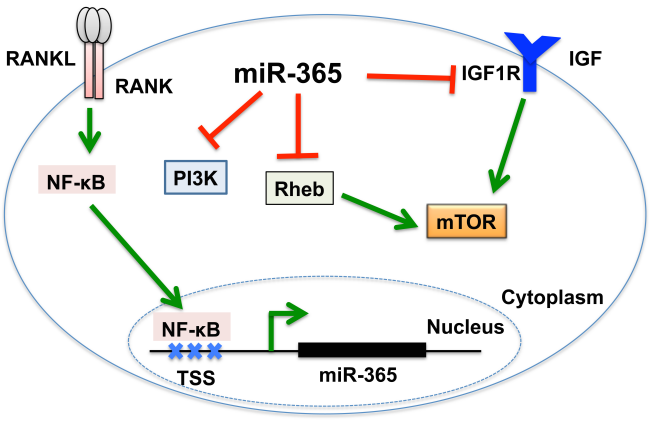

Figure 4.8. Potential working model for miR-365 inhibition of osteoclastogenesis. Negative role of miR-365 may likely involve inhibition of PI3 Kinase and mTOR signaling. Predicted miR-365 targets relevant in these signaling mechanisms include PI3K, Rheb, and IGF1R.

miR-365 is transcribed from two independent genetic loci (miR-365-2 on mouse chromosomes 11 and miR-365-1 on chromosome 16), that give rise to the identical mature miRNA and expression of miR-365-1 was shown to be activated by Sp1 and NF-κB, two

transcription factors that promote osteoclastogenesis [302]. In osteoclasts, we showed miR-365 to negatively regulate osteoclast differentiation. Our computational predictions suggest that miR-365 may regulate key signaling pathways in osteoclasts including mTOR and PI3K signaling. In osteoclasts, PI3K/ Akt and mTOR pathways coordinated to promote osteoclast differentiation, migration and resorption [280, 287, 303-305]. miR-365 levels likely play a role in this coordination to promote optimal osteoblast differentiation and function.

Recently there have been some technical advancements, to improve high throughput capture of miRNA targets. Techniques used for miRNA target capture so far include indirect and direct approaches. The indirect approaches for Ago-RNA immunoprecipitation rely on transfection of cells with miRNA mimics or inhibitors followed, by high throughput transcriptome analysis through microarray or sequencing. Transcriptome analysis fails to detect the mRNAs that are regulated primarily by translational repression. This can be overcome by proteomic analysis following AGO pulldown. A rather cost effective alternative to proteome analysis for miRNA targets is polysome profiling; where after miRNA overexpression, mRNAs bound to the ribosomes are captured and profiled by deep sequencing.

To enhance the mRNA target capture, modifications have been made to RISC immunoprecipitations, to improve the miRNA-RISC-mRNA interaction, in a technique termed CLIP (crosslinking and immunoprecipitation). For the CLIP technique, following miRNA overexpression, RISC proteins are U.V. (ultraviolet) cross-linked with the RNAs and immunoprecipitated to capture mRNA targets [89, 294, 306]. CLIP is combined with high throughput sequencing HTS-CLIP (high-throughput sequencing of CLIP- cross linking with UVc-254nm) to identify captured miRNA targets. Modifications to HTS-CLIP have been made

in form of PAR-CLIP (Photoactivatable ribonucleoside enhanced CLIP) technique. In PAR-CLIP photoreactive ribonucleoside analogues are incorporated into RNAs before their crosslinking to protein via exposure to UVa-365nm [307-309]. However, disadvantages to the above mentioned target identification techniques remain. For example, they cannot distinguish between direct and indirect miRNA targets; they enable interaction of non-miRNA targets to RISC, thereby yielding false positives; and these indirect approaches require additional computational predictions to select direct miRNA targets for experimental validation [294].

To overcome these issues, the novel technique of miR-CLIP (microRNA crosslinking and immunoprecipitation) was developed. In this technique, pre-miRNAs modified with psoralen and biotin are transfected in cells for miRNA overexpression. Following photoactivatable crosslinking of RISC protein and RNA, immunoprecipitation of both RISC and tagged miRNA is performed. In this way, mRNA targets specific for the tagged miRNA are captured and identified by deep sequencing, and the stringency in mRNA target capture is enhanced [310]. Using modifications that enable identification of physiologically relevant targets without overexpression or depletion of miRNA would be key to provide insight about miRNA regulatory mechanisms in natural environment of transcript.

To summarize we determined the function of miR-365 and miR-99b in osteoclasts, and used available miRNA target prediction computational tools to identify potential pathways that might be regulated by these miRNAs. This provides a rationale for selecting potential miRNA targets to be validated experimentally. We also optimized, in osteoclastic and osteoblastic cells, an AGO-immunoprecipitation technique that can be utilized to identify putative miRNA targets.

Chapter 5

Summary, significance and conclusions

Summary

The overall goal of this study was to understand how specific miRNAs regulate osteoblast and osteoclast differentiation and function, and thereby skeletal phenotype.

We first determined whether miRNAs play a part in the differential regulation of osteonectin 3' UTR SNP haplotypes. A previous candidate gene study had associated osteonectin 3' UTR SNP 1599 (rs1054204) with low bone mass in a cohort of idiopathic osteoporosis patients [186]. We identified the mechanism underlying this association by generating and analyzing knock-in mouse models for human osteonectin SNP 1599. We found that this SNP mediated differential regulation of the osteonectin 3' UTR, and demonstrated differential targeting by miR-433. In vivo, SNP 1599 variants displayed differences in trabecular bone volume and a differential response to a bone-anabolic PTH regimen. Ex vivo studies demonstrated that SNP 1599 caused a cell autonomous alteration in osteoblast differentiation markers and mineralized matrix deposition. Altogether, we were able to assign a function to a common variant SNP 1599, and demonstrated that SNPs can regulate skeletal phenotype through mechanisms involving miRNAs (Chapter 3).

With regard to miRNAs and osteoclasts, we determined functions of three novel miRNAs, miR-99b, -365 and -451, in osteoclast differentiation. Microarray analysis previously suggested that these miRNAs could be strongly regulated during the osteoclastic differentiation

of progenitors derived from murine primary bone marrow monocytes [138]. We observed a RANKL mediated upregulation in miR-99b and -365 levels during osteoclast differentiation; whereas expression of miR-451 declined. Our in vitro studies demonstrated that miR-99b is crucial for osteoclast differentiation; its knock down led to fewer osteoclasts. In contrast, knock down of miR-365 led to increased osteoclast number. Lastly, modulation of miR-451 levels did not impact osteoclastogenesis.

To start deciphering the molecular mechanisms that might be regulated by these miRNAs during osteoclast differentiation, we performed a computational target-pathway prediction analysis. These predictions suggested that miR-99b and miR-365 might regulate osteoclast differentiation through fine-tuning signaling in mTOR pathway. Apart from computational predictions, we aimed to design an unbiased, high throughput experimental approach involving RNA immunoprecipitation, for identifying miRNA targets in osteoblasts and osteoclasts. We optimized immunoprecipitating the AGO component of RISC complexed to miRNA:mRNA target pairs. Through immunoblotting and qRT-PCR analysis we demonstrated that these immunoprecipates are greatly enriched for miRNAs. Our subsequent studies will entail designing a miRNA overexpression system and high throughput analysis, such as RNA sequencing, to capture miR-99b and miR-365 targets in osteoclasts (Chapter 4). Through these studies we will identify new targets of miR-99b and -365, and expand our understanding of osteoclast biology.

Significance

Bone mass is a heritable trait and an increasing number of GWAS have detected BMD-associated SNPs in protein coding and the non-coding genes. Currently used fracture risk assessment models are based on clinical, demographic and anthropomorphic information such as BMD, family history and lifestyle. The addition of genetic profiling data could greatly improve the accuracy of such prognostic models, and potentially help inform treatment strategies. However, for genetic profiling data to have an important impact on fracture risk assessment, the identification of many more genetic variants with a verified function in bone mass is crucial. Our study is unique, in that we have validated and assigned a physiological function to a common SNP variant previously associated with bone mass in a candidate gene study.

Moreover, the SNP we validated is a non-coding gene variant and is a miRNA-associated SNP. Our study provides evidence for implicating miRNA-associated SNPs in skeletal diseases, and suggests miRNAs are crucial regulators of skeletal phenotype. SNP variants related to miRNA function can be incorporated into diagnostic screens for individualized risk assessment.

Although the role of microRNAs in regulating bone development and homeostasis has been recognized, the underlying mechanisms are not well understood, and such an understanding is critical for designing novel clinical interventions involving miRNA-based therapeutics. Recent studies have implicated miRNAs in the pathogenesis of osteoporosis. For example, increased levels of five circulating miRNAs were found in the serum and bone tissue of osteoporotic patients, suggesting a potential opportunity for using serum miRNAs as diagnostic biomarkers

for osteoporosis [144, 311]. Current strategies for diagnosis of osteoporosis rely on BMD measurement by DXA. Although a non-invasive, changes in BMD are small and are often detected by DXA only at the latter stages of disease progression. Circulating miRNAs may serve as improved biomarkers in the early stages of osteoporosis.

The majority of studies examining miRNA function in bone biology have narrowly focused on specific miRNA targets or one regulatory mechanism at a time. As part of our studies, we optimized the first step of a global, unbiased, high throughput approach for identifying microRNA-target interactions in bone cells. Moreover, we also demonstrated the utility of a pathway-based bioinformatic approach to miRNA target prediction, which could ease interpretation of large data sets and help establish connectivity of miRNA-dependent regulatory networks. This could facilitate building a hypothesis-driven approach to understanding the function of miRNAs in bone cells. Moreover, knowledge from our study can be used to deduce to function of miRNAs (miR-365, -99b and -433) in other tissues as well. In doing so, we have provided a ‘big picture’ approach, which will be important for therapeutic intervention, to better predict potential side effects or unintended outcomes.

Concluding remarks and future prospects

Accumulating evidence of the importance of miRNAs role in the skeleton has prompted the development in profiling approaches to identify miRNAs associated with skeletal diseases, as well as the development of new computational tools and high throughput screening techniques to discover novel miRNA-target interactions. With these developments, targeting microRNA-based regulatory mechanisms is an emerging therapeutic strategy.

In the field of miRNA-based therapeutics, developments have focused on designing and delivering stable mimetics or inhibitors for sustained alteration of miRNA activity in vivo. For augmenting the stability of miRNA mimics or inhibitors, oligonucleotide sequences are subjected to chemical modifications including 2-O-methyl (2'-O-Me), locked nucleic acid (LNA), and peptide nucleic acid (PNA) variants. For efficient delivery of chemically modified miRNA mimics or inhibitors, currently used synthetic systems include lipid-based complexes, polyethylenimine (PEI), polylactide-co-glycolide (PLGA) based particles, and modified peptides. Naturally occurring polymers that seem to enhance cell uptake, such as chitosan, protamine, atelocollagen and cell-penetrating peptides (CPP) have also been used for delivery of miRNA therapeutics [312]. With designing efficient delivery systems, focus has now shifted towards technology for cell/tissue specific delivery.

Currently, two clinical trials for miRNA-based therapeutics against hepatitis C and cancer are being conducted. The most advanced clinical trial to date examines the therapeutic potential of miR-122 inhibitor against the hepatitis C virus. miR-122 is abundantly expressed in liver, and

miR-122 binds to two closely spaced target sites within the 5' non-coding region of the hepatitis C virus genome, that is necessary to maintain the abundance of viral RNA. Sequestration of miR-122 using anti-miR reduces the virus replication. In this application, two anti-miR-122 therapeutics have been developed, one with an N-acetylegalactosamine (GalNAC) conjugate (Regulus Therapeutics) and the other with an LNA conjugate (Santaris Pharma). Of these, the LNA-anti-miR-122 termed Miravirsen has cleared phase I and is undergoing phase II of clinical trials [313].

The second microRNA therapeutic under clinical trial is MRX34, which is a miR-34a mimic developed against primary liver cancer and solid cancers that metastasize to liver. MRX34 was developed by miRNA Therapeutics Company, and is in phase I of clinical trials. Decrease in expression of miR-34a has been shown in cervical cancer, ovarian cancer, glioblastoma, hepatocellular carcinoma, colon cancer, non-small cell lung cancer (NSCLC). miR-34a, a tumor suppressor, has been shown to repress oncogenes such as CDK4 (cyclin dependent kinase 4) that promotes cell cycle progression; BCL2 (B cell lymphoma 2) that blocks apoptosis, and Wnt1/3 that promotes cell proliferation. Decreased miR-34a expression has been shown in cervical cancer, ovarian cancer, glioblastoma, hepatocellular carcinoma, colon cancer, non-small cell lung cancer (NSCLC). Increasing levels of miR-34a in cancer cells using MRX34 antagonizes key hallmarks including self-renewal and migratory potential [314, 315].

For tissue specific delivery of miRNA-therapeutics to the skeleton, biomaterials, nanoparticles and peptide-mediated approaches have been developed. As an example of

biomaterial based approach, one recent study demonstrated repair of a mouse critical size calvarial defect using a polyglycerol sebacate (PGS) scaffold loaded with BMSCs transfected with anti-miR-31. Inhibition of miR-31 was shown to promote osteoblastic differentiation and function, leading to enhanced bone formation [316].

For modulation of mesenchymal stem cells (MSCs), nanoparticle and gelatin nanofibers-based strategies have been developed for miRNA delivery [317, 318]. For example, gelatin nanofibers scaffolds incorporating miR-29a inhibitor improved extracellular matrix production by pre-osteoblasts. In osteoblasts, miR-29 family has been previously shown to inhibit extracellular matrix production and regulate Wnt signaling. Inhibition of miR-29 signaling in pre-osteoblasts promotes collagen and osteonectin synthesis, upregulates Igf1 and Tgfβ mRNA expression, and promotes osteoblastic commitment [213, 219, 318]. Another study used nanoparticles tagged to a photolabile linker to deliver miR-148b mimics to human adipose derived stem cells (hASCs). miR-148b mimics incorporated scaffolds when seeded with hASCs demonstrate improved bone formation at the critical size calvarial defect in vivo [319]. An example of peptide-mediated approaches for intracellular miRNA delivery included an arginine-rich cell penetrating peptide to deliver miR-29b mimic to human mesenchymal stem cells in vitro. This delivery greatly improved transfection efficiency and promoted their osteoblastic differentiation [320].

Strategies to enhance miRNA delivery to osteoblasts and osteoclasts have also been recently developed. For example, D-Asp8 peptide conjugated liposomes were developed to deliver anti-miR-148a to osteoclasts. D-Asp8, consisting of eight repeating sequences of

aspartate, provides enhanced specificity for binding to crystallized hydroxyapatite on bone resorptive surface. This innovative targeting system was capable of downregulating miR-148a in osteoclasts, resulting in reduced bone resorption in vivo. Non-detectable or extremely low levels of tagged-anti-miR-148a was observed in other tissues [321]. Interestingly, increased miR-148a expression has been associated with osteoporosis in other studies, providing a potential for use of miR therapeutics [144].

In conclusion, recent advances in understanding the function of miRNAs in the skeleton suggest their potential as therapeutic targets and as therapeutic entities. Since miRNAs primarily function in fine-tuning multiple signaling cascades, understanding the role of miRNA in vivo by using transgenic mouse models will be crucial. Moreover, transgenic miRNA mouse models can also prove valuable for testing miRNA-based therapeutics. Moving forward, with the implication of miRNA-SNPs in skeletal diseases and identification of miRNAs important for bone mass, we believe that miRNAs will play a crucial role in for personalized diagnostics and therapeutics for osteoporosis.

References:

[1] Cosman F, de Beur SJ, LeBoff MS, Lewiecki EM, Tanner B, Randall S, Lindsay R. Clinician's Guide to Prevention and Treatment of Osteoporosis. Osteoporos Int 2014;25: 2359-81.
[2] Yang Y. Skeletal Morphogenesis and Embryonic Development. In: Primer on the Metabolic Bone Diseases and Disorders of Mineral Metabolism: John Wiley & Sons, Inc.; 2013, p. 1-14.
[3] Raisz LG. Physiology and pathophysiology of bone remodeling. Clin Chem 1999;45: 1353-8.
[4] Raggatt LJ, Partridge NC. Cellular and molecular mechanisms of bone remodeling. J Biol Chem 2010;285: 25103-8.
[5] Neve A, Corrado A, Cantatore FP. Osteoblast physiology in normal and pathological conditions. Cell Tissue Res 2011;343: 289-302.
[6] Clarke B. Normal bone anatomy and physiology. Clin J Am Soc Nephrol 2008;3 Suppl 3: S131-9.
[7] Little RD, Carulli JP, Del Mastro RG, Dupuis J, Osborne M, Folz C, Manning SP, Swain PM, Zhao SC, Eustace B, Lappe MM, Spitzer L, Zweier S, Braunschweiger K, Benchekroun Y, Hu X, Adair R, Chee L, FitzGerald MG, Tulig C, Caruso A, Tzellas N, Bawa A, Franklin B, McGuire S, Nogues X, Gong G, Allen KM, Anisowicz A, Morales AJ, Lomedico PT, Recker SM, Van Eerdewegh P, Recker RR, Johnson ML. A mutation in the LDL receptor-related protein 5 gene results in the autosomal dominant high-bone-mass trait. Am J Hum Genet 2002;70: 11-9.
[8] Yamashita T, Takahashi N, Udagawa N. New roles of osteoblasts involved in osteoclast differentiation. World J Orthop 2012;3: 175-81.
[9] Xing L, Schwarz EM, Boyce BF. Osteoclast precursors, RANKL/RANK, and immunology. Immunol Rev 2005;208: 19-29.
[10] Bonewald LF. The amazing osteocyte. J Bone Miner Res 2011;26: 229-38.
[11] Nakashima K, de Crombrugghe B. Transcriptional mechanisms in osteoblast differentiation and bone formation. Trends Genet 2003;19: 458-66.
[12] Komori T, Yagi H, Nomura S, Yamaguchi A, Sasaki K, Deguchi K, Shimizu Y, Bronson RT, Gao YH, Inada M, Sato M, Okamoto R, Kitamura Y, Yoshiki S, Kishimoto T. Targeted disruption of Cbfa1 results in a complete lack of bone formation owing to maturational arrest of osteoblasts. Cell 1997;89: 755-64.
[13] Adhami MD, Rashid H, Chen H, Clarke JC, Yang Y, Javed A. Loss of Runx2 in committed osteoblasts impairs postnatal skeletogenesis. J Bone Miner Res 2015;30: 71-82.
[14] Adhami MD, Rashid H, Chen H, Javed A. Runx2 activity in committed osteoblasts is not essential for embryonic skeletogenesis. Connect Tissue Res 2014;55 Suppl 1: 102-6.
[15] Ducy P, Starbuck M, Priemel M, Shen J, Pinero G, Geoffroy V, Amling M, Karsenty G. A Cbfa1-dependent genetic pathway controls bone formation beyond embryonic development. Genes Dev 1999;13: 1025-36.
[16] Karsenty G, Ducy P, Starbuck M, Priemel M, Shen J, Geoffroy V, Amling M. Cbfa1 as a regulator of osteoblast differentiation and function. Bone 1999;25: 107-8.

[17] Sinha KM, Zhou X. Genetic and molecular control of osterix in skeletal formation. Journal of Cellular Biochemistry 2013;114: 975-984.
[18] Baek WY, Lee MA, Jung JW, Kim SY, Akiyama H, de Crombrugghe B, Kim JE. Positive regulation of adult bone formation by osteoblast-specific transcription factor osterix. J Bone Miner Res 2009;24: 1055-65.
[19] Canalis E, Economides AN, Gazzerro E. Bone morphogenetic proteins, their antagonists, and the skeleton. Endocr Rev 2003;24: 218-35.
[20] Broege A, Pham L, Jensen ED, Emery A, Huang TH, Stemig M, Beppu H, Petryk A, O'Connor M, Mansky K, Gopalakrishnan R. Bone morphogenetic proteins signal via SMAD and mitogen-activated protein (MAP) kinase pathways at distinct times during osteoclastogenesis. J Biol Chem 2013;288: 37230-40.
[21] Chen D, Ji X, Harris MA, Feng JQ, Karsenty G, Celeste AJ, Rosen V, Mundy GR, Harris SE. Differential roles for bone morphogenetic protein (BMP) receptor type IB and IA in differentiation and specification of mesenchymal precursor cells to osteoblast and adipocyte lineages. J Cell Biol 1998;142: 295-305.
[22] Wan M, Cao X. BMP signaling in skeletal development. Biochem Biophys Res Commun 2005;328: 651-7.
[23] Zhao M, Harris SE, Horn D, Geng Z, Nishimura R, Mundy GR, Chen D. Bone morphogenetic protein receptor signaling is necessary for normal murine postnatal bone formation. J Cell Biol 2002;157: 1049-60.
[24] Kato M, Patel MS, Levasseur R, Lobov I, Chang BH, Glass DA, 2nd, Hartmann C, Li L, Hwang TH, Brayton CF, Lang RA, Karsenty G, Chan L. Cbfa1-independent decrease in osteoblast proliferation, osteopenia, and persistent embryonic eye vascularization in mice deficient in Lrp5, a Wnt coreceptor. J Cell Biol 2002;157: 303-14.
[25] Johnson ML. LRP5 and bone mass regulation: Where are we now? Bonekey Rep 2012;1: 1.
[26] Baron R, Kneissel M. WNT signaling in bone homeostasis and disease: from human mutations to treatments. Nat Med 2013;19: 179-192.
[27] Ross FP. M-CSF, c-Fms, and signaling in osteoclasts and their precursors. Ann N Y Acad Sci 2006;1068: 110-6.
[28] Sato K, Suematsu A, Nakashima T, Takemoto-Kimura S, Aoki K, Morishita Y, Asahara H, Ohya K, Yamaguchi A, Takai T, Kodama T, Chatila TA, Bito H, Takayanagi H. Regulation of osteoclast differentiation and function by the CaMK-CREB pathway. Nat Med 2006;12: 1410-6.
[29] Charles JF, Aliprantis AO. Osteoclasts: more than 'bone eaters'. Trends Mol Med 2014;20: 449-59.
[30] Novack DV, Teitelbaum SL. The Osteoclast: Friend or Foe? Annual Review of Pathology: Mechanisms of Disease 2008;3: 457-484.
[31] Cappariello A, Maurizi A, Veeriah V, Teti A. Reprint of: The Great Beauty of the osteoclast. Archives of Biochemistry and Biophysics 2014;561: 13-21.
[32] Vaananen HK, Zhao H, Mulari M, Halleen JM. The cell biology of osteoclast function. J Cell Sci 2000;113 (Pt 3): 377-81.
[33] Grigoriadis AE, Wang ZQ, Cecchini MG, Hofstetter W, Felix R, Fleisch HA, Wagner EF. c-Fos: a key regulator of osteoclast-macrophage lineage determination and bone remodeling. Science 1994;266: 443-8.

[34] Hu R, Sharma SM, Bronisz A, Srinivasan R, Sankar U, Ostrowski MC. Eos, MITF, and PU.1 recruit corepressors to osteoclast-specific genes in committed myeloid progenitors. Mol Cell Biol 2007;27: 4018-27.
[35] Kim JH, Kim N. Regulation of NFATc1 in Osteoclast Differentiation. J Bone Metab 2014;21: 233-41.
[36] Boyce BF. Advances in the regulation of osteoclasts and osteoclast functions. J Dent Res 2013;92: 860-7.
[37] Gravallese EM, Galson DL, Goldring SR, Auron PE. The role of TNF-receptor family members and other TRAF-dependent receptors in bone resorption. Arthritis Res 2001;3: 6-12.
[38] Kanazawa K, Kudo A. TRAF2 is essential for TNF-alpha-induced osteoclastogenesis. J Bone Miner Res 2005;20: 840-7.
[39] Yen ML, Hsu PN, Liao HJ, Lee BH, Tsai HF. TRAF-6 dependent signaling pathway is essential for TNF-related apoptosis-inducing ligand (TRAIL) induces osteoclast differentiation. PLoS One 2012;7: e38048.
[40] Asagiri M, Takayanagi H. The molecular understanding of osteoclast differentiation. Bone 2007;40: 251-264.
[41] Boyle W, Simonet WS, Lacey DL. Osteoclast differentiation and activation. Nature 2003;423: 337-42.
[42] Bruzzaniti A, Baron R. Molecular regulation of osteoclast activity. Rev Endocr Metab Disord 2006;7: 123-139.
[43] Axtell MJ, Westholm JO, Lai EC. Vive la différence: biogenesis and evolution of microRNAs in plants and animals. Genome Biol. 2011;12: 221.
[44] Fabian MR, Sonenberg N. The mechanics of miRNA-mediated gene silencing: a look under the hood of miRISC. Nature Structural & Molecular Biology 2012;19: 586-593.
[45] Gaur T, Hussain S, Mudhasani R, Parulkar I, Colby JL, Frederick D, Kream BE, van Wijnen AJ, Stein JL, Stein GS, Jones SN, Lian JB. Dicer inactivation in osteoprogenitor cells compromises fetal survival and bone formation, while excision in differentiated osteoblasts increases bone mass in the adult mouse. Dev Biol 2010;340: 10-21.
[46] Mizoguchi F, Izu Y, Hayata T, Hemmi H, Nakashima K, Nakamura T, Kato S, Miyasaka N, Ezura Y, Noda M. Osteoclast-specific Dicer gene deficiency suppresses osteoclastic bone resorption. J Cell Biochem 2010;109: 866-75.
[47] Kapinas K, Delany AM. MicroRNA biogenesis and regulation of bone remodeling. Arthritis Res Ther 2011;13: 220.
[48] van Wijnen AJ, van de Peppel J, van Leeuwen JP, Lian JB, Stein GS, Westendorf JJ, Oursler MJ, Im HJ, Taipaleenmaki H, Hesse E, Riester S, Kakar S. MicroRNA functions in osteogenesis and dysfunctions in osteoporosis. Curr Osteoporos Rep 2013;11: 72-82.
[49] Genomes Project C, Abecasis GR, Auton A, Brooks LD, DePristo MA, Durbin RM, Handsaker RE, Kang HM, Marth GT, McVean GA. An integrated map of genetic variation from 1,092 human genomes. Nature 2012;491: 56-65.
[50] Estrada K, Styrkarsdottir U, Evangelou E, Hsu YH, Duncan EL, Ntzani EE, Oei L, Albagha OM, Amin N, Kemp JP, Koller DL, Li G, Liu CT, Minster RL, Moayyeri A, Vandenput L, Willner D, Xiao SM, Yerges-Armstrong LM, Zheng HF, Alonso N, Eriksson J, Kammerer CM, Kaptoge SK, Leo PJ, Thorleifsson G, Wilson SG, Wilson JF, Aalto V, Alen M, Aragaki AK, Aspelund T, Center JR, Dailiana Z, Duggan DJ, Garcia M, Garcia-Giralt N, Giroux S, Hallmans G, Hocking LJ, Husted LB, Jameson KA, Khusainova R, Kim GS, Kooperberg C, Koromila T,

Kruk M, Laaksonen M, Lacroix AZ, Lee SH, Leung PC, Lewis JR, Masi L, Mencej-Bedrac S, Nguyen TV, Nogues X, Patel MS, Prezelj J, Rose LM, Scollen S, Siggeirsdottir K, Smith AV, Svensson O, Trompet S, Trummer O, van Schoor NM, Woo J, Zhu K, Balcells S, Brandi ML, Buckley BM, Cheng S, Christiansen C, Cooper C, Dedoussis G, Ford I, Frost M, Goltzman D, Gonzalez-Macias J, Kahonen M, Karlsson M, Khusnutdinova E, Koh JM, Kollia P, Langdahl BL, Leslie WD, Lips P, Ljunggren O, Lorenc RS, Marc J, Mellstrom D, Obermayer-Pietsch B, Olmos JM, Pettersson-Kymmer U, Reid DM, Riancho JA, Ridker PM, Rousseau F, Slagboom PE, Tang NL, Urreizti R, Van Hul W, Viikari J, Zarrabeitia MT, Aulchenko YS, Castano-Betancourt M, Grundberg E, Herrera L, Ingvarsson T, Johannsdottir H, Kwan T, Li R, Luben R, Medina-Gomez C, Palsson ST, Reppe S, Rotter JI, Sigurdsson G, van Meurs JB, Verlaan D, Williams FM, Wood AR, Zhou Y, Gautvik KM, Pastinen T, Raychaudhuri S, Cauley JA, Chasman DI, Clark GR, Cummings SR, Danoy P, Dennison EM, Eastell R, Eisman JA, Gudnason V, Hofman A, Jackson RD, Jones G, Jukema JW, Khaw KT, Lehtimaki T, Liu Y, Lorentzon M, McCloskey E, Mitchell BD, Nandakumar K, Nicholson GC, Oostra BA, Peacock M, Pols HA, Prince RL, Raitakari O, Reid IR, Robbins J, Sambrook PN, Sham PC, Shuldiner AR, Tylavsky FA, van Duijn CM, Wareham NJ, Cupples LA, Econs MJ, Evans DM, Harris TB, Kung AW, Psaty BM, Reeve J, Spector TD, Streeten EA, Zillikens MC, Thorsteinsdottir U, Ohlsson C, Karasik D, Richards JB, Brown MA, Stefansson K, Uitterlinden AG, Ralston SH, Ioannidis JP, Kiel DP, Rivadeneira F. Genome-wide meta-analysis identifies 56 bone mineral density loci and reveals 14 loci associated with risk of fracture. Nat Genet 2012;44: 491-501.

[51] Rivadeneira F, Styrkarsdottir U, Estrada K, Halldorsson BV, Hsu YH, Richards JB, Zillikens MC, Kavvoura FK, Amin N, Aulchenko YS, Cupples LA, Deloukas P, Demissie S, Grundberg E, Hofman A, Kong A, Karasik D, van Meurs JB, Oostra B, Pastinen T, Pols HA, Sigurdsson G, Soranzo N, Thorleifsson G, Thorsteinsdottir U, Williams FM, Wilson SG, Zhou Y, Ralston SH, van Duijn CM, Spector T, Kiel DP, Stefansson K, Ioannidis JP, Uitterlinden AG, Genetic Factors for Osteoporosis C. Twenty bone-mineral-density loci identified by large-scale meta-analysis of genome-wide association studies. Nat Genet 2009;41: 1199-206.

[52] Richards JB, Zheng HF, Spector TD. Genetics of osteoporosis from genome-wide association studies: advances and challenges. Nat Rev Genet 2012;13: 576-88.

[53] Mann V, Hobson EE, Li B, Stewart TL, Grant SF, Robins SP, Aspden RM, Ralston SH. A COL1A1 Sp1 binding site polymorphism predisposes to osteoporotic fracture by affecting bone density and quality. J Clin Invest 2001;107: 899-907.

[54] Garcia-Giralt N, Nogues X, Enjuanes A, Puig J, Mellibovsky L, Bay-Jensen A, Carreras R, Balcells S, Diez-Perez A, Grinberg D. Two new single-nucleotide polymorphisms in the COL1A1 upstream regulatory region and their relationship to bone mineral density. J Bone Miner Res 2002;17: 384-93.

[55] Garcia-Giralt N, Enjuanes A, Bustamante M, Mellibovsky L, Nogues X, Carreras R, Diez-Perez A, Grinberg D, Balcells S. In vitro functional assay of alleles and haplotypes of two COL1A1-promoter SNPs. Bone 2005;36: 902-8.

[56] Stewart TL, Jin H, McGuigan FE, Albagha OM, Garcia-Giralt N, Bassiti A, Grinberg D, Balcells S, Reid DM, Ralston SH. Haplotypes defined by promoter and intron 1 polymorphisms of the COLIA1 gene regulate bone mineral density in women. J Clin Endocrinol Metab 2006;91: 3575-83.

[57] Grant SF, Reid DM, Blake G, Herd R, Fogelman I, Ralston SH. Reduced bone density and osteoporosis associated with a polymorphic Sp1 binding site in the collagen type I alpha 1 gene. Nat Genet 1996;14: 203-5.

[58] Arnold M, Ellwanger DC, Hartsperger ML, Pfeufer A, Stumpflen V. Cis-acting polymorphisms affect complex traits through modifications of microRNA regulation pathways. PLoS One 2012;7: e36694.
[59] Duan R, Pak C, Jin P. Single nucleotide polymorphism associated with mature miR-125a alters the processing of pri-miRNA. Hum Mol Genet 2007;16: 1124-31.
[60] Saunders MA, Liang H, Li WH. Human polymorphism at microRNAs and microRNA target sites. Proc Natl Acad Sci U S A 2007;104: 3300-5.
[61] Sun G, Yan J, Noltner K, Feng J, Li H, Sarkis DA, Sommer SS, Rossi JJ. SNPs in human miRNA genes affect biogenesis and function. RNA 2009;15: 1640-51.
[62] Mishra PJ, Mishra PJ, Banerjee D, Bertino JR. MiRSNPs or MiR-polymorphisms, new players in microRNA mediated regulation of the cell: Introducing microRNA pharmacogenomics. Cell Cycle 2008;7: 853-8.
[63] Iwai N, Naraba H. Polymorphisms in human pre-miRNAs. Biochem Biophys Res Commun 2005;331: 1439-44.
[64] Cheung KS, Sposito N, Stumpf PS, Wilson DI, Sanchez-Elsner T, Oreffo RO. MicroRNA-146a regulates human foetal femur derived skeletal stem cell differentiation by down-regulating SMAD2 and SMAD3. PLoS One 2014;9: e98063.
[65] Tye CE, Gordon JA, Martin-Buley LA, Stein JL, Lian JB, Stein GS. Could lncRNAs be the missing links in control of mesenchymal stem cell differentiation? J Cell Physiol 2015;230: 526-34.
[66] Zhu L, Xu PC. Downregulated LncRNA-ANCR promotes osteoblast differentiation by targeting EZH2 and regulating Runx2 expression. Biochem Biophys Res Commun 2013;432: 612-7.
[67] Gong J, Liu W, Zhang J, Miao X, Guo AY. lncRNASNP: a database of SNPs in lncRNAs and their potential functions in human and mouse. Nucleic Acids Res 2014.
[68] Saini HK, Griffiths-Jones S, Enright AJ. Genomic analysis of human microRNA transcripts. Proc Natl Acad Sci U S A 2007;104: 17719-24.
[69] Ha M, Kim VN. Regulation of microRNA biogenesis. Nat Rev Mol Cell Biol 2014;15: 509-24.
[70] Faller M, Toso D, Matsunaga M, Atanasov I, Senturia R, Chen Y, Zhou ZH, Guo F. DGCR8 recognizes primary transcripts of microRNAs through highly cooperative binding and formation of higher-order structures. RNA 2010;16: 1570-83.
[71] Ma H, Wu Y, Choi JG, Wu H. Lower and upper stem-single-stranded RNA junctions together determine the Drosha cleavage site. Proc Natl Acad Sci U S A 2013;110: 20687-92.
[72] Burke JM, Kelenis DP, Kincaid RP, Sullivan CS. A central role for the primary microRNA stem in guiding the position and efficiency of Drosha processing of a viral pri-miRNA. RNA 2014;20: 1068-77.
[73] Auyeung VC, Ulitsky I, McGeary SE, Bartel DP. Beyond secondary structure: primary-sequence determinants license pri-miRNA hairpins for processing. Cell 2013;152: 844-58.
[74] Davis BN, Hilyard AC, Lagna G, Hata A. SMAD proteins control DROSHA-mediated microRNA maturation. Nature 2008;454: 56-61.
[75] Ruby JG, Jan CH, Bartel DP. Intronic microRNA precursors that bypass Drosha processing. Nature 2007;448: 83-6.
[76] Yi R, Qin Y, Macara IG, Cullen BR. Exportin-5 mediates the nuclear export of pre-microRNAs and short hairpin RNAs. Genes Dev 2003;17: 3011-6.

[77] Zeng Y, Cullen BR. Structural requirements for pre-microRNA binding and nuclear export by Exportin 5. Nucleic Acids Res 2004;32: 4776-85.
[78] Bartel B. MicroRNAs directing siRNA biogenesis. Nat Struct Mol Biol 2005;12: 569-71.
[79] Bernstein E, Caudy AA, Hammond SM, Hannon GJ. Role for a bidentate ribonuclease in the initiation step of RNA interference. Nature 2001;409: 363-6.
[80] Bernstein E, Kim SY, Carmell MA, Murchison EP, Alcorn H, Li MZ, Mills AA, Elledge SJ, Anderson KV, Hannon GJ. Dicer is essential for mouse development. Nat Genet 2003;35: 215-7.
[81] Macrae IJ, Zhou K, Li F, Repic A, Brooks AN, Cande WZ, Adams PD, Doudna JA. Structural basis for double-stranded RNA processing by Dicer. Science 2006;311: 195-8.
[82] Zhang H, Kolb FA, Jaskiewicz L, Westhof E, Filipowicz W. Single processing center models for human Dicer and bacterial RNase III. Cell 2004;118: 57-68.
[83] Salzman DW, Weidhaas JB. SNPing cancer in the bud: microRNA and microRNA-target site polymorphisms as diagnostic and prognostic biomarkers in cancer. Pharmacol Ther 2013;137: 55-63.
[84] Czech B, Zhou R, Erlich Y, Brennecke J, Binari R, Villalta C, Gordon A, Perrimon N, Hannon GJ. Hierarchical rules for Argonaute loading in Drosophila. Mol Cell 2009;36: 445-56.
[85] Okamura K, Liu N, Lai EC. Distinct mechanisms for microRNA strand selection by Drosophila Argonautes. Mol Cell 2009;36: 431-44.
[86] Wilson RC, Tambe A, Kidwell MA, Noland CL, Schneider CP, Doudna JA. Dicer-TRBP Complex Formation Ensures Accurate Mammalian MicroRNA Biogenesis. Mol Cell 2014.
[87] Lewis BP, Burge CB, Bartel DP. Conserved seed pairing, often flanked by adenosines, indicates that thousands of human genes are microRNA targets. Cell 2005;120: 15-20.
[88] Brennecke J, Stark A, Russell RB, Cohen SM. Principles of microRNA-target recognition. PLoS Biol 2005;3: e85.
[89] Clark PM, Loher P, Quann K, Brody J, Londin ER, Rigoutsos I. Argonaute CLIP-Seq reveals miRNA targetome diversity across tissue types. Sci Rep 2014;4: 5947.
[90] Grimson A, Farh KK, Johnston WK, Garrett-Engele P, Lim LP, Bartel DP. MicroRNA targeting specificity in mammals: determinants beyond seed pairing. Mol Cell 2007;27: 91-105.
[91] Li J, Kim T, Nutiu R, Ray D, Hughes TR, Zhang Z. Identifying mRNA sequence elements for target recognition by human Argonaute proteins. Genome Res 2014;24: 775-85.
[92] Du T, Zamore PD. microPrimer: the biogenesis and function of microRNA. Development 2005;132: 4645-52.
[93] Subtelny AO, Eichhorn SW, Chen GR, Sive H, Bartel DP. Poly(A)-tail profiling reveals an embryonic switch in translational control. Nature 2014;508: 66-71.
[94] Meister G, Landthaler M, Patkaniowska A, Dorsett Y, Teng G, Tuschl T. Human Argonaute2 mediates RNA cleavage targeted by miRNAs and siRNAs. Mol Cell 2004;15: 185-97.
[95] Eichhorn SW, Guo H, McGeary SE, Rodriguez-Mias RA, Shin C, Baek D, Hsu SH, Ghoshal K, Villen J, Bartel DP. mRNA destabilization is the dominant effect of mammalian microRNAs by the time substantial repression ensues. Mol Cell 2014;56: 104-15.

[96] Liang H, Zhang J, Zen K, Zhang CY, Chen X. Nuclear microRNAs and their unconventional role in regulating non-coding RNAs. Protein Cell 2013;4: 325-30.
[97] Schanen BC, Li X. Transcriptional regulation of mammalian miRNA genes. Genomics 2011;97: 1-6.
[98] Guo Z, Maki M, Ding R, Yang Y, Zhang B, Xiong L. Genome-wide survey of tissue-specific microRNA and transcription factor regulatory networks in 12 tissues. Sci Rep 2014;4: 5150.
[99] Alexiou P, Vergoulis T, Gleditzsch M, Prekas G, Dalamagas T, Megraw M, Grosse I, Sellis T, Hatzigeorgiou AG. miRGen 2.0: a database of microRNA genomic information and regulation. Nucleic Acids Res 2010;38: D137-41.
[100] Schmeier S, Schaefer U, MacPherson CR, Bajic VB. dPORE-miRNA: polymorphic regulation of microRNA genes. PLoS One 2011;6: e16657.
[101] Luo X, Yang W, Ye DQ, Cui H, Zhang Y, Hirankarn N, Qian X, Tang Y, Lau YL, de Vries N, Tak PP, Tsao BP, Shen N. A functional variant in microRNA-146a promoter modulates its expression and confers disease risk for systemic lupus erythematosus. PLoS Genet 2011;7: e1002128.
[102] Ji J, Cha E, Lee W. Association of miR-146a polymorphisms with systemic lupus erythematosus: a meta-analysis. Lupus 2014;23: 1023-1030.
[103] Ceribelli A, Nahid MA, Satoh M, Chan EK. MicroRNAs in rheumatoid arthritis. FEBS Lett 2011;585: 3667-74.
[104] Nakasa T, Miyaki S, Okubo A, Hashimoto M, Nishida K, Ochi M, Asahara H. Expression of microRNA-146 in rheumatoid arthritis synovial tissue. Arthritis Rheum 2008;58: 1284-92.
[105] Nakasa T, Shibuya H, Nagata Y, Niimoto T, Ochi M. The inhibitory effect of microRNA-146a expression on bone destruction in collagen-induced arthritis. Arthritis Rheum 2011;63: 1582-90.
[106] Polesskaya A, Cuvellier S, Naguibneva I, Duquet A, Moss EG, Harel-Bellan A. Lin-28 binds IGF-2 mRNA and participates in skeletal myogenesis by increasing translation efficiency. Genes Dev 2007;21: 1125-38.
[107] Jazdzewski K, Liyanarachchi S, Swierniak M, Pachucki J, Ringel MD, Jarzab B, de la Chapelle A. Polymorphic mature microRNAs from passenger strand of pre-miR-146a contribute to thyroid cancer. Proc Natl Acad Sci U S A 2009;106: 1502-5.
[108] Jazdzewski K, Murray EL, Franssila K, Jarzab B, Schoenberg DR, de la Chapelle A. Common SNP in pre-miR-146a decreases mature miR expression and predisposes to papillary thyroid carcinoma. Proc Natl Acad Sci U S A 2008;105: 7269-74.
[109] Wei WJ, Wang YL, Li DS, Wang Y, Wang XF, Zhu YX, Yang YJ, Wang ZY, Ma YY, Wu Y, Jin L, Ji QH, Wang JC. Association between the rs2910164 polymorphism in pre-Mir-146a sequence and thyroid carcinogenesis. PLoS One 2013;8: e56638.
[110] Wang J, Bi J, Liu X, Li K, Di J, Wang B. Has-miR-146a polymorphism (rs2910164) and cancer risk: a meta-analysis of 19 case-control studies. Mol Biol Rep 2012;39: 4571-9.
[111] Dai ZJ, Shao YP, Wang XJ, Xu D, Kang HF, Ren HT, Min WL, Lin S, Wang M, Song ZJ. Five Common Functional Polymorphisms in microRNAs (rs2910164, rs2292832, rs11614913, rs3746444, rs895819) and the Susceptibility to Breast Cancer: Evidence from 8361 Cancer Cases and 8504 Controls. Curr Pharm Des 2015;21: 1455-63.
[112] Garcia AI, Cox DG, Barjhoux L, Verny-Pierre C, Barnes D, Gemo Study C, Antoniou AC, Stoppa-Lyonnet D, Sinilnikova OM, Mazoyer S. The rs2910164:G>C SNP in the MIR146A

gene is not associated with breast cancer risk in BRCA1 and BRCA2 mutation carriers. Hum Mutat 2011;32: 1004-7.
[113] Xu X, Yang X, Ru G, Wu Y, Zhang S, Xing C, Wu Y, Cao J. miR-146a gene polymorphism rs2910164 and the risk of digestive tumors: A meta-analysis of 21 case-control studies. Oncol Rep 2014;31: 472-9.
[114] Huang GL, Chen ML, Li YZ, Lu Y, Pu XX, He YX, Tang SY, Che H, Zou Y, Ding C, He Z. Association of miR-146a gene polymorphism with risk of nasopharyngeal carcinoma in the central-southern Chinese population. J Hum Genet 2014;59: 141-4.
[115] Chen HF, Hu TT, Zheng XY, Li MQ, Luo MH, Yao YX, Chen Q, Yu SY. Association between miR-146a rs2910164 polymorphism and autoimmune diseases susceptibility: a meta-analysis. Gene 2013;521: 259-64.
[116] Li K, Tie H, Hu N, Chen H, Yin X, Peng C, Wan J, Huang W. Association of two polymorphisms rs2910164 in miRNA-146a and rs3746444 in miRNA-499 with rheumatoid arthritis: a meta-analysis. Hum Immunol 2014;75: 602-8.
[117] Wang EA, Rosen V, D'Alessandro JS, Bauduy M, Cordes P, Harada T, Israel DI, Hewick RM, Kerns KM, LaPan P, et al. Recombinant human bone morphogenetic protein induces bone formation. Proc Natl Acad Sci U S A 1990;87: 2220-4.
[118] Ashique AM, Fu K, Richman JM. Signalling via type IA and type IB bone morphogenetic protein receptors (BMPR) regulates intramembranous bone formation, chondrogenesis and feather formation in the chicken embryo. Int J Dev Biol 2002;46: 243-53.
[119] Suzuki A, Thies RS, Yamaji N, Song JJ, Wozney JM, Murakami K, Ueno N. A truncated bone morphogenetic protein receptor affects dorsal-ventral patterning in the early Xenopus embryo. Proc Natl Acad Sci U S A 1994;91: 10255-9.
[120] Dewulf N, Verschueren K, Lonnoy O, Moren A, Grimsby S, Vande Spiegle K, Miyazono K, Huylebroeck D, Ten Dijke P. Distinct spatial and temporal expression patterns of two type I receptors for bone morphogenetic proteins during mouse embryogenesis. Endocrinology 1995;136: 2652-63.
[121] Zou H, Wieser R, Massague J, Niswander L. Distinct roles of type I bone morphogenetic protein receptors in the formation and differentiation of cartilage. Genes Dev 1997;11: 2191-203.
[122] Saetrom P, Biesinger J, Li SM, Smith D, Thomas LF, Majzoub K, Rivas GE, Alluin J, Rossi JJ, Krontiris TG, Weitzel J, Daly MB, Benson AB, Kirkwood JM, O'Dwyer PJ, Sutphen R, Stewart JA, Johnson D, Larson GP. A risk variant in an miR-125b binding site in BMPR1B is associated with breast cancer pathogenesis. Cancer Res 2009;69: 7459-65.
[123] Helms MW, Packeisen J, August C, Schittek B, Boecker W, Brandt BH, Buerger H. First evidence supporting a potential role for the BMP/SMAD pathway in the progression of oestrogen receptor-positive breast cancer. J Pathol 2005;206: 366-76.
[124] Esquela-Kerscher A, Slack FJ. Oncomirs - microRNAs with a role in cancer. Nat Rev Cancer 2006;6: 259-69.
[125] Feng N, Xu B, Tao J, Li P, Cheng G, Min Z, Mi Y, Wang M, Tong N, Tang J, Zhang Z, Wu H, Zhang W, Wang Z, Hua L. A miR-125b binding site polymorphism in bone morphogenetic protein membrane receptor type IB gene and prostate cancer risk in China. Mol Biol Rep 2012;39: 369-73.
[126] Chang CY, Chen Y, Lai MT, Chang HW, Cheng J, Chan C, Chen CM, Lee SC, Lin YJ, Wan L, Tsai PW, Yang SH, Chung C, Sheu JJ, Tsai FJ. BMPR1B up-regulation via a miRNA binding

site variation defines endometriosis susceptibility and CA125 levels. PLoS One 2013;8: e80630.
[127] Sun Q, Zhao X, Liu X, Wang Y, Huang J, Jiang B, Chen Q, Yu J. miR-146a functions as a tumor suppressor in prostate cancer by targeting Rac1. Prostate 2014;74: 1613-21.
[128] He Y, Huang C, Sun X, Long XR, Lv XW, Li J. MicroRNA-146a modulates TGF-beta1-induced hepatic stellate cell proliferation by targeting SMAD4. Cell Signal 2012;24: 1923-30.
[129] Garcia AI, Buisson M, Bertrand P, Rimokh R, Rouleau E, Lopez BS, Lidereau R, Mikaelian I, Mazoyer S. Down-regulation of BRCA1 expression by miR-146a and miR-146b-5p in triple negative sporadic breast cancers. EMBO Mol Med 2011;3: 279-90.
[130] Taganov KD, Boldin MP, Chang KJ, Baltimore D. NF-kappaB-dependent induction of microRNA miR-146, an inhibitor targeted to signaling proteins of innate immune responses. Proc Natl Acad Sci U S A 2006;103: 12481-6.
[131] Park H, Huang X, Lu C, Cairo MS, Zhou X. MicroRNA-146a and MicroRNA-146b Regulate Human Dendritic Cell Apoptosis and Cytokine Production by Targeting TRAF6 and IRAK1 Proteins. J Biol Chem 2015;290: 2831-41.
[132] Rusca N, Monticelli S. MiR-146a in Immunity and Disease. Mol Biol Int 2011;2011: 437301.
[133] Li X, Gibson G, Kim JS, Kroin J, Xu S, van Wijnen AJ, Im HJ. MicroRNA-146a is linked to pain-related pathophysiology of osteoarthritis. Gene 2011;480: 34-41.
[134] Kim JH, Jin HM, Kim K, Song I, Youn BU, Matsuo K, Kim N. The mechanism of osteoclast differentiation induced by IL-1. J Immunol 2009;183: 1862-70.
[135] Jin LEI, Zhao J, Jing W, Yan S, Wang XIN, Xiao C, Ma B. Role of miR-146a in human chondrocyte apoptosis in response to mechanical pressure injury in vitro. International Journal of Molecular Medicine 2014;34: 451-463.
[136] Li J, Huang J, Dai L, Yu D, Chen Q, Zhang X, Dai K. miR-146a, an IL-1beta responsive miRNA, induces vascular endothelial growth factor and chondrocyte apoptosis by targeting Smad4. Arthritis Res Ther 2012;14: R75.
[137] Yamasaki K, Nakasa T, Miyaki S, Ishikawa M, Deie M, Adachi N, Yasunaga Y, Asahara H, Ochi M. Expression of MicroRNA-146a in osteoarthritis cartilage. Arthritis Rheum 2009;60: 1035-41.
[138] Franceschetti T, Dole NS, Kessler CB, Lee SK, Delany AM. Pathway analysis of microRNA expression profile during murine osteoclastogenesis. PLoS One 2014;9: e107262.
[139] Scott GK, Goga A, Bhaumik D, Berger CE, Sullivan CS, Benz CC. Coordinate suppression of ERBB2 and ERBB3 by enforced expression of micro-RNA miR-125a or miR-125b. J Biol Chem 2007;282: 1479-86.
[140] de la Rica L, Garcia-Gomez A, Comet NR, Rodriguez-Ubreva J, Ciudad L, Vento-Tormo R, Company C, Alvarez-Errico D, Garcia M, Gomez-Vaquero C, Ballestar E. NF-kappaB-direct activation of microRNAs with repressive effects on monocyte-specific genes is critical for osteoclast differentiation. Genome Biol 2015;16: 2.
[141] Guo LJ, Liao L, Yang L, Li Y, Jiang TJ. MiR-125a TNF receptor-associated factor 6 to inhibit osteoclastogenesis. Exp Cell Res 2014;321: 142-52.
[142] Huang K, Fu J, Zhou W, Li W, Dong S, Yu S, Hu Z, Wang H, Xie Z. MicroRNA-125b regulates osteogenic differentiation of mesenchymal stem cells by targeting Cbfbeta in vitro. Biochimie 2014;102: 47-55.

[143] Mizuno Y, Yagi K, Tokuzawa Y, Kanesaki-Yatsuka Y, Suda T, Katagiri T, Fukuda T, Maruyama M, Okuda A, Amemiya T, Kondoh Y, Tashiro H, Okazaki Y. miR-125b inhibits osteoblastic differentiation by down-regulation of cell proliferation. Biochem Biophys Res Commun 2008;368: 267-72.
[144] Seeliger C, Karpinski K, Haug AT, Vester H, Schmitt A, Bauer JS, van Griensven M. Five freely circulating miRNAs and bone tissue miRNAs are associated with osteoporotic fractures. J Bone Miner Res 2014;29: 1718-28.
[145] Matsukawa T, Sakai T, Yonezawa T, Hiraiwa H, Hamada T, Nakashima M, Ono Y, Ishizuka S, Nakahara H, Lotz MK, Asahara H, Ishiguro N. MicroRNA-125b regulates the expression of aggrecanase-1 (ADAMTS-4) in human osteoarthritic chondrocytes. Arthritis Res Ther 2013;15: R28.
[146] Lehmann TP, Korski K, Ibbs M, Zawierucha P, Grodecka-Gazdecka S, Jagodzinski PP. rs12976445 variant in the pri-miR-125a correlates with a lower level of hsa-miR-125a and ERBB2 overexpression in breast cancer patients. Oncol Lett 2013;5: 569-573.
[147] Hu Y, Liu CM, Qi L, He TZ, Shi-Guo L, Hao CJ, Cui Y, Zhang N, Xia HF, Ma X. Two common SNPs in pri-miR-125a alter the mature miRNA expression and associate with recurrent pregnancy loss in a Han-Chinese population. RNA Biol 2011;8: 861-72.
[148] Hu Y, Huo ZH, Liu CM, Liu SG, Zhang N, Yin KL, Qi L, Ma X, Xia HF. Functional Study of One Nucleotide Mutation in Pri-MiR-125a Coding Region which Related to Recurrent Pregnancy Loss. PLoS One 2014;9: e114781.
[149] Jiao L, Zhang J, Dong Y, Duan B, Yu H, Sheng H, Huang J, Gao H. Association between miR-125a rs12976445 and survival in breast cancer patients. Am J Transl Res 2014;6: 869-75.
[150] Zakany J, Duboule D. The role of Hox genes during vertebrate limb development. Curr Opin Genet Dev 2007;17: 359-66.
[151] Alexander T, Nolte C, Krumlauf R. Hox Genes and Segmentation of the Hindbrain and Axial Skeleton. Annual Review of Cell and Developmental Biology 2009;25: 431-456.
[152] McGlinn E, Yekta S, Mansfield JH, Soutschek J, Bartel DP, Tabin CJ. In ovo application of antagomiRs indicates a role for miR-196 in patterning the chick axial skeleton through Hox gene regulation. Proc Natl Acad Sci U S A 2009;106: 18610-5.
[153] Yekta S, Shih IH, Bartel DP. MicroRNA-directed cleavage of HOXB8 mRNA. Science 2004;304: 594-6.
[154] Kim YJ, Bae SW, Yu SS, Bae YC, Jung JS. miR-196a regulates proliferation and osteogenic differentiation in mesenchymal stem cells derived from human adipose tissue. J Bone Miner Res 2009;24: 816-25.
[155] Candini O, Spano C, Murgia A, Grisendi G, Veronesi E, Piccinno MS, Ferracin M, Negrini M, Giacobbi F, Bambi F, Horwitz EM, Conte P, Paolucci P, Dominici M. Mesenchymal Progenitors Aging Highlights a miR-196 Switch Targeting HOXB7 as Master Regulator of Proliferation and Osteogenesis. Stem Cells 2015;33: 939-50.
[156] Juan AH, Lei H, Bhargava P, Lebrun M, Ruddle FH. Multiple roles of hoxc8 in skeletal development. Ann N Y Acad Sci 2006;1068: 87-94.
[157] Lei H, Wang H, Juan AH, Ruddle FH. The identification of Hoxc8 target genes. Proceedings of the National Academy of Sciences of the United States of America 2005;102: 2420-2424.

[158] Zheng YJ, Chung HJ, Min H, Kang M, Kim SH, Gadi J, Kim MH. In vitro osteoblast differentiation is negatively regulated by Hoxc8. Appl Biochem Biotechnol 2010;160: 891-900.
[159] Braig S, Mueller DW, Rothhammer T, Bosserhoff AK. MicroRNA miR-196a is a central regulator of HOX-B7 and BMP4 expression in malignant melanoma. Cell Mol Life Sci 2010;67: 3535-48.
[160] Xu M, Qiang F, Gao Y, Kang M, Wang M, Tao G, Gong W, Zhu H, Wu D, Zhang Z, Zhao Q. Evaluation of a novel functional single-nucleotide polymorphism (rs35010275 G>C) in MIR196A2 promoter region as a risk factor of gastric cancer in a Chinese population. Medicine (Baltimore) 2014;93: e173.
[161] Hua HB, Yan TT, Sun QM. miRNA polymorphisms and risk of gastric cancer in Asian population. World J Gastroenterol 2014;20: 5700-7.
[162] Hoffman AE, Zheng T, Yi C, Leaderer D, Weidhaas J, Slack F, Zhang Y, Paranjape T, Zhu Y. microRNA miR-196a-2 and Breast Cancer: A Genetic and Epigenetic Association Study and Functional Analysis. Cancer Research 2009;69: 5970-5977.
[163] Chamorro-Jorganes A, Araldi E, Rotllan N, Cirera-Salinas D, Suarez Y. Autoregulation of glypican-1 by intronic microRNA-149 fine tunes the angiogenic response to FGF2 in human endothelial cells. J Cell Sci 2014;127: 1169-78.
[164] Diaz-Prado S, Cicione C, Muinos-Lopez E, Hermida-Gomez T, Oreiro N, Fernandez-Lopez C, Blanco FJ. Characterization of microRNA expression profiles in normal and osteoarthritic human chondrocytes. BMC Musculoskelet Disord 2012;13: 144.
[165] Santini P, Politi L, Vedova PD, Scandurra R, Scotto d'Abusco A. The inflammatory circuitry of miR-149 as a pathological mechanism in osteoarthritis. Rheumatol Int 2014;34: 711-6.
[166] He B, Pan Y, Cho WC, Xu Y, Gu L, Nie Z, Chen L, Song G, Gao T, Li R, Wang S. The association between four genetic variants in microRNAs (rs11614913, rs2910164, rs3746444, rs2292832) and cancer risk: evidence from published studies. PLoS One 2012;7: e49032.
[167] Hu Y, Yu C-Y, Wang J-L, Guan J, Chen H-Y, Fang J-Y. MicroRNA sequence polymorphisms and the risk of different types of cancer. Sci. Rep. 2014;4.
[168] Hassan MQ, Gordon JA, Beloti MM, Croce CM, van Wijnen AJ, Stein JL, Stein GS, Lian JB. A network connecting Runx2, SATB2, and the miR-23a~27a~24-2 cluster regulates the osteoblast differentiation program. Proc Natl Acad Sci U S A 2010;107: 19879-84.
[169] Hassan MQ, Tare R, Lee SH, Mandeville M, Weiner B, Montecino M, van Wijnen AJ, Stein JL, Stein GS, Lian JB. HOXA10 controls osteoblastogenesis by directly activating bone regulatory and phenotypic genes. Mol Cell Biol 2007;27: 3337-52.
[170] Xu Q, He C-y, Liu J-w, Yuan Y. Pre-miR-27a rs895819A/G Polymorphisms in Cancer: A Meta-Analysis. PLoS ONE 2013;8: e65208.
[171] Wang Z, Sun X, Wang Y, Liu X, Xuan Y, Hu S. Association between miR-27a genetic variants and susceptibility to colorectal cancer. Diagnostic Pathology 2014;9: 146.
[172] Yang Q, Jie Z, Ye S, Li Z, Han Z, Wu J, Yang C, Jiang Y. Genetic variations in miR-27a gene decrease mature miR-27a level and reduce gastric cancer susceptibility. Oncogene 2014;33: 193-202.
[173] Zhou Q, Long L, Shi G, Zhang J, Wu T, Zhou B. Research of the Methylation Status of miR-124a Gene Promoter among Rheumatoid Arthritis Patients. Clinical and Developmental Immunology 2013;2013: 4.

[174] Lee Y, Kim HJ, Park CK, Kim YG, Lee HJ, Kim JY, Kim HH. MicroRNA-124 regulates osteoclast differentiation. Bone 2013;56: 383-9.
[175] Qadir AS, Um S, Lee H, Baek K, Seo BM, Lee G, Kim GS, Woo KM, Ryoo HM, Baek JH. miR-124 Negatively Regulates Osteogenic Differentiation and In vivo Bone Formation of Mesenchymal Stem Cells. J Cell Biochem 2015;116: 730-42.
[176] Laine SK, Alm JJ, Virtanen SP, Aro HT, Laitala-Leinonen TK. MicroRNAs miR-96, miR-124, and miR-199a regulate gene expression in human bone marrow-derived mesenchymal stem cells. J Cell Biochem 2012;113: 2687-95.
[177] Nakamachi Y, Ohnuma K, Uto K, Noguchi Y, Saegusa J, Kawano S. MicroRNA-124 inhibits the progression of adjuvant-induced arthritis in rats. Annals of the Rheumatic Diseases 2015.
[178] Qi L, Hu Y, Zhan Y, Wang J, Wang BB, Xia HF, Ma X. A SNP site in pri-miR-124 changes mature miR-124 expression but no contribution to Alzheimer's disease in a Mongolian population. Neurosci Lett 2012;515: 1-6.
[179] Peacock M, Turner CH, Econs MJ, Foroud T. Genetics of osteoporosis. Endocr Rev 2002;23: 303-26.
[180] Lei SF, Papasian CJ, Deng HW. Polymorphisms in predicted miRNA binding sites and osteoporosis. J Bone Miner Res 2011;26: 72-8.
[181] Naganawa T, Xiao L, Coffin JD, Doetschman T, Sabbieti MG, Agas D, Hurley MM. Reduced expression and function of bone morphogenetic protein-2 in bones of Fgf2 null mice. J Cell Biochem 2008;103: 1975-88.
[182] Fei Y, Xiao L, Hurley MM. The impaired bone anabolic effect of PTH in the absence of endogenous FGF2 is partially due to reduced ATF4 expression. Biochem Biophys Res Commun 2011;412: 160-4.
[183] Su N, Jin M, Chen L. Role of FGF/FGFR signaling in skeletal development and homeostasis: learning from mouse models. Bone Research 2014;2: 14003.
[184] Kalajzic I, Kalajzic Z, Hurley MM, Lichtler AC, Rowe DW. Stage specific inhibition of osteoblast lineage differentiation by FGF2 and noggin. J Cell Biochem 2003;88: 1168-76.
[185] Okada Y, Montero A, Zhang X, Sobue T, Lorenzo J, Doetschman T, Coffin JD, Hurley MM. Impaired osteoclast formation in bone marrow cultures of Fgf2 null mice in response to parathyroid hormone. J Biol Chem 2003;278: 21258-66.
[186] Delany AM, McMahon DJ, Powell JS, Greenberg DA, Kurland ES. Osteonectin/SPARC polymorphisms in Caucasian men with idiopathic osteoporosis. Osteoporos Int 2008;19: 969-78.
[187] Dole NS, Kapinas K, Kessler CB, Yee SP, Adams DJ, Pereira RC, Delany AM. A single nucleotide polymorphism in osteonectin 3' untranslated region regulates bone volume and is targeted by miR-433. J Bone Miner Res 2014.
[188] Boskey AL, Moore DJ, Amling M, Canalis E, Delany AM. Infrared analysis of the mineral and matrix in bones of osteonectin-null mice and their wildtype controls. J Bone Miner Res 2003;18: 1005-11.
[189] Delany AM, Kalajzic I, Bradshaw AD, Sage EH, Canalis E. Osteonectin-null mutation compromises osteoblast formation, maturation, and survival. Endocrinology 2003;144: 2588-96.
[190] Delany AM, Amling M, Priemel M, Howe C, Baron R, Canalis E. Osteopenia and decreased bone formation in osteonectin-deficient mice. J Clin Invest 2000;105: 915-23.

[191] Kim EJ, Kang IH, Lee JW, Jang WG, Koh JT. MiR-433 mediates ERRgamma-suppressed osteoblast differentiation via direct targeting to Runx2 mRNA in C3H10T1/2 cells. Life Sci 2013;92: 562-8.
[192] Hu R, Liu W, Li H, Yang L, Chen C, Xia ZY, Guo LJ, Xie H, Zhou HD, Wu XP, Luo XH. A Runx2/miR-3960/miR-2861 regulatory feedback loop during mouse osteoblast differentiation. J Biol Chem 2011;286: 12328-39.
[193] Li H, Xie H, Liu W, Hu R, Huang B, Tan YF, Xu K, Sheng ZF, Zhou HD, Wu XP, Luo XH. A novel microRNA targeting HDAC5 regulates osteoblast differentiation in mice and contributes to primary osteoporosis in humans. J Clin Invest 2009;119: 3666-77.
[194] Jeon E-J, Lee K-Y, Choi N-S, Lee M-H, Kim H-N, Jin Y-H, Ryoo H-M, Choi J-Y, Yoshida M, Nishino N, Oh B-C, Lee K-S, Lee YH, Bae S-C. Bone Morphogenetic Protein-2 Stimulates Runx2 Acetylation. Journal of Biological Chemistry 2006;281: 16502-16511.
[195] Chassaing N, Siani V, Carles D, Delezoide AL, Alberti EM, Battin J, Chateil JF, Gilbert-Dussardier B, Coupry I, Arveiler B, Saura R, Lacombe D. X-linked dominant chondrodysplasia with platyspondyly, distinctive brachydactyly, hydrocephaly, and microphthalmia. Am J Med Genet A 2005;136A: 307-12.
[196] Simon D, Laloo B, Barillot M, Barnetche T, Blanchard C, Rooryck C, Marche M, Burgelin I, Coupry I, Chassaing N, Gilbert-Dussardier B, Lacombe D, Grosset C, Arveiler B. A mutation in the 3'-UTR of the HDAC6 gene abolishing the post-transcriptional regulation mediated by hsa-miR-433 is linked to a new form of dominant X-linked chondrodysplasia. Hum Mol Genet 2010;19: 2015-27.
[197] Westendorf JJ, Zaidi SK, Cascino JE, Kahler R, van Wijnen AJ, Lian JB, Yoshida M, Stein GS, Li X. Runx2 (Cbfa1, AML-3) interacts with histone deacetylase 6 and represses the p21(CIP1/WAF1) promoter. Mol Cell Biol 2002;22: 7982-92.
[198] Thompson CL, Chapple JP, Knight MM. Primary cilia disassembly down-regulates mechanosensitive hedgehog signalling: a feedback mechanism controlling ADAMTS-5 expression in chondrocytes. Osteoarthritis Cartilage 2014;22: 490-8.
[199] Ding S-L, Wang J-X, Jiao J-Q, Tu X, Wang Q, Liu F, Li Q, Gao J, Zhou Q-Y, Gu D-F, Li P-F. A Pre-microRNA-149 (miR-149) Genetic Variation Affects miR-149 Maturation and Its Ability to Regulate the Puma Protein in Apoptosis. Journal of Biological Chemistry 2013;288: 26865-26877.
[200] Ralston. Genetic Control of Susceptibility to Osteoporosis. The Journal of Clinical Endocrinology and Metabolism 2002;87: 2460-2466.
[201] Kurt O, Yilmaz-Aydogan H, Uyar M, Isbir T, Seyhan MF, Can A. Evaluation of ERalpha and VDR gene polymorphisms in relation to bone mineral density in Turkish postmenopausal women. Mol Biol Rep 2012;39: 6723-30.
[202] Yamada Y. Association of polymorphisms of the transforming growth factor-beta1 gene with genetic susceptibility to osteoporosis. Pharmacogenetics 2001;11: 765-71.
[203] Shen L, Qiu Y, Xing S, Chen D, Zhu Y, He X, Wang J, Lai J, Shi G, Liao T, Tan J. Association between osteoprotegerin genetic variants and bone mineral density in Chinese women. Int Immunopharmacol 2013;16: 275-8.
[204] Falcon-Ramirez E, Casas-Avila L, Miranda A, Diez P, Castro C, Rubio J, Gomez R, Valdes-Flores M. Sp1 polymorphism in collagen I alpha1 gene is associated with osteoporosis in lumbar spine of Mexican women. Mol Biol Rep 2011;38: 2987-92.
[205] Yamada Y, Ando F, Niino N, Shimokata H. Association of polymorphisms of interleukin-6, osteocalcin, and vitamin D receptor genes, alone or in combination, with

bone mineral density in community-dwelling Japanese women and men. J Clin Endocrinol Metab 2003;88: 3372-8.
[206] Koller DL, Econs MJ, Morin PA, Christian JC, Hui SL, Parry P, Curran ME, Rodriguez LA, Conneally PM, Joslyn G, Peacock M, Johnston CC, Foroud T. Genome screen for QTLs contributing to normal variation in bone mineral density and osteoporosis. J Clin Endocrinol Metab 2000;85: 3116-20.
[207] Delany AM, Amling M, Priemel M, Howe C, Baron R, Canalis E. Osteopenia and decreased bone formation in osteonectin-deficient mice. J Clin Invest 2000;105: 1325.
[208] Machado do Reis L, Kessler CB, Adams DJ, Lorenzo J, Jorgetti V, Delany AM. Accentuated osteoclastic response to parathyroid hormone undermines bone mass acquisition in osteonectin-null mice. Bone 2008;43: 264-73.
[209] Kurland ES, Chan FK, Rosen CJ, Bilezikian JP. Normal growth hormone secretory reserve in men with idiopathic osteoporosis and reduced circulating levels of insulin-like growth factor-I. J Clin Endocrinol Metab 1998;83: 2576-9.
[210] Kurland ES, Rosen CJ, Cosman F, McMahon D, Chan F, Shane E, Lindsay R, Dempster D, Bilezikian JP. Insulin-like growth factor-I in men with idiopathic osteoporosis. J Clin Endocrinol Metab 1997;82: 2799-805.
[211] Mendell JT, Dietz HC. When the message goes awry: disease-producing mutations that influence mRNA content and performance. Cell 2001;107: 411-4.
[212] Harris SA, Enger RJ, Riggs BL, Spelsberg TC. Development and characterization of a conditionally immortalized human fetal osteoblastic cell line. J Bone Miner Res 1995;10: 178-86.
[213] Kapinas K, Kessler C, Ricks T, Gronowicz G, Delany AM. miR-29 modulates Wnt signaling in human osteoblasts through a positive feedback loop. J Biol Chem 2010;285: 25221-31.
[214] Lee EC, Yu D, Martinez de Velasco J, Tessarollo L, Swing DA, Court DL, Jenkins NA, Copeland NG. A highly efficient Escherichia coli-based chromosome engineering system adapted for recombinogenic targeting and subcloning of BAC DNA. Genomics 2001;73: 56-65.
[215] Ingram RT, Clarke BL, Fisher LW, Fitzpatrick LA. Distribution of noncollagenous proteins in the matrix of adult human bone: evidence of anatomic and functional heterogeneity. J Bone Miner Res 1993;8: 1019-29.
[216] Bouxsein ML, Boyd SK, Christiansen BA, Guldberg RE, Jepsen KJ, Muller R. Guidelines for assessment of bone microstructure in rodents using micro-computed tomography. J Bone Miner Res 2010;25: 1468-86.
[217] Parfitt AM, Drezner MK, Glorieux FH, Kanis JA, Malluche H, Meunier PJ, Ott SM, Recker RR. Bone histomorphometry: standardization of nomenclature, symbols, and units. Report of the ASBMR Histomorphometry Nomenclature Committee. J Bone Miner Res 1987;2: 595-610.
[218] Rehmsmeier M, Steffen P, Hochsmann M, Giegerich R. Fast and effective prediction of microRNA/target duplexes. RNA 2004;10: 1507-17.
[219] Kapinas K, Kessler CB, Delany AM. miR-29 suppression of osteonectin in osteoblasts: regulation during differentiation and by canonical Wnt signaling. J Cell Biochem 2009;108: 216-24.

[220] Sheng MH, Lau KH, Beamer WG, Baylink DJ, Wergedal JE. In vivo and in vitro evidence that the high osteoblastic activity in C3H/HeJ mice compared to C57BL/6J mice is intrinsic to bone cells. Bone 2004;35: 711-9.
[221] Shultz KL, Donahue LR, Bouxsein ML, Baylink DJ, Rosen CJ, Beamer WG. Congenic strains of mice for verification and genetic decomposition of quantitative trait loci for femoral bone mineral density. J Bone Miner Res 2003;18: 175-85.
[222] Bradshaw AD, Sage EH. SPARC, a matricellular protein that functions in cellular differentiation and tissue response to injury. J Clin Invest 2001;107: 1049-54.
[223] Kapinas K, Lowther KM, Kessler CB, Tilbury K, Lieberman JR, Tirnauer JS, Campagnola P, Delany AM. Bone matrix osteonectin limits prostate cancer cell growth and survival. Matrix Biol 2012;31: 299-307.
[224] Rentz TJ, Poobalarahi F, Bornstein P, Sage EH, Bradshaw AD. SPARC regulates processing of procollagen I and collagen fibrillogenesis in dermal fibroblasts. J Biol Chem 2007;282: 22062-71.
[225] Chen LJ, Tam PO, Tham CC, Liang XY, Chiang SW, Canlas O, Ritch R, Rhee DJ, Pang CP. Evaluation of SPARC as a candidate gene of juvenile-onset primary open-angle glaucoma by mutation and copy number analyses. Mol Vis 2010;16: 2016-25.
[226] Turner RT, Evans GL, Lotinun S, Lapke PD, Iwaniec UT, Morey-Holton E. Dose-response effects of intermittent PTH on cancellous bone in hindlimb unloaded rats. J Bone Miner Res 2007;22: 64-71.
[227] Delany AM, Canalis E. Basic fibroblast growth factor destabilizes osteonectin mRNA in osteoblasts. Am J Physiol 1998;274: C734-40.
[228] Chamboredon S, Briggs J, Vial E, Hurault J, Galvagni F, Oliviero S, Bos T, Castellazzi M. v-Jun downregulates the SPARC target gene by binding to the proximal promoter indirectly through Sp1/3. Oncogene 2003;22: 4047-61.
[229] Dominguez P, Ibaraki K, Robey PG, Hefferan TE, Termine JD, Young MF. Expression of the osteonectin gene potentially controlled by multiple cis- and trans-acting factors in cultured bone cells. J Bone Miner Res 1991;6: 1127-36.
[230] Ibaraki K, Robey PG, Young MF. Partial characterization of a novel 'GGA' factor which binds to the osteonectin promoter in bovine bone cells. Gene 1993;130: 225-32.
[231] Ng KW, Manji SS, Young MF, Findlay DM. Opposing influences of glucocorticoid and retinoic acid on transcriptional control in preosteoblasts. Mol Endocrinol 1989;3: 2079-85.
[232] Sauk JJ, Norris K, Kerr JM, Somerman MJ, Young MF. Diverse forms of stress result in changes in cellular levels of osteonectin/SPARC without altering mRNA levels in osteoligament cells. Calcif Tissue Int 1991;49: 58-62.
[233] Chen XD, Xiao P, Lei SF, Liu YZ, Guo YF, Deng FY, Tan LJ, Zhu XZ, Chen FR, Recker RR, Deng HW. Gene expression profiling in monocytes and SNP association suggest the importance of the STAT1 gene for osteoporosis in both Chinese and Caucasians. J Bone Miner Res 2010;25: 339-55.
[234] De Bonis P, Laborante A, Pizzicoli C, Stallone R, Barbano R, Longo C, Mazzilli E, Zelante L, Bisceglia L. Mutational screening of VSX1, SPARC, SOD1, LOX, and TIMP3 in keratoconus. Mol Vis 2011;17: 2482-94.
[235] Lagan AL, Pantelidis P, Renzoni EA, Fonseca C, Beirne P, Taegtmeyer AB, Denton CP, Black CM, Wells AU, du Bois RM, Welsh KI. Single-nucleotide polymorphisms in the SPARC gene are not associated with susceptibility to scleroderma. Rheumatology (Oxford) 2005;44: 197-201.

[236] Segat L, Milanese M, Pirulli D, Trevisiol C, Lupo F, Salizzoni M, Amoroso A, Crovella S. Secreted protein acidic and rich in cysteine (SPARC) gene polymorphism association with hepatocellular carcinoma in Italian patients. J Gastroenterol Hepatol 2009;24: 1840-6.
[237] Zhou X, Tan FK, Reveille JD, Wallis D, Milewicz DM, Ahn C, Wang A, Arnett FC. Association of novel polymorphisms with the expression of SPARC in normal fibroblasts and with susceptibility to scleroderma. Arthritis Rheum 2002;46: 2990-9.
[238] Sherry ST, Ward MH, Kholodov M, Baker J, Phan L, Smigielski EM, Sirotkin K. dbSNP: the NCBI database of genetic variation. Nucleic Acids Res 2001;29: 308-11.
[239] Hochberg MC. Racial differences in bone strength. Trans Am Clin Climatol Assoc 2007;118: 305-15.
[240] George A, Tracy JK, Meyer WA, Flores RH, Wilson PD, Hochberg MC. Racial differences in bone mineral density in older men. J Bone Miner Res 2003;18: 2238-44.
[241] Gong G, Haynatzki G, Haynatzka V, Howell R, Kosoko-Lasaki S, Fu YX, Yu F, Gallagher JC, Wilson MR. Bone mineral density-affecting genes in Africans. J Natl Med Assoc 2006;98: 1102-8.
[242] Gibson G. Rare and common variants: twenty arguments. Nat Rev Genet 2011;13: 135-45.
[243] Nguyen TV, Eisman JA. Genetics and the individualized prediction of fracture. Curr Osteoporos Rep 2012;10: 236-44.
[244] Mitchell BD, Streeten EA. Clinical impact of recent genetic discoveries in osteoporosis. Appl Clin Genet 2013;6: 75-85.
[245] Tondravi MM, McKercher SR, Anderson K, Erdmann JM, Quiroz M, Maki R, Teitelbaum SL. Osteopetrosis in mice lacking haematopoietic transcription factor PU.1. Nature 1997;386: 81-4.
[246] Dahl R, Simon MC. The importance of PU.1 concentration in hematopoietic lineage commitment and maturation. Blood Cells Mol Dis 2003;31: 229-33.
[247] Dahl R, Walsh JC, Lancki D, Laslo P, Iyer SR, Singh H, Simon MC. Regulation of macrophage and neutrophil cell fates by the PU.1:C/EBPalpha ratio and granulocyte colony-stimulating factor. Nat Immunol 2003;4: 1029-36.
[248] Kwon OH, Lee CK, Lee YI, Paik SG, Lee HJ. The hematopoietic transcription factor PU.1 regulates RANK gene expression in myeloid progenitors. Biochem Biophys Res Commun 2005;335: 437-46.
[249] Sharma SM, Bronisz A, Hu R, Patel K, Mansky KC, Sif S, Ostrowski MC. MITF and PU.1 recruit p38 MAPK and NFATc1 to target genes during osteoclast differentiation. J Biol Chem 2007;282: 15921-9.
[250] Matsuo K, Galson DL, Zhao C, Peng L, Laplace C, Wang KZ, Bachler MA, Amano H, Aburatani H, Ishikawa H, Wagner EF. Nuclear factor of activated T-cells (NFAT) rescues osteoclastogenesis in precursors lacking c-Fos. J Biol Chem 2004;279: 26475-80.
[251] Takayanagi H, Kim S, Matsuo K, Suzuki H, Suzuki T, Sato K, Yokochi T, Oda H, Nakamura K, Ida N, Wagner EF, Taniguchi T. RANKL maintains bone homeostasis through c-Fos-dependent induction of interferon-beta. Nature 2002;416: 744-9.
[252] Boyce BF, Yamashita T, Yao Z, Zhang Q, Li F, Xing L. Roles for NF-kappaB and c-Fos in osteoclasts. J Bone Miner Metab 2005;23 Suppl: 11-5.
[253] Takayanagi H, Kim S, Koga T, Nishina H, Isshiki M, Yoshida H, Saiura A, Isobe M, Yokochi T, Inoue J, Wagner EF, Mak TW, Kodama T, Taniguchi T. Induction and activation of

the transcription factor NFATc1 (NFAT2) integrate RANKL signaling in terminal differentiation of osteoclasts. Dev Cell 2002;3: 889-901.
[254] Lomaga MA, Yeh WC, Sarosi I, Duncan GS, Furlonger C, Ho A, Morony S, Capparelli C, Van G, Kaufman S, van der Heiden A, Itie A, Wakeham A, Khoo W, Sasaki T, Cao Z, Penninger JM, Paige CJ, Lacey DL, Dunstan CR, Boyle WJ, Goeddel DV, Mak TW. TRAF6 deficiency results in osteopetrosis and defective interleukin-1, CD40, and LPS signaling. Genes Dev 1999;13: 1015-24.
[255] Sugatani T, Hruska KA. Impaired micro-RNA pathways diminish osteoclast differentiation and function. J Biol Chem 2009;284: 4667-78.
[256] Cheng Y, Kuang W, Hao Y, Zhang D, Lei M, Du L, Jiao H, Zhang X, Wang F. Downregulation of miR-27a* and miR-532-5p and upregulation of miR-146a and miR-155 in LPS-induced RAW264.7 macrophage cells. Inflammation 2012;35: 1308-13.
[257] Zhang J, Zhao H, Chen J, Xia B, Jin Y, Wei W, Shen J, Huang Y. Interferon-beta-induced miR-155 inhibits osteoclast differentiation by targeting SOCS1 and MITF. FEBS Lett 2012;586: 3255-62.
[258] Mann M, Barad O, Agami R, Geiger B, Hornstein E. miRNA-based mechanism for the commitment of multipotent progenitors to a single cellular fate. Proc Natl Acad Sci U S A 2010;107: 15804-9.
[259] Sugatani T, Hruska KA. MicroRNA-223 is a key factor in osteoclast differentiation. J Cell Biochem 2007;101: 996-9.
[260] Sugatani T, Vacher J, Hruska KA. A microRNA expression signature of osteoclastogenesis. Blood 2011;117: 3648-57.
[261] Mizoguchi F, Murakami Y, Saito T, Miyasaka N, Kohsaka H. miR-31 controls osteoclast formation and bone resorption by targeting RhoA. Arthritis Res Ther 2013;15: R102.
[262] Franceschetti T, Kessler CB, Lee SK, Delany AM. miR-29 promotes murine osteoclastogenesis by regulating osteoclast commitment and migration. J Biol Chem 2013;288: 33347-60.
[263] Kagiya T, Nakamura S. Expression profiling of microRNAs in RAW264.7 cells treated with a combination of tumor necrosis factor alpha and RANKL during osteoclast differentiation. J Periodontal Res 2013;48: 373-85.
[264] Dobson KR, Reading L, Haberey M, Marine X, Scutt A. Centrifugal isolation of bone marrow from bone: an improved method for recovery and quantitation of bone marrow osteoprogenitor cells from rat tibiae and femurae. Calcif Tissue Int 1999;65: 411-413.
[265] Keene JD, Komisarow JM, Friedersdorf MB. RIP-Chip: the isolation and identification of mRNAs, microRNAs and protein components of ribonucleoprotein complexes from cell extracts. Nat Protoc 2006;1: 302-7.
[266] Wang WX, Wilfred BR, Hu Y, Stromberg AJ, Nelson PT. Anti-Argonaute RIP-Chip shows that miRNA transfections alter global patterns of mRNA recruitment to microribonucleoprotein complexes. RNA 2010;16: 394-404.
[267] Jacquin C, Gran DE, Lee SK, Lorenzo JA, Aguila HL. Identification of multiple osteoclast precursor populations in murine bone marrow. J Bone Miner Res 2006;21: 67-77.
[268] Jacome-Galarza CE, Lee SK, Lorenzo JA, Aguila HL. Identification, characterization, and isolation of a common progenitor for osteoclasts, macrophages, and dendritic cells from murine bone marrow and periphery. J Bone Miner Res 2013;28: 1203-13.

[269] Guo SL, Ye H, Teng Y, Wang YL, Yang G, Li XB, Zhang C, Yang X, Yang ZZ, Yang X. Akt-p53-miR-365-cyclin D1/cdc25A axis contributes to gastric tumorigenesis induced by PTEN deficiency. Nat Commun 2013;4: 2544.
[270] Hamada S, Masamune A, Miura S, Satoh K, Shimosegawa T. MiR-365 induces gemcitabine resistance in pancreatic cancer cells by targeting the adaptor protein SHC1 and pro-apoptotic regulator BAX. Cell Signal 2014;26: 179-85.
[271] Kloosterman WP, Steiner FA, Berezikov E, de Bruijn E, van de Belt J, Verheul M, Cuppen E, Plasterk RH. Cloning and expression of new microRNAs from zebrafish. Nucleic Acids Res 2006;34: 2558-69.
[272] Yu D, dos Santos CO, Zhao G, Jiang J, Amigo JD, Khandros E, Dore LC, Yao Y, D'Souza J, Zhang Z, Ghaffari S, Choi J, Friend S, Tong W, Orange JS, Paw BH, Weiss MJ. miR-451 protects against erythroid oxidant stress by repressing 14-3-3zeta. Genes Dev 2010;24: 1620-33.
[273] Alexiou P, Maragkakis M, Papadopoulos GL, Simmosis VA, Zhang L, Hatzigeorgiou AG. The DIANA-mirExTra web server: from gene expression data to microRNA function. PLoS One 2010;5: e9171.
[274] Betel D, Koppal A, Agius P, Sander C, Leslie C. Comprehensive modeling of microRNA targets predicts functional non-conserved and non-canonical sites. Genome Biol 2010;11: R90.
[275] Friedman RC, Farh KK, Burge CB, Bartel DP. Most mammalian mRNAs are conserved targets of microRNAs. Genome Res 2009;19: 92-105.
[276] Sun D, Lee YS, Malhotra A, Kim HK, Matecic M, Evans C, Jensen RV, Moskaluk CA, Dutta A. miR-99 family of MicroRNAs suppresses the expression of prostate-specific antigen and prostate cancer cell proliferation. Cancer Res 2011;71: 1313-24.
[277] Wei F, Liu Y, Guo Y, Xiang A, Wang G, Xue X, Lu Z. miR-99b-targeted mTOR induction contributes to irradiation resistance in pancreatic cancer. Mol Cancer 2013;12: 81.
[278] Jin Y, Tymen SD, Chen D, Fang ZJ, Zhao Y, Dragas D, Dai Y, Marucha PT, Zhou X. MicroRNA-99 family targets AKT/mTOR signaling pathway in dermal wound healing. PLoS One 2013;8: e64434.
[279] Sugatani T, Hruska KA. Akt1/Akt2 and Mammalian Target of Rapamycin/Bim Play Critical Roles in Osteoclast Differentiation and Survival, Respectively, Whereas Akt Is Dispensable for Cell Survival in Isolated Osteoclast Precursors. Journal of Biological Chemistry 2005;280: 3583-3589.
[280] Glantschnig H, Fisher JE, Wesolowski G, Rodan GA, Reszka AA. M-CSF, TNFalpha and RANK ligand promote osteoclast survival by signaling through mTOR/S6 kinase. Cell Death Differ 2003;10: 1165-77.
[281] Indo Y, Takeshita S, Ishii KA, Hoshii T, Aburatani H, Hirao A, Ikeda K. Metabolic regulation of osteoclast differentiation and function. J Bone Miner Res 2013;28: 2392-9.
[282] Guntur AR, Rosen CJ. IGF-1 regulation of key signaling pathways in bone. BoneKEy Rep 2013;2.
[283] Wang Y, Nishida S, Elalieh HZ, Long RK, Halloran BP, Bikle DD. Role of IGF-I Signaling in Regulating Osteoclastogenesis. Journal of Bone and Mineral Research 2006;21: 1350-1358.
[284] Saucedo LJ, Gao X, Chiarelli DA, Li L, Pan D, Edgar BA. Rheb promotes cell growth as a component of the insulin/TOR signalling network. Nat Cell Biol 2003;5: 566-71.

[285] Sato T, Umetsu A, Tamanoi F. Characterization of the Rheb-mTOR signaling pathway in mammalian cells: constitutive active mutants of Rheb and mTOR. Methods Enzymol 2008;438: 307-20.
[286] Heard JJ, Fong V, Bathaie SZ, Tamanoi F. Recent progress in the study of the Rheb family GTPases. Cellular Signalling 2014;26: 1950-1957.
[287] Gingery A, Bradley E, Shaw A, Oursler MJ. Phosphatidylinositol 3-kinase coordinately activates the MEK/ERK and AKT/NFkappaB pathways to maintain osteoclast survival. J Cell Biochem 2003;89: 165-79.
[288] Oikawa T, Kuroda Y, Matsuo K. Regulation of osteoclasts by membrane-derived lipid mediators. Cellular and Molecular Life Sciences 2013;70: 3341-3353.
[289] Grey A, Chaussade C, Empson V, Lin J-M, Watson M, O'Sullivan S, Rewcastle G, Naot D, Cornish J, Shepherd P. Evidence for a role for the p110-α isoform of PI3K in skeletal function. Biochemical and Biophysical Research Communications 2010;391: 564-569.
[290] Shinohara M, Nakamura M, Masuda H, Hirose J, Kadono Y, Iwasawa M, Nagase Y, Ueki K, Kadowaki T, Sasaki T, Kato S, Nakamura H, Tanaka S, Takayanagi H. Class IA phosphatidylinositol 3-kinase regulates osteoclastic bone resorption through protein kinase B-mediated vesicle transport. J Bone Miner Res 2012;27: 2464-75.
[291] Easow G, Teleman AA, Cohen SM. Isolation of microRNA targets by miRNP immunopurification. RNA 2007;13: 1198-204.
[292] Hong X, Hammell M, Ambros V, Cohen SM. Immunopurification of Ago1 miRNPs selects for a distinct class of microRNA targets. Proc Natl Acad Sci U S A 2009;106: 15085-90.
[293] Karginov FV, Conaco C, Xuan Z, Schmidt BH, Parker JS, Mandel G, Hannon GJ. A biochemical approach to identifying microRNA targets. Proc Natl Acad Sci U S A 2007;104: 19291-6.
[294] Martinez-Sanchez A, Murphy CL. MicroRNA Target Identification-Experimental Approaches. Biology (Basel) 2013;2: 189-205.
[295] Okamura K, Ishizuka A, Siomi H, Siomi MC. Distinct roles for Argonaute proteins in small RNA-directed RNA cleavage pathways. Genes Dev 2004;18: 1655-66.
[296] Nelson PT, De Planell-Saguer M, Lamprinaki S, Kiriakidou M, Zhang P, O'Doherty U, Mourelatos Z. A novel monoclonal antibody against human Argonaute proteins reveals unexpected characteristics of miRNAs in human blood cells. RNA 2007;13: 1787-92.
[297] Tanic M, Zajac M, Gomez-Lopez G, Benitez J, Martinez-Delgado B. Integration of BRCA1-mediated miRNA and mRNA profiles reveals microRNA regulation of TRAF2 and NFkappaB pathway. Breast Cancer Res Treat 2012;134: 41-51.
[298] Turcatel G, Rubin N, El-Hashash A, Warburton D. MIR-99a and MIR-99b modulate TGF-beta induced epithelial to mesenchymal plasticity in normal murine mammary gland cells. PLoS One 2012;7: e31032.
[299] Singh Y, Kaul V, Mehra A, Chatterjee S, Tousif S, Dwivedi VP, Suar M, Van Kaer L, Bishai WR, Das G. Mycobacterium tuberculosis controls microRNA-99b (miR-99b) expression in infected murine dendritic cells to modulate host immunity. J Biol Chem 2013;288: 5056-61.
[300] Yasui T, Kadono Y, Nakamura M, Oshima Y, Matsumoto T, Masuda H, Hirose J, Omata Y, Yasuda H, Imamura T, Nakamura K, Tanaka S. Regulation of RANKL-induced osteoclastogenesis by TGF-beta through molecular interaction between Smad3 and Traf6. J Bone Miner Res 2011;26: 1447-56.

[301] Landstrom M. The TAK1-TRAF6 signalling pathway. Int J Biochem Cell Biol 2010;42: 585-9.
[302] Xu Z, Xiao SB, Xu P, Xie Q, Cao L, Wang D, Luo R, Zhong Y, Chen HC, Fang LR. miR-365, a novel negative regulator of interleukin-6 gene expression, is cooperatively regulated by Sp1 and NF-kappaB. J Biol Chem 2011;286: 21401-12.
[303] Adapala NS, Barbe MF, Langdon WY, Nakamura MC, Tsygankov AY, Sanjay A. The loss of Cbl-phosphatidylinositol 3-kinase interaction perturbs RANKL-mediated signaling, inhibiting bone resorption and promoting osteoclast survival. J Biol Chem 2010;285: 36745-58.
[304] Kang H, Chang W, Hurley M, Vignery A, Wu D. Important roles of PI3Kgamma in osteoclastogenesis and bone homeostasis. Proc Natl Acad Sci U S A 2010;107: 12901-6.
[305] Kawamura N, Kugimiya F, Oshima Y, Ohba S, Ikeda T, Saito T, Shinoda Y, Kawasaki Y, Ogata N, Hoshi K, Akiyama T, Chen WS, Hay N, Tobe K, Kadowaki T, Azuma Y, Tanaka S, Nakamura K, Chung UI, Kawaguchi H. Akt1 in osteoblasts and osteoclasts controls bone remodeling. PLoS One 2007;2: e1058.
[306] Jaskiewicz L, Bilen B, Hausser J, Zavolan M. Argonaute CLIP--a method to identify in vivo targets of miRNAs. Methods 2012;58: 106-12.
[307] Chi SW, Zang JB, Mele A, Darnell RB. Argonaute HITS-CLIP decodes microRNA-mRNA interaction maps. Nature 2009;460: 479-86.
[308] Ascano M, Hafner M, Cekan P, Gerstberger S, Tuschl T. Identification of RNA-protein interaction networks using PAR-CLIP. Wiley Interdiscip Rev RNA 2012;3: 159-77.
[309] Hafner M, Lianoglou S, Tuschl T, Betel D. Genome-wide identification of miRNA targets by PAR-CLIP. Methods 2012;58: 94-105.
[310] Imig J, Brunschweiger A, Brummer A, Guennewig B, Mittal N, Kishore S, Tsikrika P, Gerber AP, Zavolan M, Hall J. miR-CLIP capture of a miRNA targetome uncovers a lincRNA H19-miR-106a interaction. Nat Chem Biol 2015;11: 107-14.
[311] Huang J, Chen D. miRNAs in circulation: mirroring bone conditions? J Bone Miner Res 2014;29: 1715-7.
[312] Zhang Y, Wang Z, Gemeinhart RA. Progress in MicroRNA Delivery. Journal of controlled release : official journal of the Controlled Release Society 2013;172: 962-974.
[313] van Rooij E, Kauppinen S. Development of microRNA therapeutics is coming of age. EMBO Molecular Medicine 2014;6: 851-864.
[314] Misso G, Di Martino MT, De Rosa G, Farooqi AA, Lombardi A, Campani V, Zarone MR, Gulla A, Tagliaferri P, Tassone P, Caraglia M. Mir-34: A New Weapon Against Cancer? Mol Ther Nucleic Acids 2014;3: e194.
[315] Di Martino MT, Leone E, Amodio N, Foresta U, Lionetti M, Pitari MR, Cantafio ME, Gulla A, Conforti F, Morelli E, Tomaino V, Rossi M, Negrini M, Ferrarini M, Caraglia M, Shammas MA, Munshi NC, Anderson KC, Neri A, Tagliaferri P, Tassone P. Synthetic miR-34a mimics as a novel therapeutic agent for multiple myeloma: in vitro and in vivo evidence. Clin Cancer Res 2012;18: 6260-70.
[316] Deng Y, Bi X, Zhou H, You Z, Wang Y, Gu P, Fan X. Repair of critical-sized bone defects with anti-miR-31-expressing bone marrow stromal stem cells and poly(glycerol sebacate) scaffolds. Eur Cell Mater 2014;27: 13-24; discussion 24-5.
[317] Schade A, Delyagina E, Scharfenberg D, Skorska A, Lux C, David R, Steinhoff G. Innovative strategy for microRNA delivery in human mesenchymal stem cells via magnetic nanoparticles. Int J Mol Sci 2013;14: 10710-26.

[318] James EN, Delany AM, Nair LS. Post-transcriptional regulation in osteoblasts using localized delivery of miR-29a inhibitor from nanofibers to enhance extracellular matrix deposition. Acta Biomater 2014;10: 3571-80.
[319] Qureshi AT, Doyle A, Chen C, Coulon D, Dasa V, Del Piero F, Levi B, Monroe WT, Gimble JM, Hayes DJ. Photoactivated miR-148b-nanoparticle conjugates improve closure of critical size mouse calvarial defects. Acta Biomater 2015;12: 166-73.
[320] Suh JS, Lee JY, Choi YS, Chong PC, Park YJ. Peptide-mediated intracellular delivery of miRNA-29b for osteogenic stem cell differentiation. Biomaterials 2013;34: 4347-4359.
[321] Liu J, Dang L, Li D, Liang C, He X, Wu H, Qian A, Yang Z, Au DWT, Chiang MWL, Zhang B-T, Han Q, Yue KKM, Zhang H, Lv C, Pan X, Xu J, Bian Z, Shang P, Tan W, Liang Z, Guo B, Lu A, Zhang G. A delivery system specifically approaching bone resorption surfaces to facilitate therapeutic modulation of microRNAs in osteoclasts. Biomaterials 2015;52: 148-160.